# Pulsatile Flows

## Experimental Investigation of fully turbulent pulsatile pipe flows

Abhiroop Bhadra

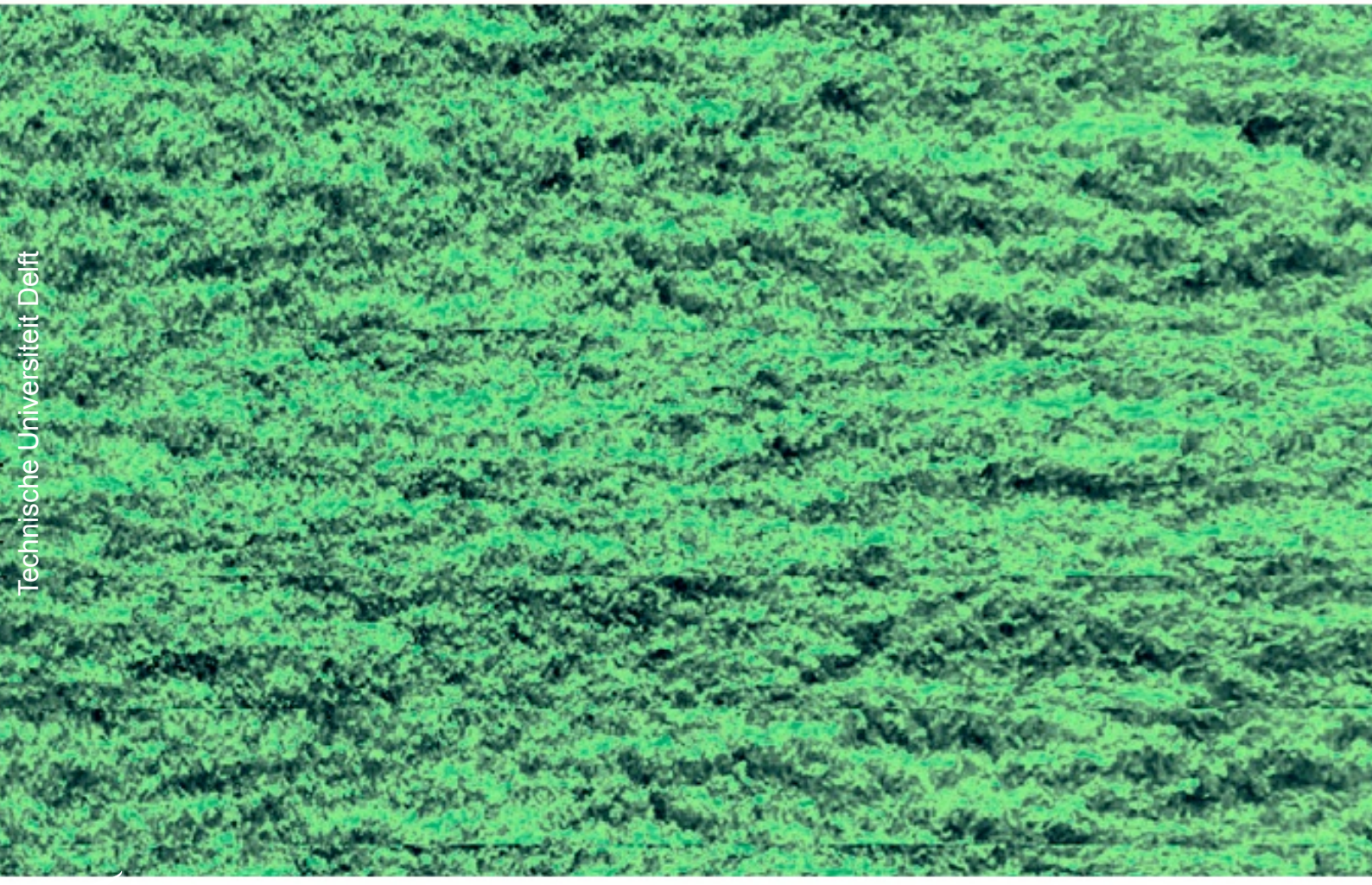

Technische Universiteit Delft

# Pulsatile Flows

## Experimental Investigation of fully turbulent pulsatile pipe flows

by

Abhiroop Bhadra

to obtain the degree of Master of Science at the Delft University of Technology, to be defended publicly on Tuesday November 27, 2018 at 11:00 AM.

| | | |
|---|---|---|
| Student Number: | 4518268 | |
| P&E Report Number: | 2931 | |
| Supervisor: | Prof. dr. ir. Jerry Westerweel, | TU Delft |
| Daily Supervisor: | Melika Gül, | TU Delft |
| Thesis Committee: | Dr. ir. Gerrit Elsinga, | TU Delft |
| | Dr.ir. R. Pecnik, | TU Delft |
| | Dr. Andrea Sciacchitano, | TU Delft |

An electronic version of this report is available at http://repository.tudelft.nl/

TU Delft Delft University of Technology

# Acknowledgements

I am grateful to my supervisor **Prof.dr.ir. J. Westerweel** for giving me the opportunity to work on this topic and for his feedback during our meetings which helped me to critically review my work. A special thanks goes out to my daily supervisor **Melika Gül** for making me familiar with experimental research through the constant aid and discussions. I would also like to thank **Edwin Overmars** for making me acquainted with 2D3C PIV experiments. Heartiest thanks to **Jasper Ruijgrok** and **Jan Graafland** for removing all the setbacks that I frequently encountered during the experimental work which ultimately helped me to complete the experiments in the targeted time. The thesis committee includes **Dr.ir. Gerrit E. Elsinga**, **Dr.ir. Rene Pecnik** and **Dr. Andrea Sciacchitano**: Thank you for agreeing to be present in the thesis committee.

Thank you, **Ankur** and **Digvijay** for giving me feedback on my report.Also, a special thanks to **Ankit**, **Aditya**, **Antaran** and everyone in the lab for creating a dynamic environment to work in.

Last but definitely not the least, I am grateful to my parents for having faith in me throughout this whole time.

*Abhiroop Bhadra*

*Delft, November 2018*

# Abstract

Turbulence is a commonly encountered state of fluid dynamics. Unsteady turbulent flows in pipes are present in many engineering applications and also in biological flows. However, the various processes active in such flows are not well understood. The present work employs stereo-PIV to investigate the effects of a sinusoidal pressure gradient on the various turbulence parameters, including the terms of the turbulent kinetic energy budget equation. The bulk flow rate was oscillated with a frequency of 0.5 Hz with a mean $Re_D$ 26,000 and an amplitude of modulation, 0.23 times the mean value. It is seen that there is a delay in the response of turbulence to the oscillations of the bulk flow and the delay increases with increasing distance from the wall. The axial and the in-plane turbulence parameters show a difference in the delay of their responses. This delay extends into the small scales responsible for the dissipation of turbulent kinetic energy. Changes are also observed in azimuthal length scales when the flow oscillates.The effects of oscillation on the streaks of low momentum are also discussed and the structural organization in unsteady pipe flows are found to be different from that in steady pipe flows.

# Contents

# List of Figures

# List of Tables

# Abbreviations

| Acronym | Full Form |
|---|---|
| **PIV** | **P**article **I**mage **V**elocimetry |
| **TKE** | **T**urbulent **K**inetic **E**nergy |

# List of Symbols

| Symbol | Usage |
|---|---|
| $\alpha$ | Womersley Number |
| $D$ | Diameter of pipe |
| $\delta_v$ | Viscous wall unit |
| $\epsilon$ | Rate of dissipation of turbulent kinetic energy |
| $f$ | Frequency of oscillation |
| $\phi$ | Phase |
| $\rho$ | Density |
| $\mu$ | Dynamic Viscosity |
| $\nu$ | Kinematic Viscosity |
| $\nu_\tau$ | Eddy Viscosity |
| $\eta$ | Kolmogorov Length Scale |
| $P$ | Pressure |
| $R$ | Radius of pipe |
| $r$ | Distance from the center of the pipe |
| $Re_D$ | Bulk reynolds Number |
| $St$ | Strouhal number |
| $t$ | time |
| $\theta$ | Azimuthal angle |
| $T_{osc}$ | Time period of oscillaton |
| $\tau$ | Wall shear stress |
| $u_\tau$ | Friction velocity of the mean flow |
| $U_b$ | Bulk velocity of the mean flow |
| $u_\tau^*$ | Friction velocity of the instantaneous flow |
| $\omega$ | Angular frequency of oscillation |
| $y$ | Distance from the pipe wall |

# 1

# Introduction

## 1.1. Motivation

Turbulent flows are ubiquitous in nature and are encountered in many engineering applications. Statistically unsteady turbulent flows, commonly referred to as unsteady turbulent flows, are encountered in fields like turbomachinery [1], aerodynamics [2], biological flows [3], [4], etc. A thorough understanding of such flows would not only facilitate the development of such fields but would also foster a greater understanding of the various mechanisms active in turbulent flows in general. The unsteady nature of the flow reveals several aspects of turbulence which are difficult to isolate in steady turbulent flows [5].

Pulsatile flows in a pipe are a class of unsteady flows where the pressure difference across the ends of the pipe is varied in a periodic manner. These flows are found in engineering applications like combustion engines [6], heat exchangers [7], reciprocatory pumps [8],etc. In biological studies these flows are present in the respiratory track of land animals, in blood vessels [9], etc. If the rate of change of pressure is high enough, the behaviour of these flows deviates from that of a steady flow with the same flow rate. Research on pulsatile flows has been going on since the second half of the $20^{th}$ century, yet the processes responsible for the deviation of their behaviour from steady pipe flows are not well understood.

The present work aims to investigate the effects of sinusoidally varying pressure on the terms of the turbulent kinetic energy budget equation. The flow rate in the pipe varies sinusoidally about a mean flow rate. The processes responsible for creating, distributing and ultimately destroying turbulence in such flows are decoupled from one another and studying how the terms vary in an oscillation will aid in understanding the physics involved in these flows.

## 1.2. Literature Review

The early investigators of pulsatile flows in pipes (**Brown *et al.* (1969)** [10]; **Ohmi & Usui (1976)** [11]) have analyzed pulsatile flows with a constant eddy viscosity (the eddy viscosity being that of the Reynolds number of the mean flow rate) and predicted the velocity profile using finite difference techniques. They observed that the results are in close agreement with experimental results only at high oscillation frequencies.

**Ohmi *et al.*(1978)** [12] repeated the calculations using a time dependent eddy viscosity (eddy viscosity of the flow at a specific phase of oscillation was assumed to be that of the instantaneous flowrate at that phase. i.e. a quasi-steady eddy viscosity was assumed ). It was found that the results matched experimental results only at low oscillation frequencies.

**Mizushina, *et al.* (1973)**[13] took measurements of pulsatile flows in a pipe using an electrochemical method. They observed that if the frequency of pulsation is comparable to the mean bursting frequency of turbulence of the steady mean flow rate, significant changes in the turbulence parameters are observed. They also showed that the eddy viscosity changes throughout the time period of pulsation indicating that standard eddy viscosity models cannot be applied in the case of pulsatile flows.

**Mizushina,*et al.* (1975)**[14] extended their previous work and studied the generation and propagation of turbulence in pulsatile flows. The temporal characteristics of the propagation of 'turbulence' generated near the wall was presented. The average time delay of the turbulence, in reaching the centerline, was observed to be same as the mean bursting period of turbulence of the steady mean flow rate, therefore, if the period of pulsation is less than the bursting period, the intensity of turbulence is localized near the wall. Hence, the authors arrived at an approach to characterize pulsatile flows based on the time period of bursting of the steady mean flow rate.

**Shermer,*et al.* (1982)**[15] studied the structure of turbulence in a pipe using a rake of 9 hot wires. They studied the effect of oscillations on the time mean profiles of various turbulence parameters. Their measurements, however, were confined to the low frequency quasi-steady regime of a fairly low Reynolds number (based on bulk velocity). In this regime, the time mean properties of the flow showed no difference with the corresponding steady values.

**Ramaprian & Tu (Part 1) (1983)**[16] investigated the effects of pulsation in a pipe flow, on the time mean properties of the flow and also the structure of turbulence, using a single channel Laser Doppler Anemometry and direct wall shear stress was measured using a flush mounted film gauge. Experiments were performed at a fairly high Reynolds number 50,000 (based on bulk velocity). Two frequencies of oscillations- 0.5Hz (65% amplitude) and 3.6 Hz (15% amplitude) were studied.

A time-mean velocity profile of a quasi steady flow was obtained by averaging the velocity profiles of steady flows within the range of the amplitude of modulation of the pulsating flow. It was then compared with the time averaged velocity of the pulsating flow. Differences were detected in the time mean

profile of the flow with the higher frequency. These findings were contradictory to those of previous investigators.

At the higher frequency the ensemble averaged velocity profile looked similar to one another. At the lower frequency the ensemble averaged velocity profiles showed differences from each other and even inflection points were found in the velocity profiles. The ensemble averaged velocity profiles did not follow the 'log law'.

For the higher frequency studied, the ensemble averaged turbulence intensities did not show any modulation near the central region, while for the lower frequency it varied significantly throughout the pipe. The authors described the turbulence to be 'frozen' in the central region at the higher frequencies. As the lower frequency was at a higher amplitude of oscillation the authors inferred that the amplitude plays a weaker role than the frequency of oscillation in causing changes to the flow parameters.

**Ramaprian & Tu (Part 2) (1983)** [17] continued their previous work and repeated the experiments with a constant amplitude (25%) and different frequencies ranging from 0.5 Hz to 3.0 Hz.

On comparing the modulation amplitude of the ensemble averaged velocity profile (normalized by the modulation amplitude of the cross sectional averaged velocity) along different points in the radius it was seen that the overshoot of the amplitude is more diffused in turbulent flows than those of oscillating laminar flows. The overshoot for the turbulent flow occurs much further away from the wall than for the laminar flow. Thus, showing the Stokes number which is used to characterize oscillating laminar flow cannot be used as a relevant parameter in turbulent flows.

The 'frozen' turbulence observed at the center was explained in terms of the time taken for the turbulence to reach the center of the pipe from its production near the wall being higher relative to the time period of the imposed oscillations.

Mizushina *et al.*[14] reported that this delay period was comparable to the time period of bursting of the mean flow rate and they also produces a histogram of the time between bursts for different Reynolds numbers . Using the highest measured bursting frequency ($\omega_{bU}$), the mean bursting frequency ($\overline{\omega_b}$) and the lowest measured bursting frequency ($\omega_{bL}$) of bursting of the mean flowrate; five regimes of pulsatile flows were defined as, (here $\frac{\omega D}{\overline{u_t}}$ refers to the Strouhal number of the mean steady flow, D is the diameter of the pipe, $\omega$ is the circular frequency of oscillation and $\overline{u_t}$ is the friction velocity of the mean flow rate.)

$1^{st}$ regime ($\frac{\omega D}{\overline{u_t}} \leq 0.1$)-The flow will behave as a quasi steady flow.

$2^{nd}$ regime ($0.1 \leq \frac{\omega D}{\overline{u_t}} \leq 10$)- The oscillations will not affect the structure of turbulence but will not be completely quasi steady in nature.

$3^{rd}$ regime ($\frac{\omega_{bL} D}{\overline{u_t}} \leq \frac{\omega D}{\overline{u_t}} \leq \frac{\overline{\omega_b} D}{\overline{u_t}}$)-The structure of turbulence will start interacting with the imposed oscillations.

$4^{th}$ regime ($\frac{\overline{\omega_b} D}{\overline{u_t}} \leq \frac{\omega D}{\overline{u_t}} \leq \frac{\omega_{bU} D}{\overline{u_t}}$)-The effects of oscillation will be confined to a thin region (0.1D) near the wall.

$5^{th}$ regime ($\frac{\omega_{bU} D}{\overline{u_t}} \leq \frac{\omega D}{\overline{u_t}}$)-The flow will behave as a plug flow with effects of oscillations confined to around 0.01D.

**Mao & Hanratty *et. al.* (1984)**[18] investigated the effects of the imposed oscillations on the wall shear stress in a pipe. **Tardu *et al.* (1991)**[19] investigated the logarithmic region and near wall region in a channel with high frequency and high amplitude oscillating flow. It was reported in both these studies that the time mean properties of the flow did not show any difference from that of the steady flow and a phase difference existed between the oscillation and the turbulence parameters.

**He & Jackson *et al.* (1997)**[5] performed experiments on unsteady flows in a pipe with ramp-up and ramp-down velocity changes, using double channel Laser Dopppler Anemometry. The parameter $\frac{D}{u_{\tau o}}(\frac{1}{U_{bo}}\frac{dU_b}{dt}$, where $U_b$ is the bulk velocity, $u_{\tau o}$ and $U_{bo}$ are the friction velocity and bulk velocity respectively of the initial Reynolds number in the transient) was used to characterize the flows. This parameter is the ratio of the time scale of diffusion to the time scale of the transient. Observations included a delay period in the response of the axial component of turbulence in reaching the center during the transient and a longer delay in the response of the non-axial components. This can be explained with the longer time scales of the processes distributing energy to the non-axial velocity components . Reynolds stress showed a behavior similar to the non-axial components.

In the experiments conducted two types of delays in the response of turbulence were detected- delays in diffusion and delays in redistribution (for non-axial components). A third type delay in production was hypothesized to be present for faster transients.In the experiments conducted by the authors, the delay in diffusion in the outer layer dominates the lag in turbulence response and hence $\frac{D}{u_{\tau o}}$ is used as the time scale for characterization. For faster transients the delay in production caused by change in the velocity gradient of the buffer region dominates the entire delay and the inner layers variables $\frac{\nu}{u_{\tau o}^2}$ ($\nu$ is the kinematic viscosity) would be used to scale time.

**Scotti & Piomelli (2000)**[20] used Direct numerical Simulation (DNS) and Large-Eddy Simulation (LES) data to study pulsatile flows in a channel over a range of imposed oscillating frequencies. In order to facilitate their study and classify the flows, the authors introduced the concept of turbulent Stokes layer thickness ($l_t$). The Stokes layer thickness is given as, $l_s = \sqrt{\frac{2\nu}{\omega}}$. Motivated by the laminar version, the turbulent Stokes layer thickness in wall units is given as $l_t^+ = \frac{u_t}{\nu}\sqrt{\frac{2(\nu+\nu_t)}{\omega}}$, ($\nu_t$ is the eddy viscosity) , replacing $\nu_t = \kappa \nu_t l_t$, where $\kappa$ is the Von Karman constant, the following is derived $l_t^+ = l_s^+[\frac{\kappa l_s^+}{2} + \sqrt{1+(\frac{\kappa l_s^+}{2})^2}]$ ,

The turbulent Stokes layer thickness in wall units was presented as a parameter to determine how far the oscillations generated near the wall would penetrate into the flow. For $l_t^+ >> h^+ (h^+$ is the channel half-width in wall units) the turbulence has enough time to adjust to the modulation and a quasi steady flow will be obtained. On increasing the frequency, in the regime $l_t^+ < \frac{h^+}{2}$ the central region of the channel would not show any changes due to the imposed oscillations and there would be a phase difference between the turbulence parameters in the region towards the wall where changes are

observed. For $l_t^+ << h^+$ the changes due to oscillations would be confined to a very thin region near the wall.

The literature on fully turbulent pulsatile flow is vast as this class of flows has been actively investigated over the past years. For a detailed literature review of fully turbulent pulsatile flows, the reader is referred to **Gundogdu & Carpinlioglu (1992)**[21]. Only the works that are relevant to the present project have been reviewed in the present report.

It is seen from the review of literature that a major hurdle in the study of pulsatile flows is their characterization. This arises from the fact that two additional parameters- the frequency of modulation and the amplitude of modulation appear in pulsatile flows. Therefore three non-dimensional parameters are required to fully characterize the system (unlike only one parameter, the Reynolds number in steady flows). Most authors have reported the modulation amplitude of the flowrate to be a non-significant parameter ( as long it is less than the mean flow rate itself) and the number of non-dimensional parameters reduces to two. The choice of these parameters have varied with authors and a consensus on the parameters to be used is yet to be arrived at. Moreover, the physical mechanisms responsible for causing a delay of the flow variables with respect to the bulk flowrate are not well understood.

## 1.3. Outline of the thesis

The report has the following outline. Chapter 1 gives an introduction to pulsatile flows and gives a description of the existing work. Chapter 2 describes the experiment test setup used in measuring the data, the design of experiment and the validation of the data obtained. Chapter 3 shows the statistical results obtained. It includes the effects of oscillation on the terms of the Navier Stokes equation, the turbulent kinetic energy equations and the various turbulence parameters- Eddy viscosity, Reynolds stress, Wall shear stress, etc. Chapter 4 describes the effects of oscillations on the regions of low momentum which are seen in wall turbulence and finally Chapter 5 gives the conclusion and the recommendations for future work.

# 2

# Measurement Technique

## 2.1. Experimental Setup

The experimental setup used for the present work is represented schematically in Figure 2.1. It consists of a rigid Perspex pipe 9.1 m in length, 40 mm inner diameter and 5mm thickness. A gear pump (Liquiflo Rotogear Sealed Pump 37 F) is used to generate pulsatile flow in the pipe. A settling chamber with grids and a contraction is used to terminate any swirls that arise due to the motion of the pump. The flow rate is monitored using a ultrasound flow meter (Krohne UFC 500).

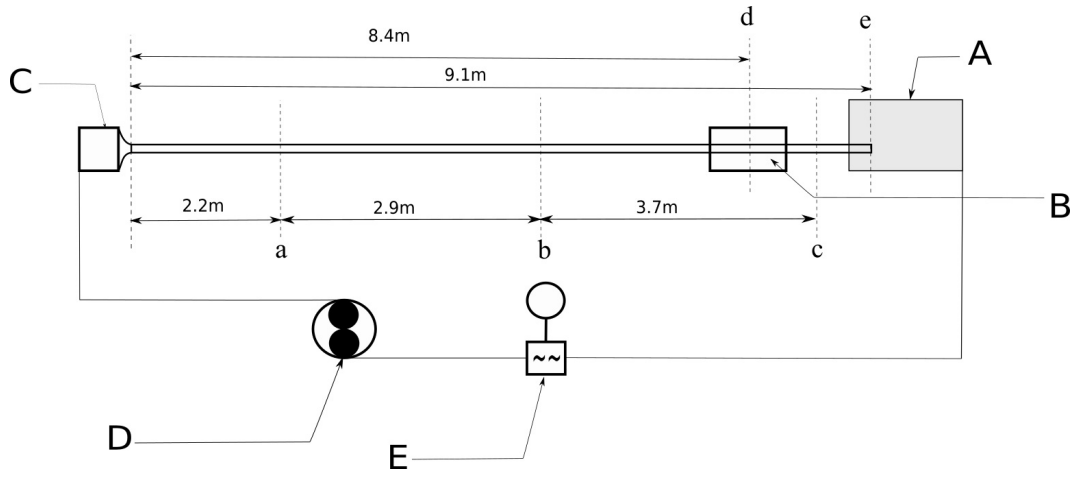


Figure 2.1: Layout of the experimental setup; A- Discharge Tank; B- Test section; C-Settling Chamber; D- Gear Pump; E- Ultrasound Flowmeter; a- Pressure port 1; b-Pressure port 2; c-Pressure port 3; d- Measurement plane; e- End of pipe

In order to investigate the terms of the energy budget equation, three components of the velocity field

over the entire cross section of the pipe are required. Thus, Stereo PIV (S-PIV) was used with the laser sheet cutting across the pipe. Two cameras (Phantom VEO-640L) were used to record the images and a Nd:YLF laser system (Pegasus-PIV) was used to generate the light sheet for the measurements. Scheimpflug adapters were used to obtain uniform focusing of the measurement plane on the image plane (See figure 2.2). 10-12 um hollow glass spheres with a bulk density of 1.1 ($\pm$ 0.5) g/cc (Sphericell 110P8, Potters Industries) are used as tracer particles. The laser and cameras were synchronized with the oscillating flow using a Programmable Timing Unit (PTU), allowing the capturing of images at a specific phase of oscillation. The vector fields are obtained using the commercial software Davis 8.4.0.

The measurement section is 8.4m (210D) downstream of the inlet. In the measurement section the Perspex pipe section is replaced with a glass pipe with the same inner diameter but a reduced thickness of 1.6mm. The glass pipe itself is within a glass-walled rectangular cuboid box filled with water (Test Section). This reduces the optical distortions due to the curvature of the pipe. Two water-filled prisms are on the side of the Test Section facing the cameras, in order to reduce the extent of refraction at the interface and also avoid Total Internal Reflection.

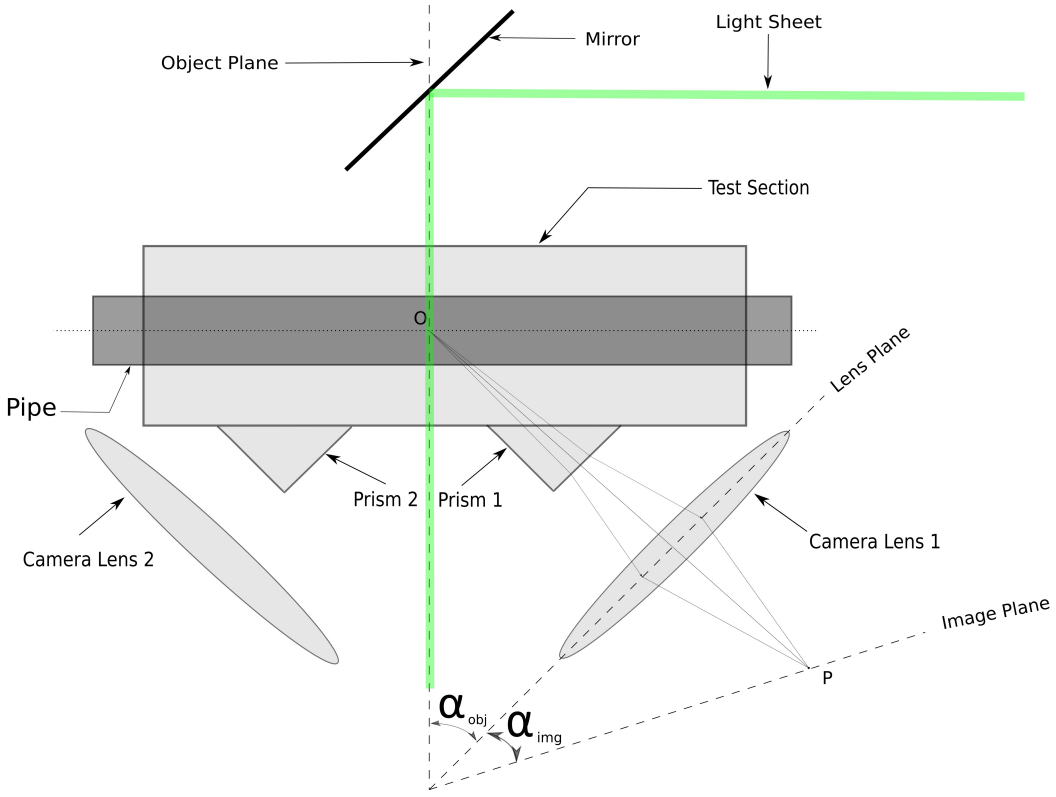


Figure 2.2: Schematic showing the action of prisms and Scheimpflug adapters

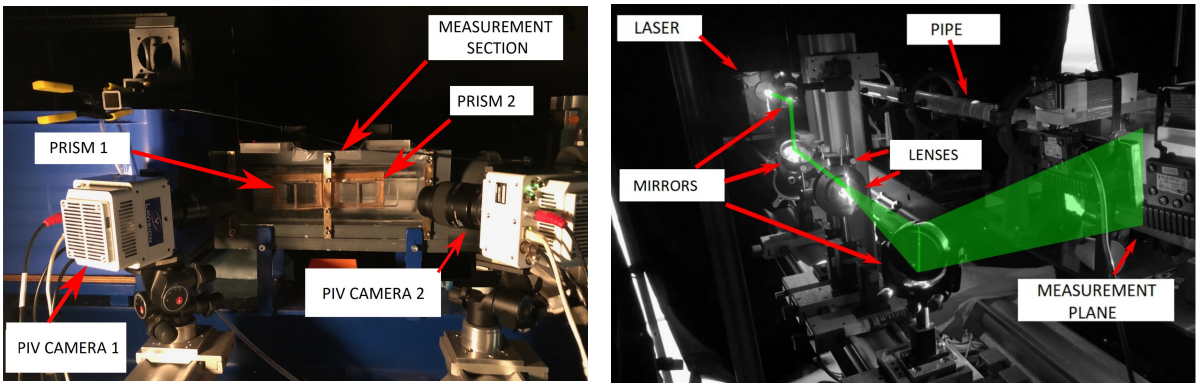


(a) (b)

Figure 2.3: **Figure (a)** the experimental setup near the measurement section. **Figure (b)** the generation of the light sheet is shown

Pressure measurements were made to confirm that the flow is 'fully developed' in the measurement section. As the measurement section was very close to the end of the pipe, the pressure measurements would also be used to inspect whether the exit length which is not significant for steady turbulent flows would play any role in the measurement of fully turbulent pulsatile flows. The pressure data was recorded using a differential pressure transducer (Validyne Engineering Corp., Model DP15-26).Static pressure holes in the pipe were made at distances 2.2m (point **a**), 5.1m (point **b**)and 8.8 m (point **c**) from the entrance plane (Figure 2.1). The measurement plane was present between the holes at point **b** and point **c**. The Darcy–Weisbach friction factor calculated from the pressure drop between points **b** and **c** in steady flows were compared with the theoretical friction factor in a smooth pipe predicted by the Blasius correlation (See Figure 2.4)

The pressure drop (for pulsatile flow) between points **a** and **b** was compared with that between **b** and **c** to establish if the exit length would influence the S-PIV measurements. The differences observed were within 2% of the measured values, which is within the accuracy range. (See Table 2.1).The pressure drop ($\frac{\Delta P}{L}$) is related to the wall shear stress ($\tau$) as follows, (here, $\rho$ is the density of the fluid and L is the length of the pipe section)

$$\frac{\Delta P}{L} = \rho \frac{dU_b}{dt} + 4\frac{\tau}{D} \tag{2.1}$$

As the term $\rho \frac{dU_b}{dt}$ remains the same in all sections of the pipe (due to mass conservation), Table 2.1 shows that the wall shear stress does not vary spatially in the pipe section. Hence, the pulsatile flow is 'fully developed' in the measurement plane.

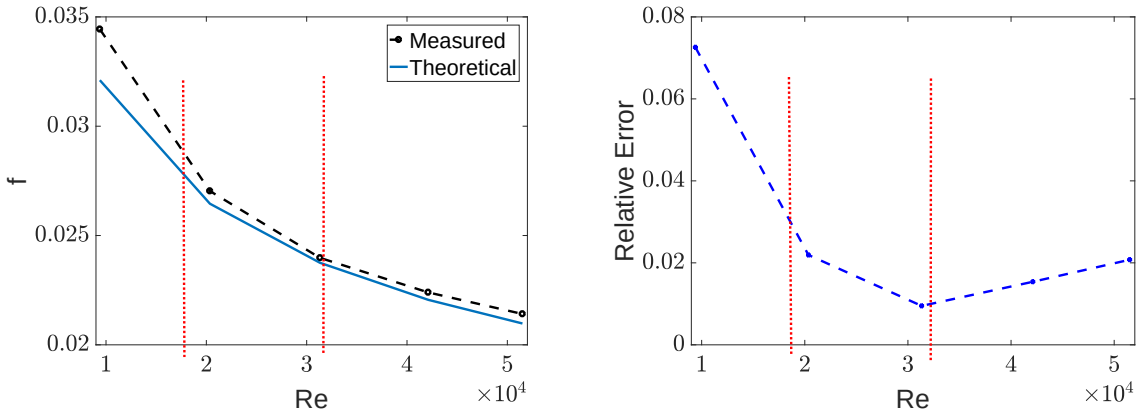


Figure 2.4: **Figure (a)** Comparison of the measured pressure drop between pressure ports at points *b* and *c*. **Figure (b)** the error between the theoretical and calculated values of the Darcy–Weisbach friction factor are shown, the present project deals with Reynolds numbers between the two red lines

| | P.D. across points **a** and **b** | | P.D. across points **b** and **c** | | Error percentage | |
|---|---|---|---|---|---|---|
| Frequency (Hz) | $(\frac{\Delta P}{L})_{Mean}$ | $(\frac{\Delta P}{L})_{Amp}$ | $(\frac{\Delta P}{L})_{Mean}$ | $(\frac{\Delta P}{L})_{Amp}$ | $(\frac{\Delta P}{L})_{Mean}$ | $(\frac{\Delta P}{L})_{Amp}$ |
| 0.32 | 152.3 | 292.46 | 149.78 | 294.31 | 1.65 % | 0.62 % |
| 0.4 | 152.2 | 397.94 | 150.17 | 402.48 | 1.32 % | 1.12 % |
| 0.5 | 152 | 526.67 | 149.97 | 537.246 | 1.32 % | 1.96 % |

Table 2.1: Comparisons of unsteady pressure drop (P.D.) measurements between points **a** and **b**; **b** and **c** (The flow has a mean flowrate bulk Reynolds number 26000 and amplitude (0.23%); **P.D has the units Pa/m)**

A brief descritption of PIV and S-PIV is presented in **Appendix 2**, however for a detailed review of the techniques the following are to be referred to - Adrian and Westerweel[22], Prasad[23], Soloff,*et al.*[24]. The laser sheet thickness for the S-PIV measurements was measured to be ≈ 0.5 mm using the technique described in Wieneke[25].

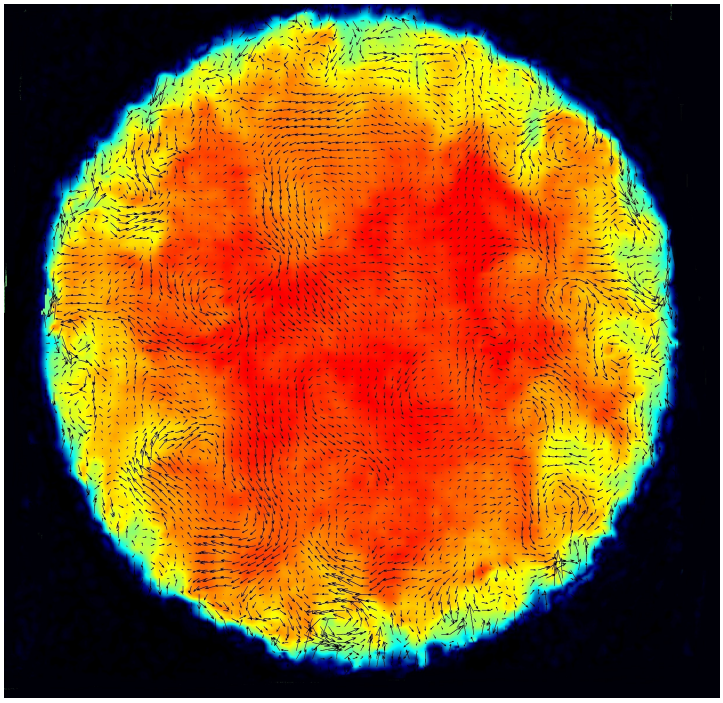

Figure 2.5: Sample vector field of pipe cross section (Arrows represent in-plane velocity vectors)

## 2.2. Design of experiments

Data is collected at a mean Reynolds number, $Re_D$ ($= \frac{U_b D}{\nu}$) ≡ 26,000 with an oscillating frequency, $f_{osc}$ ≡ 0.5 Hz. The pusatile flow is in the data is taken in the 'third regime' as defined by Ramaprian & Tu (Part 2) [17] and has a Womersley number, $\alpha$ ($= R\sqrt{\frac{\omega}{\nu}}$) ≡ 36. This is done to ensure that the effects of flow oscillations are visible in the 'outer layer' of the pipe. The amplitude of modulation of the flowrate is 0.23 times the mean flowrate. Steady flow measurements were taken at $Re_D$ 25,900 which is nearly the same as the mean flowrate and also at $Re_D$ 20,495 and $Re_D$ 30,947. The multi-pass interrogation scheme was used. An interogation window size of 64x64 pixels with 50% overlap was reduced to 24x24 pixels with 75% overlap. The FoV of the cameras were 45x33 mm. The in-plane resolution obtained is $8.5\eta$ and the vector spacing is $2.12\eta$, ($\eta$ = 5.86 x $10^{-5}$m is the Kolmogorov length scale of the measured steady flow). The temperature during the measurements was $20.2^o$C. The friction velocities ($u_\tau$) measured for steady flows at $Re_D$ 30,947, $Re_D$ 25,900 and $Re_D$ 20,495 were 0.0422 m/s, 0.0359 m/s and 0.0292 m/s respectively. These values were higher by 2.9 %, 2.5 % and 2.0 % of the theoretical values calculated by using the Blasius correlation for steady flows at the current temperature.

### 2.2.1. Statistical data

Ensemble averaging was used to measure the statistical data. PIV vector fields were obtained at specific phase points in repeating oscillations. The quantities obtained at a specific phase of unsteady flows are decomposed as, $\psi = \langle\psi\rangle + \psi' + \mathcal{E}_\psi$, here $\langle\psi\rangle$ denotes an ensemble average over the images captured at the same phase in different oscillation cycles, $\psi'$ denotes the fluctuating part and $\mathcal{E}_\psi$ represents measurement error.

$$\langle\psi\rangle = \frac{\sum_{n=1}^{N}\psi}{N} \tag{2.2}$$

N is the number of oscillations over which images are captured. In the present experiments N=1077. The fluctuating terms are calculated as $\psi' + \mathcal{E}_\psi = \psi - \langle\psi\rangle$, random measurement errors are included in fluctuating terms and as the fluctuating terms are themselves subjected to further averaging ( $\langle\acute{u}_z^2\rangle$, $\langle\acute{u}_z\acute{u}_r\rangle$, $\langle\acute{u}_z^2\acute{u}_r\rangle$ etc.), the effect of random errors in the measurements will reduce. Moreover, filtering is applied to the velocity fields to reduce random errors.

The phase averaged velocity may be further decomposed as $\langle\psi\rangle = \overline{\psi} + \psi_{osc}$, where $\overline{\psi}$ refers to the time averaged part, i.e. an average of all images captured at different phase points within a time period and $\psi_{osc}$ refers to the modulating part of the quantity. For statiscally steady flows, $\psi_{osc} = 0$.

$$\overline{\psi} = \frac{\sum_{n=1}^{M}\langle\psi\rangle}{M} \tag{2.3}$$

M is the number of phases over which images are captured within one oscillation. In the present experiments M=4 which is a small number, making the time averaged parameter susceptible to errors.

Hence, time averaging has been avoided in the present report.

Images were intended to be captured at the 4 phase points ( the two mean positions, the crest and the trough) as shown in Fig.2.6a. However, there was a delay of 0.2s in the trigger mechanism and the images are obtained at points shown in Fig. 2.6b. The bulk velocity measured using PIV images at these specific phases had a standard deviation of 0.004 m/s, 0.007 m/s, 0.005 m/s and 0.004 m/s which is 0.5%, 0.9%, 0.8% and 0.7% respectively of the average bulk velocity of all the vector fields at that particular phase, indicating that the same phase points were captured in every oscillation.

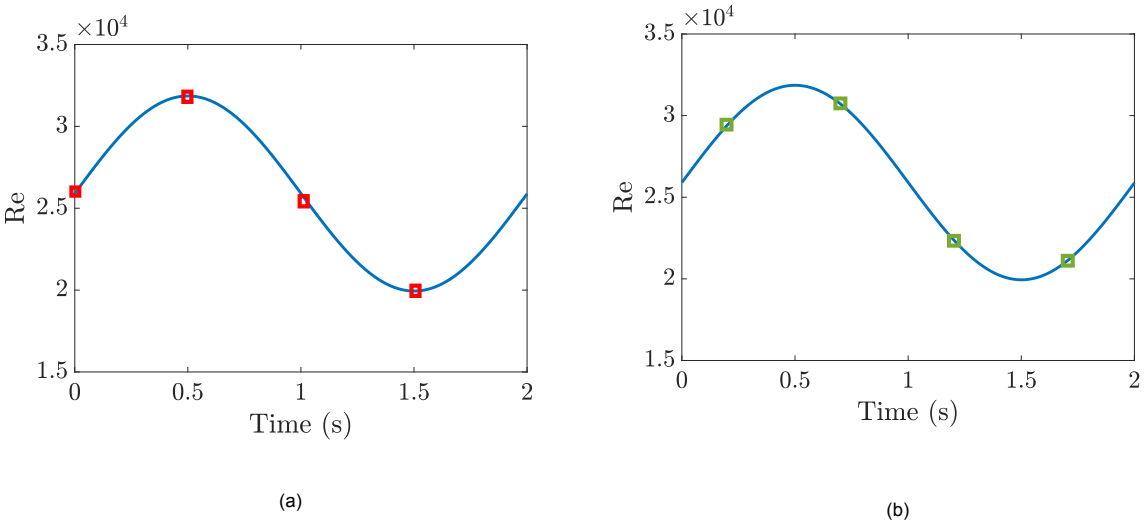


Figure 2.6: In **Figure (a)** Points at which images were planned to be captured at for $f_{osc}$ = 0.5 Hz (marked in red, Re # - 26,000 (mean); 31,860 (crest) & 19,970 (trough)). In **Figure (b)** Points at which images were obtained for $f_{osc}$ = 0.5 Hz (marked in green, Re # - 29,649; 31,000; 22,510 & 21,165.)

The commercial software Davis 8.4.0 generates the vector fields in Cartesian coordinates (X,Y) and as the polar coordinates is a natural choice for pipe geometry, the data was linearly interpolated into Polar coordinates (r, $\theta$) using MATLAB. All axial gradient terms in the energy budget equations [for instance, $\langle(\frac{\partial \cdot}{\partial z})^2\rangle$], have been obtained using Taylor's hypothesis of frozen turbulence, $\langle(\frac{\partial \cdot}{\partial z})^2\rangle = \langle(-\frac{\partial \cdot}{U_c \partial t})^2\rangle$. To facilitate this, 5 vector fields were obtained around a specific point in a phase with a sampling rate of 859 Hz. The local phase averaged axial velocity $\langle u_z \rangle$ has been used as the convective velocity $U_c$. Though the flow is statistically unsteady it is assumed that the changes to the turbulence parameters within such a small time interval ($\frac{1}{859}$ s=$10^{-3}$ s) will be negligible and the turbulence will thus be 'frozen'. A smoothing spline was applied to data to calculate derivatives.

A 3-D Gaussian smoothing kernel with standard deviation of 1.1 and a kernel size of 3x3x3 is used for filtering the data at 3 images using the 5 images collected at a phase point. All gradients are calculated using the central difference scheme of finite differences.

### 2.2.2. Time series data

In order to capture the low speed streaks, time series data was captured with a sampling rate of 859 Hz. 10 sets of 1799 images were recorded for 2.04 seconds each, which would encompass the entire oscillation. As the bulk flow rate changes over the oscillation cycle, the average displacement of the seeding particles in the cross-section, changes with time in the same recording. The time interval between the laser pulses was chosen such that, when the bulk flow rate was high, the displacement was small enough to avoid loss of particles in the interrogation window and when the the bulk flow was low, the displacements would be large enough to produce good correlation peaks. This would not be possible in pulsatile flows with large amplitudes of oscillations, but it was a sufficient remedy in the present case.

## 2.3. Data Validation

The data from steady flow measurements are compared with the data measured by Toonder and Nieuwstadt[26] in order to check the quality of the present measurements.

The following parameters are used - y, the distance from the wall; $u_\tau$, the friction velocity ; $u^+(=\frac{u}{u_\tau})$, the dimensionless velocity; $y^+(=\frac{yu_\tau}{\nu})$, the distance from the wall made dimensionless by inner parameters and $r$,the distance from the center.

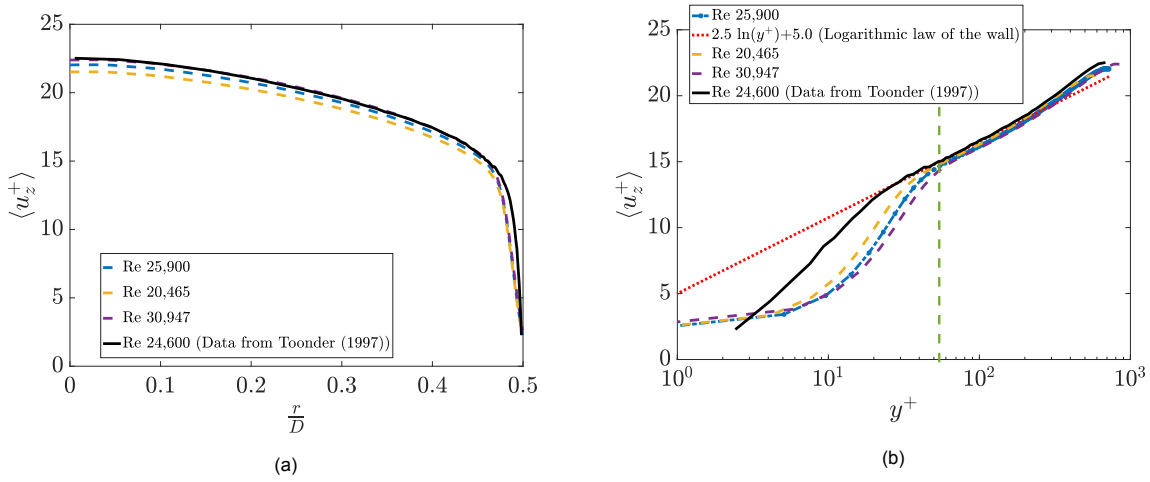


Figure 2.7: **Figure (a)** Average axial velocity scaled on outer variables. **Figure (b)** Average axial velocity scaled on inner variables, showing a detailed view of the log-layer

The mean velocity profile is lower than that measured by Toonder and Nieuwstadt[26] by 2.1% at the center and 1.6% at r=0.42D ($y^+ = 104$).

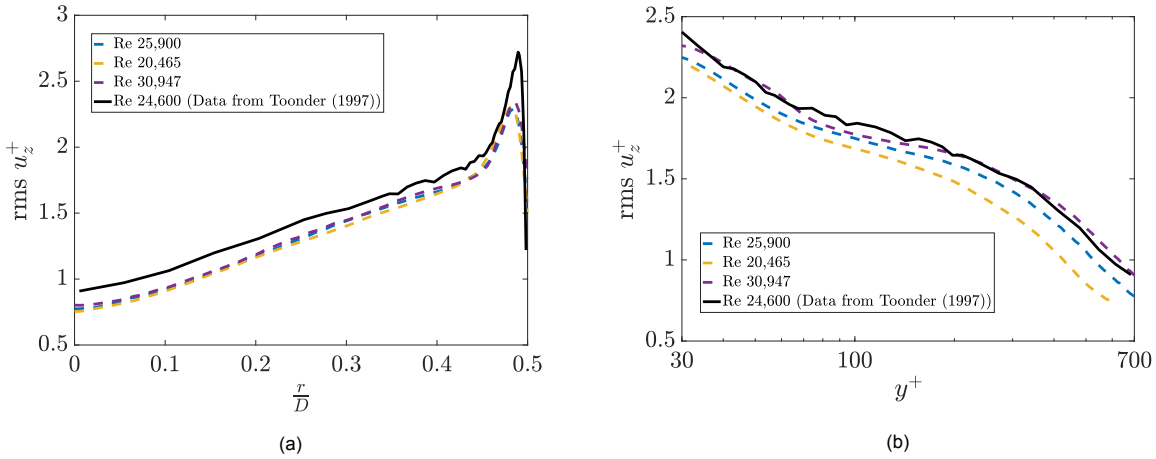


(a) (b)

Figure 2.8: **Figure (a)** RMS profile of the axial velocity profile scaled on outer variables. **Figure (b)** RMS profile of the axial velocity scaled on inner variables

The RMS profiles have a higher error, the RMS profile of the axial velocity is lower by 14.36% close to the centre and the error reduces to 6.2% at r=0.42D.

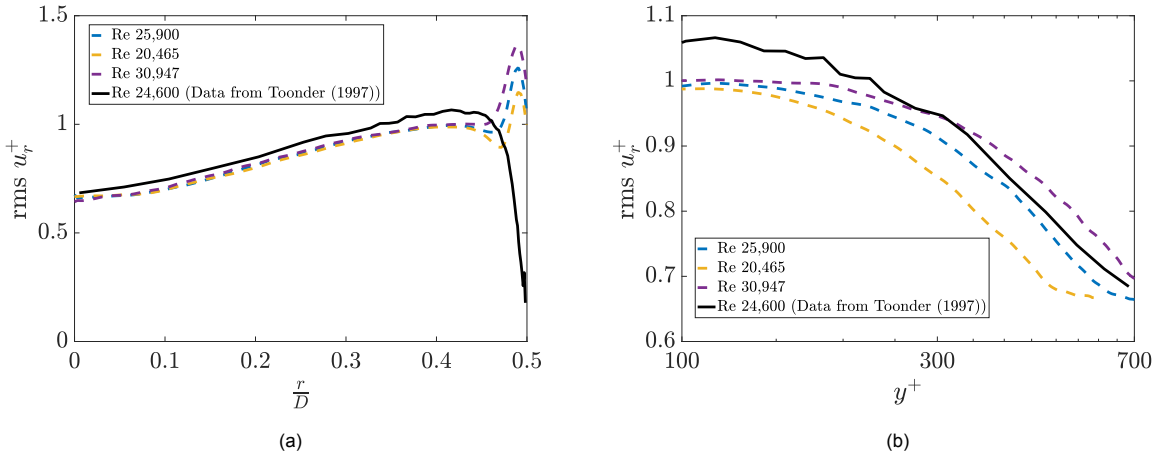


(a) (b)

Figure 2.9: **Figure (a)** RMS profile of the radial velocity scaled on outer variables. **Figure (b)** RMS profile of the radial velocity profile scaled on inner variables

The RMS profile of the radial velocity has a lower error (3.2%) close to the centre and the error increases to 6.1% at r=0.42D.

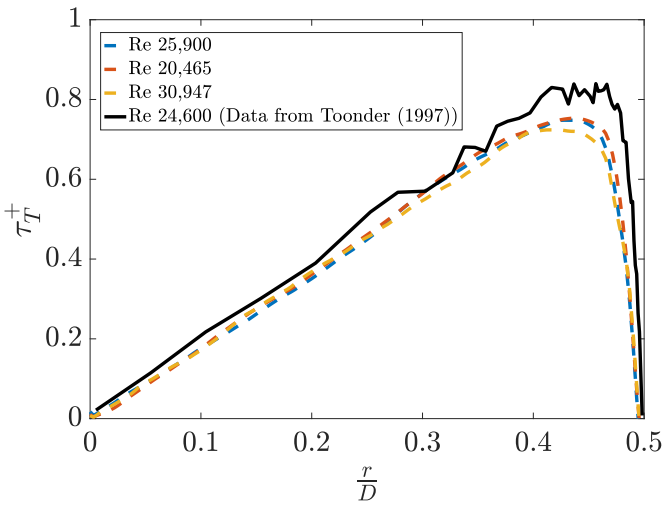


Figure 2.10: Reynolds shear stress scaled on outer variables

The Reynolds stress profile is close to that measured by Toonder and Nieuwstadt[26] towards the centre but the error increases to 9.4% at r=0.42D. It is noticeable that although there is a negative offset in the acquired data sets with respect to the reference data but the trend of the former matches the latter. Moreover, PIV accuracy near the wall has long being an issue and the measurements near the wall are not reliable due to various causes like distortion due to the pipe, reflection of laser light from the pipe, strong velocity gradients, etc.

To further assess the measurement quality a histogram of the divergence error and a scatter plot of -$(\frac{\partial u_z}{\partial z}).\Delta t$ versus $(\frac{\partial u_r}{\partial r}+\frac{\partial u_\theta}{r\partial \theta}+\frac{u_r}{r}).\Delta t$ is shown in Fig 2.11. A gaussian distribution fitting the histogram has a standard deviation of 0.015. The ellipse describing the scatter plot has an aspect ratio of $\frac{1}{2.814}$. The scatter plot should be elongated along the line representing the divergence free condition ($(\nabla.\overline{u}) = 0$). However it is seen that the axial gradients are underestimated. Increasing the strength of the filter did not improve the scatter plot significantly (See Appendix 3) and in order to preserve the small scale motions needed to quantify the rate of dissipation, the present filter strength is chosen.

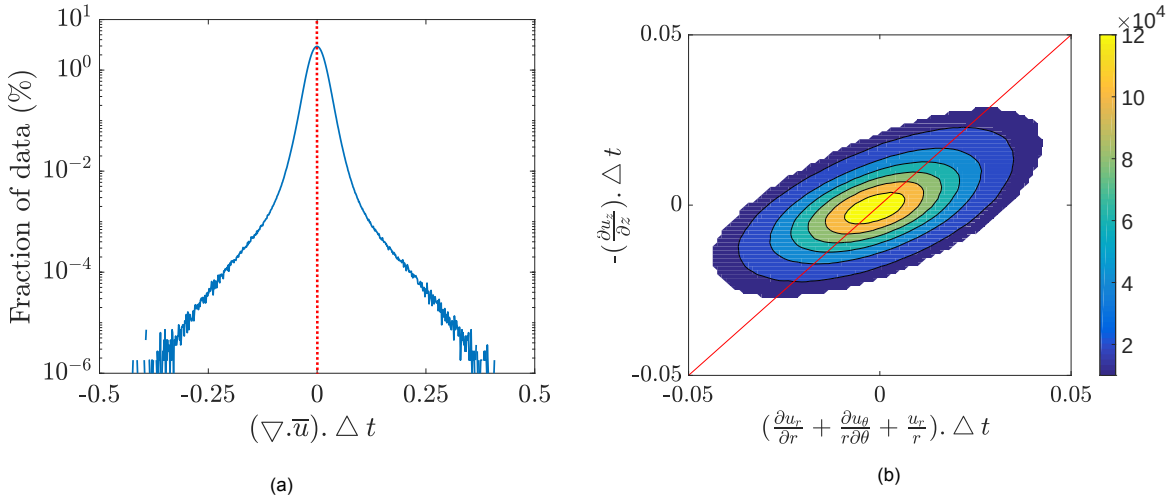


Figure 2.11: **Figure (a)** Histogram of divergence error. **Figure (b)** Scatter plot of -($\frac{\partial u_z}{\partial z}$). $\triangle t$ vs ($\frac{\partial u_r}{\partial r}+\frac{\partial u_\theta}{r\partial\theta}+\frac{u_r}{r}$). $\triangle t$ for 1000 images. Red lines represents the divergence free ($(\nabla.\overline{u})=0$) condition.

It is conjectured that the quantities might be underestimated as the laser sheet thickness was higher than the optimum, leading to a loss of resolution. This could not be checked and the experiment could not be repeated due to high demand of the experimental setup for other running projects in the lab.

# 3

# Results (Phase averaged)

In this chapter, the effects of oscillation on the statistical properties of the flow are discussed. The effects of oscillation on the phase averaged velocity profile, the turbulence parameters like Eddy viscosity, Reynolds stress, Turbulent kinetic energy, the terms of the Navier-Stokes Equation and the Turbulent Kinetic Energy Budget equation are discussed. As energy in turbulent flows is transferred from the mean velocity field to the turbulent velocity field and the turbulent flow field is responsible for the transport of momentum which ultimately influences the mean flow field, it is relevant to investigate the effects of oscillation on this interaction between the mean flow field and turbulent flow field. In the figures shown in this chapter the distance from the center '$r$' is non-dimensionalized with the radius R=0.02m and time '$t$' is non-dimensionalized with with the time period of oscillation, $T_{osc}$=2s.

## 3.1. Phase averaged velocity profile

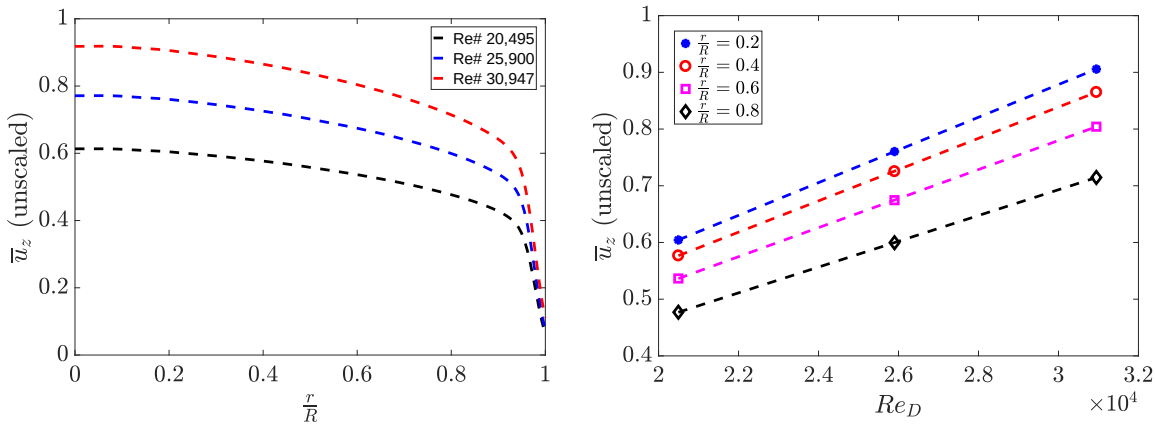


(a) Steady flow measurements. Here and in all following figures, R is the radius of the pipe and r is the distance from the centre.

(b) Linear dependency of velocity on bulk Re #. Dashed lines represent fitted curve and marked points represent the actual data measured

Figure 3.1: Curve fitting to obtain steady flow profiles

In order to analyze the effects of oscillation on averaged axial velocity profiles, the phase averaged axial velocity profiles are compared with the mean axial velocity profiles of the corresponding steady flow. The data for steady flows were acquired at bulk flow $Re_D$ 25,900, 30,947 and 20,465. These were the Reynolds numbers at which the data for the unsteady flow was planned to be acquired. However, as the trigger was delayed, steady velocity profiles at $Re_D$ 29,649, 31,000, 22,510 and 21,165 were required for comparison.

The velocity profiles for $Re_D$ 25,900, 30,947 and 20,465 are shown in Fig 3.1a. It is seen that the mean velocity at a radial point is linearly dependent of the on bulk flow $Re_D$ (Fig 3.1b). This trend may be justified using the power law velocity profiles of turbulent flows. It is given as,

$$u = U_{max}(1 - \frac{r}{R})^{\frac{1}{n}} \tag{3.1}$$

Here, n is an exponent that depends on the $Re_D$, $U_{max}$ depends on the bulk velocity ($U_b$) as follows,

$$U_{max} = U_b(\frac{2n^2 + 3n + 1}{2n^2}) \tag{3.2}$$

The exponent n changes negligibly with changing $Re_D$ and in most cases n=7 gives an accurate representation of the velocity profile [27]. It is seen that the velocity at a particular radial location is a linear function of the bulk velocity and hence a linear function of the $Re_D$ (at constant temperature). This trend may exist only for a small range of $Re_D$ (where n is constant), however, for the present study it is sufficient to perform a curve fitting with a linear polynomial to obtain the local mean velocity at each radial point for the $Re_D$ required. The velocity profiles generated using this method follow the 'log law'. ( Fig 3.2 and Fig 3.3). Moreover, as the data measured is offset to a certain extent, in order to remove bias, the phase averaged velocity profiles of the unsteady flows are compared with the profiles obtained by interpolation rather than that obtained by using the power law.

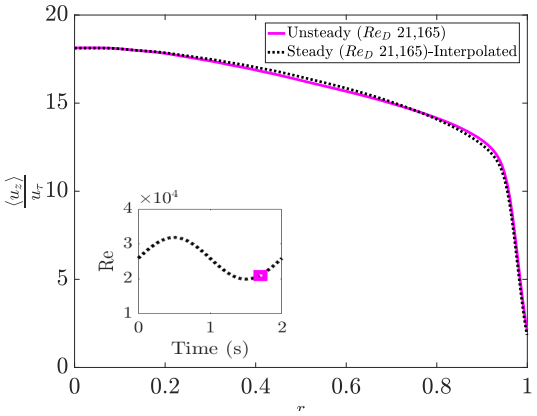


(a) Mean velocity profile when the bulk flow rate starts to accelerate (Inset image shows phase point at which velocity profile is measured).

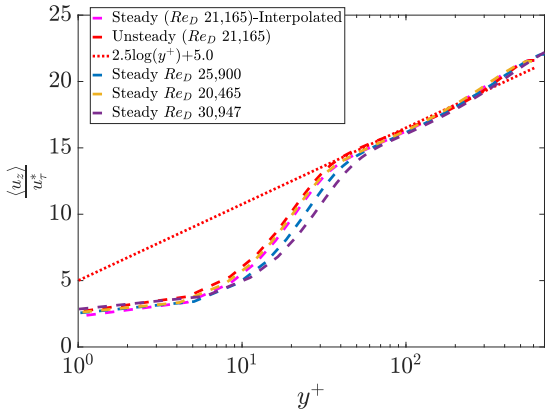


(b) Logarithmic velocity profile at the start of acceleration.

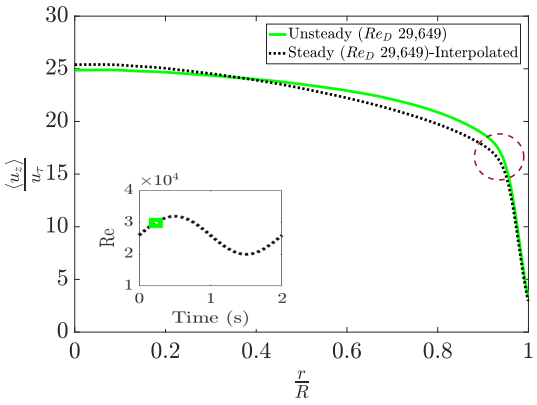


(c) Mean velocity profile towards the end of acceleration of the bulk flow.Circle represents the region with $\frac{\partial \langle u_z \rangle}{\partial r}$ higher than steady flow.

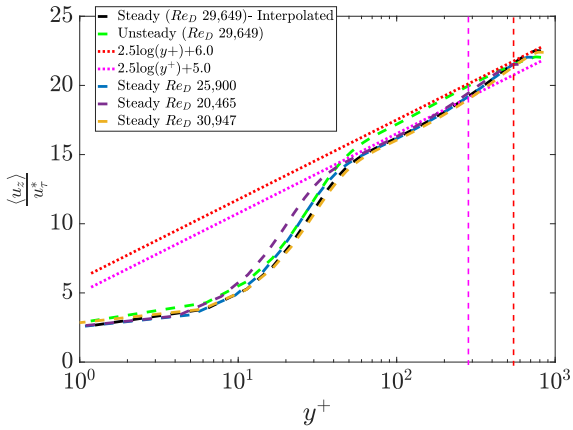


(d) Logarithmic velocity profile at the end of acceleration (Vertical lines represent the extent of the log layer for the different profiles).

Figure 3.2: Comparison of phase averaged velocity profile with steady velocity profiles during acceleration.

In Fig 3.2 and Fig 3.3 the profiles of the unsteady flow at different phases are compared with the corresponding steady flow velocity profiles. In these figures and in all following figures of this chapter, in order to non-dimensionalize the statistical quantities, the frictional velocity of the steady flow of the mean $Re_D$ 26,000 ($u_\tau$) is used. In order to compare the logarithmic velocity profile the mean flow is non-dimensionalized using the frictional velocity of the steady flow of the instantaneous $Re_D$ ($u_\tau^*$).

It is seen that in the beginning of acceleration the velocity gradient ($\frac{\partial \langle u_z \rangle}{\partial r}$) in the unsteady flow is similar to that of the corresponding steady flow and the logarithmic velocity profiles are similar.

However, at the end of acceleration the velocity gradient of the unsteady flow in the region $r < 0.85R$ is lower than that of the corresponding steady flow with the same $Re_D$, but it is higher near the wall **(denoted by in circle in Fig 3.2c)**.The log velocity profile for the unsteady flow is displaced 'upwards' and the extent of the 'log layer' is increased (as shown by the vertical lines in Fig 3.2d).

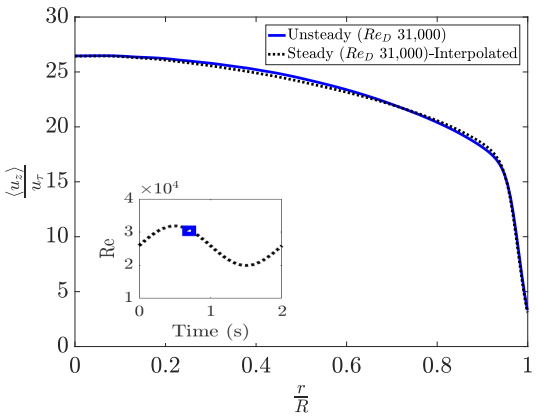


(a) Mean velocity profile when the bulk flow rate starts to deceleration

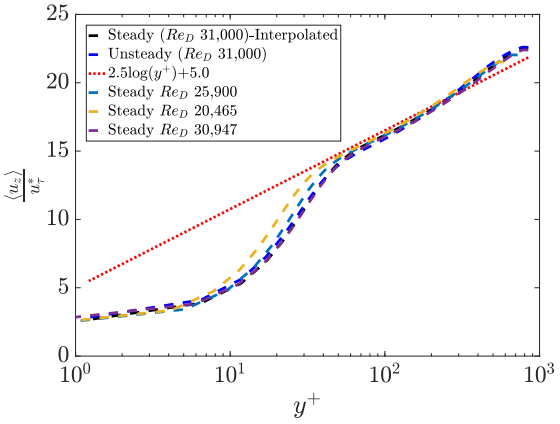


(b) Logarithmic velocity profile at the start of deceleration

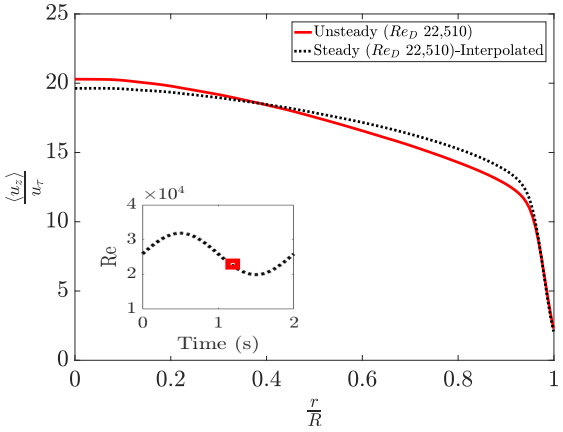


(c) Mean velocity profile towards the end of deceleration of the bulk flow. Velocity gradient in the unsteady flow is higher than that of the corresponding steady flow in the wake region.

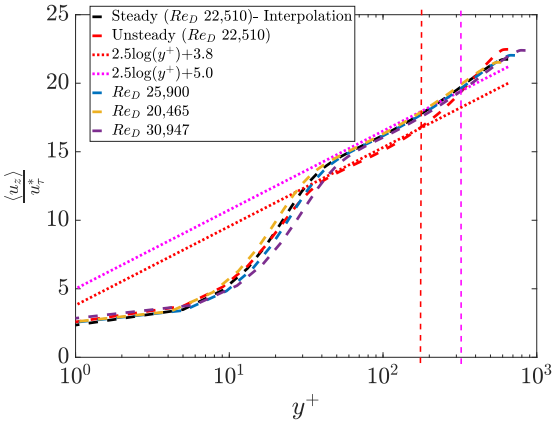


(d) Logarithmic velocity profile at the end of deceleration.(Vertical lines represent the extent of the log layer for the different profiles)

Figure 3.3: Comparison of phase averaged velocity profile with steady velocity profiles during deceleration.

As the bulk flow rate starts to decrease, the fluid in the central region of the pipe retains a higher momentum than that in the central region of the corresponding steady flow. Towards the end of deceleration, the velocity gradient is higher than that of the corresponding steady flow throughout $r < 0.85R$ (Fig 3.3c) but lower towards the wall. The logarithmic velocity profile for the unsteady flow is lowered and the extent of the 'log layer' is decreased (Fig 3.3d).

As energy in turbulent flow is transferred from the mean flow field, in quasi-steady pulsatile flows the turbulence characteristics in an oscillation are the same as that of the steady flow with the same Reynolds number. However, as the rate of change of velocity is increased, the difference in the mean velocity gradient between pulsatile and the steady flows is responsible for the difference in turbulence characteristics created.

## 3.2. Effect of oscillation on phase averaged parameters

The phase averaged turbulence parameters can be described as a Fourier series of the form:

$$\langle \psi \rangle = \overline{\psi} + \sum_{n=1}^{\infty} A_n sin(n\omega t + \phi) \tag{3.3}$$

Here, $A_n$ is the amplitude of the $n^{th}$ node. It has been mentioned in previous literature ([15], [16], [19]) that the parameters can be described by using the fundamental mode of frequency, as the higher modes are comparatively very small. This has been used in the present project to examine the behaviour of the parameters during one period of oscillation.

## 3.3. Effect of oscillation on Wall shear stress

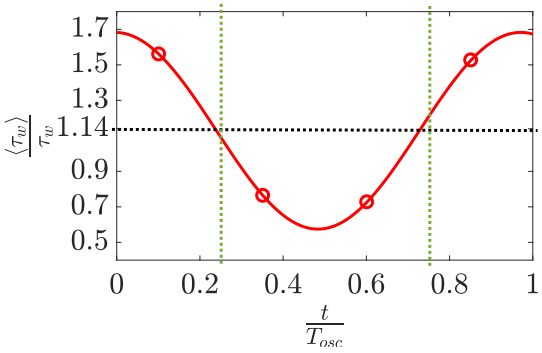


Figure 3.4: $\frac{\langle \tau_w \rangle}{\tau_w}$ is the phase averaged wall shear stress scaled by the wall shear stress of the steady flow. Bulk flow is decelerating between the two vertical lines. Here and in all following figures $t$ is time and $T_{osc} = 2$s is the time period of oscillation. Marked points represent actual data measured and the solid line represents the fitted sine wave.

The phase averaged wall shear stress is calculated indirectly using the integral momentum balance equation 2.1. It reaches its lowest value at the $t = 0.48T_{osc}$ and highest value at $t = 0.97T_{osc}$. The time averaged wall shear stress as well as the pressure drop is obtained to be 1.14 times that of the steady flow.

## 3.4. Effect of oscillation on the terms of the Navier Stokes Equation

The Reynolds Averaged Navier Stokes (RANS) equation for the phase averaged axial velocity for pipe flow is given as,

$$\frac{\partial \langle u_z \rangle}{\partial t} = -\frac{1}{\rho}\frac{\partial \langle p \rangle}{\partial z} + \upsilon\left(\frac{1}{r}\frac{\partial}{\partial r}\left(r\frac{\partial \langle u_z \rangle}{\partial r}\right)\right) - \frac{1}{r}\frac{\partial r\langle u_z' u_r' \rangle}{\partial r} \tag{3.4}$$

**Calculating the unsteady term ($\frac{\partial \langle u_z \rangle}{\partial t}$)**

The phase averaged axial velocity displays sinusoidal behaviour with time at different radial points (Fig 3.4). The time derivative of this sinusoidal curve provides the term $\frac{\partial \langle u_z \rangle}{\partial t}$. This term can also be measured by applying the central difference technique to the vector fields captured at a high sampling rate around a phase point. However, as the term $\langle u_z \rangle$ is calculated from the statistical averaging of

data from a finite sample size there might be a scattering of the value calculated around the'true' mean value, leading to a noisy derivative being calculated.(Fig 3.4). Thus, for further analysis the derivative obtained by taking a derivative of the fitted curve is utilized.

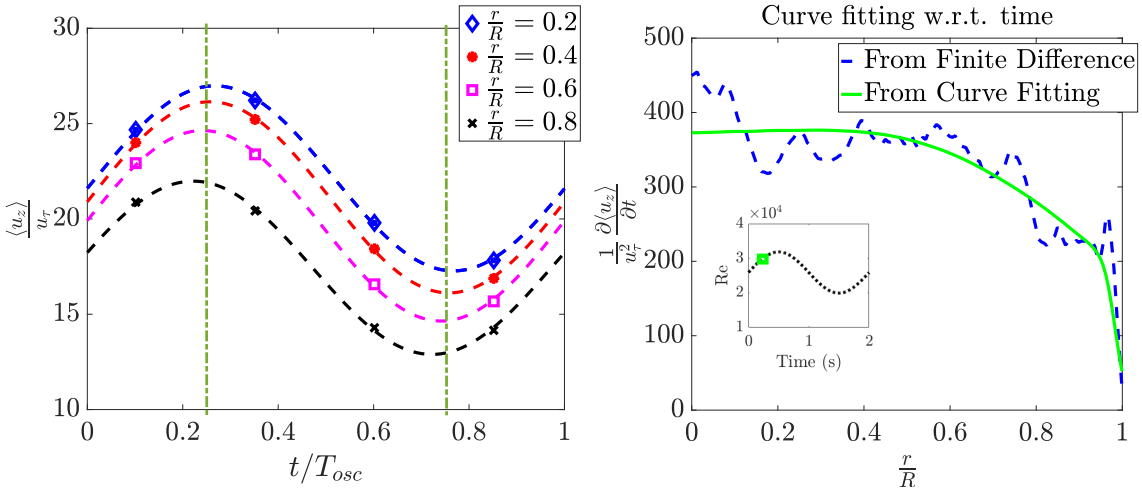


The terms of the RANS equation at different radial points are shown in Fig.3.5. A phase shift is observed in the terms- $\frac{1}{r}\frac{\partial r\langle -u_z' u_r' \rangle}{\partial r}$ and $\frac{\partial \langle u_z \rangle}{\partial t}$ at different radial locations. The term $\upsilon(\frac{1}{r}\frac{\partial}{\partial r}(r\frac{\partial \langle u_z \rangle}{\partial r}))$ is negligible on being compared to the other terms.

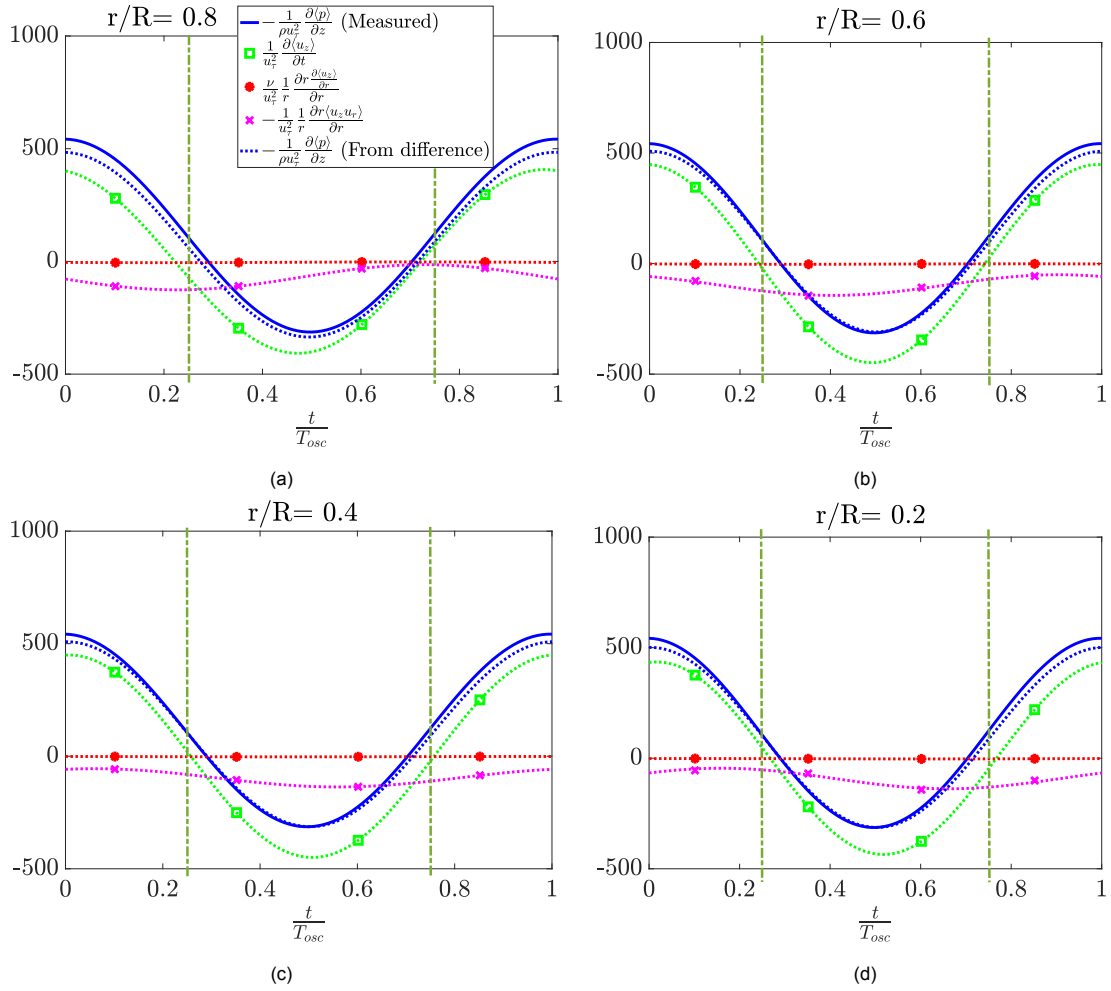


Figure 3.5: Comparison of terms of the NS equation at different phase points. Bulk flow is decelerating between vertical lines. The marked points represents the measured data and the dashed line represents a curve fitted using the fundamental mode of oscillation. The pressure gradient has been calculated by applying the fitted curves to the NS equation and directly measured by the pressure transducer as well. The phase of the measured pressure gradient has been **shifted** to match the pressure gradient calculated from the NS equation. The shift is the same in all the radial points and the shifted pressure gradient agrees well with the calculated pressure gradient in all radial positions. The phase shift can be justified in that there there might be a lag in the data captured by the pressure transducer.

During deceleration of the bulk flow, in the region r=0.2R the term $-\frac{1}{r}\frac{\partial r\langle u_z' u_r'\rangle}{\partial r}$, which represents the retarding force per unit volume produced by the Reynolds stress, has a lower magnitude towards the onset of deceleration and increases as the bulk flow continues to decelerate. In the region around r=0.8R the term shows the opposite behaviour, resulting in a delay in the response of the fluid near the centre to the adverse pressure gradient during deceleration.

This delay deforms the mean velocity profile such that during deceleration, the term $\frac{\partial\langle u_z\rangle}{\partial r}$ in the wake region of the pipe is higher than the that of the corresponding steady flow at the same Reynolds number. Hence excess turbulence is generated in the wake region due to the excess shear created by deceleration.

During the onset of acceleration of the bulk flow, the term $-\frac{1}{r}\frac{\partial r\langle u_z' u_r'\rangle}{\partial r}$ has a higher magnitude at r=0.2R and as the bulk flowrate increases, the value of the term the decreases. Hence, velocity during the favourable pressure gradient is more uniform in the wake region leading to a lower value of $\frac{\partial\langle u_z\rangle}{\partial r}$. However, the 'no-slip' constraint on the wall surface leads to a higher vale of $\frac{\partial\langle u_z\rangle}{\partial r}$ in the region near the wall towards the end of acceleration (shown by circle in Fig. 3.2c). Mathematically, the term $\langle u_z' u_r'\rangle\frac{\partial\langle u_z\rangle}{\partial r}$ gives a measure of the transfer of mean kinetic energy of the flow to the turbulent kinetic energy.

### 3.4.1. Effect of oscillation on Eddy Viscosity

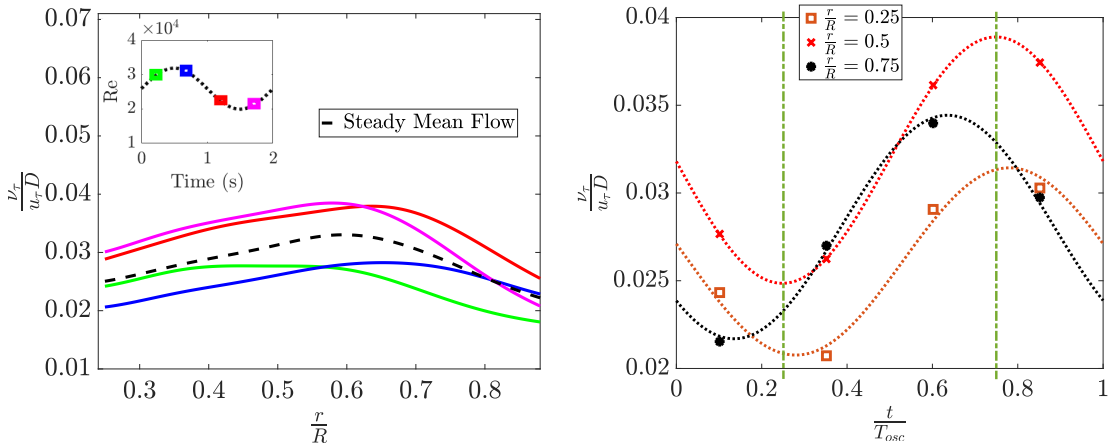


(a) Eddy viscosity profiles. Inset shows phase points (shown in same colour) at which eddy viscosity is measured.

(b) Change of eddy viscosity with time at different radial points. Bulk flow is decelerating between vertical lines.

Figure 3.6: Comparison of eddy viscosity profiles

Fig.3.6a shows the eddy viscosity ($\nu_\tau$) profiles at different phase points. It is seen that the eddy viscosity values change during an oscillation cycle indicating that standard eddy viscosity models will be unable to model pulsatile flows. Fig.3.6b shows that the eddy viscosity at different radial points can be represented as a sinusoidal function of time.

### 3.4.2. Effect of oscillation on the Reynolds stress

The phase averaged Reynolds stress terms are shown in Fig 3.7. As seen in fig 3.7b, the measured data at particular phase point can be fitted with a sinusoidal function of time. There is a delay in the response of the Reynolds stress to the oscillating flow rate. This is manifested as a phase difference in the fitted curve with respect to the oscillation of the flow rate. This delay or phase difference increases with increasing distance from the wall.

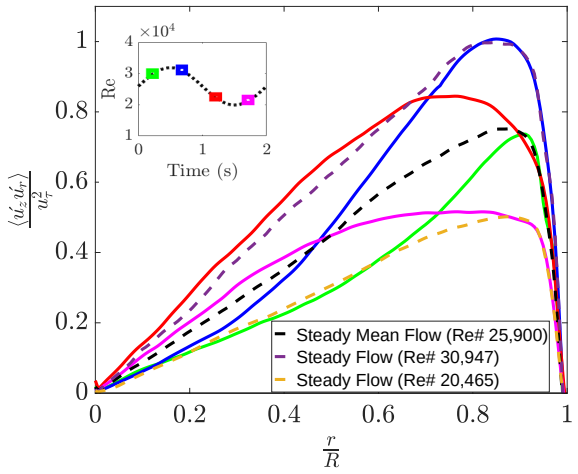


(a) Phase averaged Reynolds Stress profiles at different radial locations.Inset shows phase points (shown in same colour) at which values are measured.

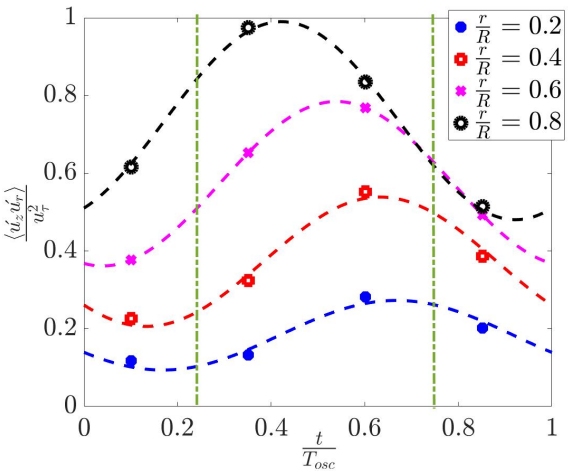


(b) Marked points represent points at which data is measured and dashed line represents the fitted curve.

Figure 3.7: Reynolds stress.

### 3.4.3. Effect of oscillation on the intensities of turbulence

The terms ($\langle u_z'^2 \rangle$ and $\langle u_r'^2 \rangle$), which represent twice the phase averaged axial and radial turbulence kinetic energies respectively are shown in Fig. 3.8. As seen in the Reynolds stress there is a delay in the response of the turbulence to the oscillation of the bulk flow rate, which is expressed as a phase lag in the fitted curve.This is in agreement with the results of Ramaprian and Tu[16], He and Jackson[5], Brereton,*et al.*[28].

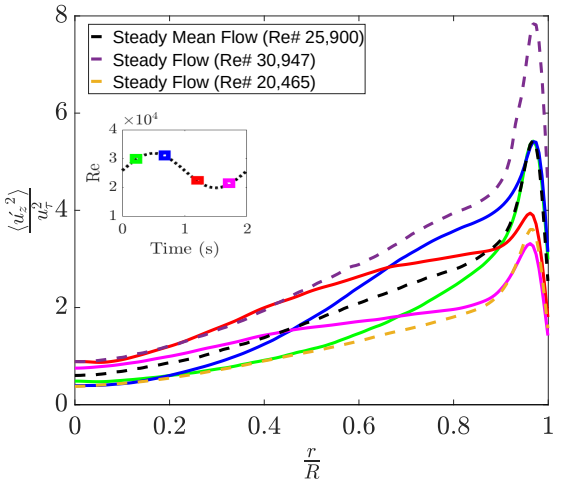


(a) Phase averaged axial Velocity turbulence intensity profiles. Inset shows phase points (shown in same colour) at which values measured.

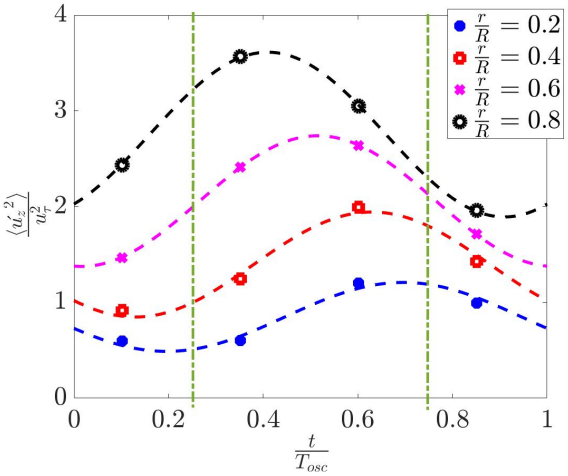


(b) Phase averaged axial turbulence intensity at different radial location.Bulk flow is decelerating between vertical lines.

Figure 3.8: Comparison of phase averaged turbulence intensity profiles

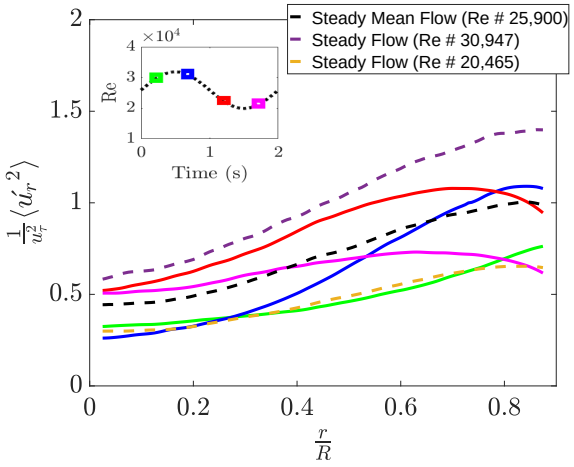


(a) Phase averaged radial Velocity turbulence intensity profiles. Inset shows phase points (shown in same colour) at which values measured.

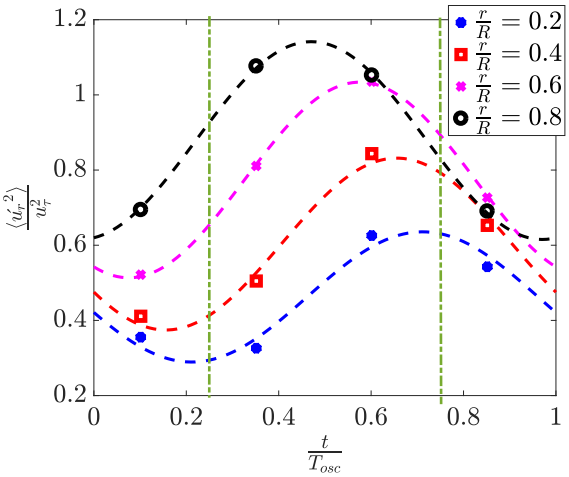


(b) Radial turbulence intensity at different radial location.Bulk flow is decelerating between vertical lines.

Figure 3.9: Turbulence at radial locations.

The axial ($\langle u_z'^2\rangle$) and in-plane turbulence ($\langle u_r'^2\rangle$ & $\langle u_\theta'^2\rangle$) display different responses to the oscillating flow rate. Towards the wall there is a greater difference between the delay in the response of the in-plane turbulence and the axial turbulence and the difference decreases towards the centre. (See Fig 3.13a). The radial and azimuthal turbulence did not display any phase difference between them. This is in agreement with the results of He and Jackson[29]. The time derivative of the curves fitted to these terms are used to measure the unsteady terms of the turbulent kinetic energy budget equation used subsequently in this work.

## 3.5. Effect of oscillation on the terms of Turbulent Kinetic Energy Equation

The Turbulent Kinetic Energy (TKE) Equation for pipe flows are given as, (for complete derivation refer to Appendix 1)

In the axial direction,

$$\begin{aligned}&\frac{1}{2}\frac{\partial\langle u_z'^2\rangle}{\partial t}+\frac{1}{2}\frac{\partial\langle u_z'^2u_r'\rangle}{\partial r}+\langle u_z'u_r'\rangle\frac{\partial\langle u_z\rangle}{\partial r}+\frac{\langle u_z'^2u_r'\rangle}{2r}\\&=\langle\frac{\acute{p}}{\rho}\frac{\partial u_z'}{\partial z}\rangle+2\upsilon(\frac{\partial\langle ru_z's_{rz}'\rangle}{r\partial r}+\frac{\partial\langle u_z's_{z\theta}'\rangle}{r\partial\theta}+\frac{\partial\langle u_z's_{zz}'\rangle}{\partial z}\\&-\langle s_{rz}'\frac{\partial u_z'}{\partial r}\rangle-\langle s_{z\theta}'\frac{\partial u_z'}{r\partial\theta}\rangle-\langle s_{zz}'\frac{\partial u_z'}{\partial z}\rangle)\end{aligned}\tag{3.5}$$

In the azimuthal direction,

$$\begin{aligned}&\frac{1}{2}\frac{\partial\langle \acute{u_\theta}^2\rangle}{\partial t}+\frac{1}{2}\frac{\partial\langle \acute{u_\theta}^2\acute{u_r}\rangle}{\partial r}+\frac{\langle 3\acute{u_\theta}^2\acute{u_r}\rangle}{2r}\\&=\langle\frac{\acute{p}}{r\rho}\frac{\partial\acute{u_\theta}}{\partial\theta}\rangle+2\upsilon(\frac{\partial\langle r\acute{u_\theta}s'_{r\theta}\rangle}{r\partial r}+\frac{\partial\langle\acute{u_\theta}s'_{\theta\theta}\rangle}{r\partial\theta}+\frac{\partial\langle\acute{u_\theta}s'_{z\theta}\rangle}{\partial z}\\&-\langle s'_{r\theta}\frac{\partial\acute{u_\theta}}{\partial r}\rangle-\langle s'_{\theta\theta}\frac{\partial\acute{u_\theta}}{r\partial\theta}\rangle-\langle s'_{z\theta}\frac{\partial\acute{u_\theta}}{\partial z}\rangle+\langle\frac{\acute{u_\theta}s'_{r\theta}}{r}\rangle)\end{aligned}\tag{3.6}$$

In the radial direction,

$$\begin{aligned}&\frac{1}{2}\frac{\partial\langle \acute{u_r}^2\rangle}{\partial t}+\frac{1}{2}\frac{\partial\langle \acute{u_r}^3\rangle}{\partial r}+\frac{\langle \acute{u_r}^3\rangle}{2r}-\frac{\langle \acute{u_\theta}^2\acute{u_r}\rangle}{r}\\&=\langle\frac{\acute{p}}{\rho}\frac{\partial\acute{u_r}}{\partial r}\rangle-\frac{1}{\rho}\frac{\partial\langle\acute{u_r}\acute{p}\rangle}{\partial r}+2\upsilon(\frac{\partial\langle r\acute{u_r}s'_{rr}\rangle}{r\partial r}+\frac{\partial\langle\acute{u_r}s'_{r\theta}\rangle}{r\partial\theta}+\frac{\partial\langle\acute{u_r}s'_{rz}\rangle}{\partial z}\\&-\langle s'_{rr}\frac{\partial\acute{u_r}}{\partial r}\rangle-\langle s'_{r\theta}\frac{\partial\acute{u_r}}{r\partial\theta}\rangle-\langle s'_{rz}\frac{\partial\acute{u_r}}{\partial z}\rangle-\langle\frac{\acute{u_r}s'_{\theta\theta}}{r}\rangle)\end{aligned}\tag{3.7}$$

The TKE is given as,

$$\begin{aligned}&\frac{\partial\langle q\rangle}{\partial t}=-\langle\frac{1}{r}\frac{\partial r\acute{u_r}(\frac{\acute{p}}{\rho}+q)}{\partial r}\rangle-\langle\acute{u_z}\acute{u_r}\rangle\frac{\partial\langle u_z\rangle}{\partial r}\\&+2\upsilon(\frac{\partial\langle r\acute{u_z}s'_{rz}\rangle}{r\partial r}+\frac{\partial\langle\acute{u_z}s'_{z\theta}\rangle}{r\partial\theta}+\frac{\partial\langle\acute{u_z}s'_{zz}\rangle}{\partial z}\\&\frac{\partial\langle r\acute{u_\theta}s'_{r\theta}\rangle}{r\partial r}+\frac{\partial\langle\acute{u_\theta}s'_{\theta\theta}\rangle}{r\partial\theta}+\frac{\partial\langle\acute{u_\theta}s'_{z\theta}\rangle}{\partial z}\\&\frac{\partial\langle r\acute{u_r}s'_{rr}\rangle}{r\partial r}+\frac{\partial\langle\acute{u_r}s'_{r\theta}\rangle}{r\partial\theta}+\frac{\partial\langle\acute{u_r}s'_{rz}\rangle}{\partial z}\\&-\langle s'_{rz}\frac{\partial\acute{u_z}}{\partial r}\rangle-\langle s'_{z\theta}\frac{\partial\acute{u_z}}{r\partial\theta}\rangle-\langle s'_{zz}\frac{\partial\acute{u_z}}{\partial z}\rangle\\&-\langle s'_{r\theta}\frac{\partial\acute{u_\theta}}{\partial r}\rangle-\langle s'_{\theta\theta}\frac{\partial\acute{u_\theta}}{r\partial\theta}\rangle-\langle s'_{z\theta}\frac{\partial\acute{u_\theta}}{\partial z}\rangle+\langle\frac{\acute{u_\theta}s'_{r\theta}}{r}\rangle\\&-\langle s'_{rr}\frac{\partial\acute{u_r}}{\partial r}\rangle-\langle s'_{r\theta}\frac{\partial\acute{u_r}}{r\partial\theta}\rangle-\langle s'_{rz}\frac{\partial\acute{u_r}}{\partial z}\rangle-\langle\frac{\acute{u_r}s'_{\theta\theta}}{r}\rangle)\end{aligned}\tag{3.8}$$

The terms can be classified as-

**Unsteady term**-

$$\frac{\partial\langle q\rangle}{\partial t}\tag{3.9}$$

**Pressure Diffusion Term**-

$$-\langle\frac{1}{\rho r}\frac{\partial r\acute{u_r}\acute{p})}{\partial r}\rangle\tag{3.10}$$

**Production Term**-

$$-\langle\acute{u_z}\acute{u_r}\rangle\frac{\partial\langle u_z\rangle}{\partial r}\tag{3.11}$$

**Turbulent Diffusion Term**-

$$-\langle\frac{1}{\rho r}\frac{\partial(r\acute{u_r}q)}{\partial r}\rangle\tag{3.12}$$

**Viscous Diffusion Term-**

$$2\upsilon\left(\frac{\partial\langle r\acute{u}_z s'_{rz}\rangle}{r\partial r}+\frac{\partial\langle \acute{u}_z s'_{z\theta}\rangle}{r\partial\theta}+\frac{\partial\langle \acute{u}_z s'_{zz}\rangle}{\partial z}\right.$$
$$\frac{\partial\langle r\acute{u}_\theta s'_{r\theta}\rangle}{r\partial r}+\frac{\partial\langle \acute{u}_\theta s'_{\theta\theta}\rangle}{r\partial\theta}+\frac{\partial\langle \acute{u}_\theta s'_{z\theta}\rangle}{\partial z} \tag{3.13}$$
$$\left.\frac{\partial\langle r\acute{u}_r s'_{rr}\rangle}{r\partial r}+\frac{\partial\langle \acute{u}_r s'_{r\theta}\rangle}{r\partial\theta}+\frac{\partial\langle \acute{u}_r s'_{rz}\rangle}{\partial z}\right)$$

**Viscous Dissipation Term-**

$$-2\upsilon\langle s'_{ij}s'_{ij}\rangle \tag{3.14}$$

The viscous diffusion term is known to be negligible in the outer region of the pipe and has been omitted from the subsequent results.

The pressure diffusion term measured by using the other terms of the total kinetic energy equation and balancing them.

The pressure strain term in each components are measured by using the other terms of the kinetic energy equation in the respective components and balancing them.

### 3.5.1. Effect of oscillation on the Production Term

The phase averaged production term ($\langle u_z\acute{u}_r\rangle\frac{\partial\langle u_z\rangle}{\partial r}$) profiles and the curves fitted to the points measured at different phase points is shown Fig 3.10.

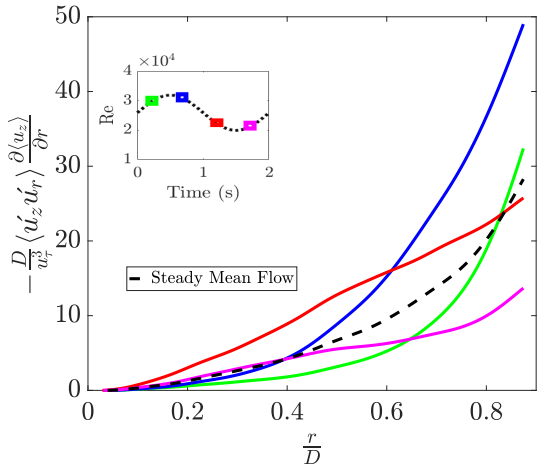


(a) Phase averaged production term at different phase points.Inset shows phase points (shown in same colour) at which values measured.

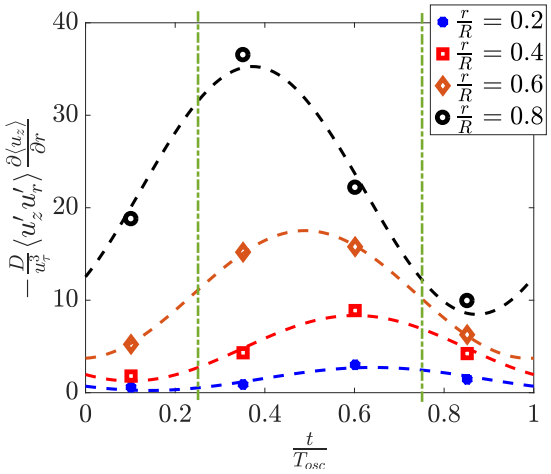


(b) Curves fitted to production terms measured at phase points.Bulk flow is decelerating between vertical lines.

Figure 3.10: Production term

### 3.5.2. Measuring the rate of dissipation

The dissipation rate is measured using the large eddy approach [30]. This is done to measure dissipation in the sub-grid scales as the resolution of the data is not enough to measure the true dissipation

using the velocity gradients in the small scales. The Smagorinsky model is used with the value of the Smagorinsky constant as 0.17. The value of this constant is expected to change at different filter lengths and finite difference schemes [31]. However, the consequences of the change of the constant on the dissipation rates measured are assumed to be too small to cause any change in the interpretation of results.

Fig 3.11a shows the measured dissipation rate of the steady mean flow along with the dissipation after adding the contribution of the sub-grid scales. The Production term is also shown for comparison.Fig 3.11b shows the convergence of the dissipation term. The dissipation rate obtained is qualitatively similar to that obtained by Laufer[32] and Lawn[33] (See Appendix 3). The average dissipation rate for the mean steady flow ($\epsilon = \frac{\Delta P U_z}{\rho L}$) is 0.0771 $m^2/s^3$. The resolved dissipation rate averaged over the cross-section from r=0.02R to r=0.86R (y+=100) is 0.0033 $m^2/s^3$ and after adding the dissipation rate in the sub-grid scale, it is 0.0079 $m^2/s^3$. The inconsistency with the theoretical dissipation rate arises from the fact that the dissipation rate close to the wall has not been taken into account.

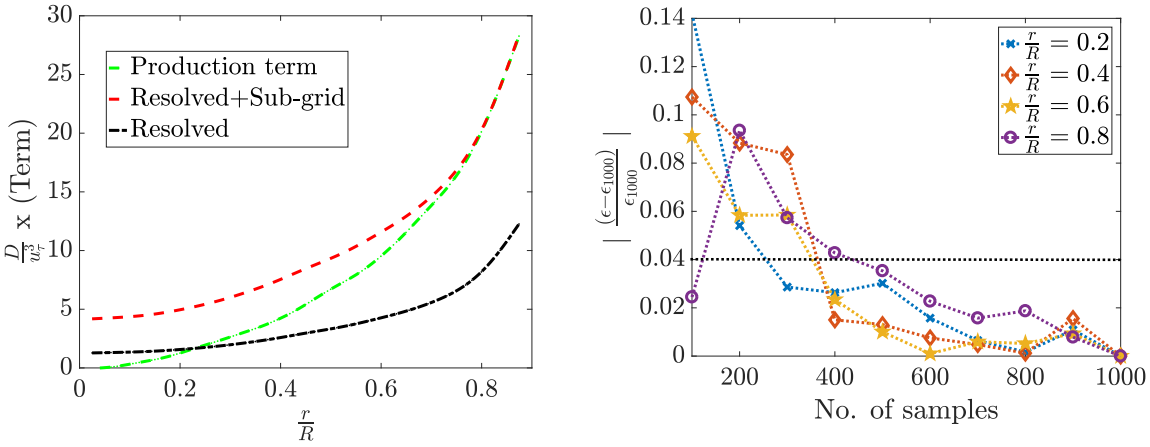


(a) Resolved dissipation rates and the dissipation rates obtained by large eddy PIV method

(b) Convergence of dissipation rates measured at various radial locations

Figure 3.11: Measuring the rate of dissipation

### 3.5.3. Effect of oscillations on the rate of dissipation

Fig 3.12a shows the dissipation at different points of the oscillation. The curves fitted to the measured point is also shown in Fig 3.12.

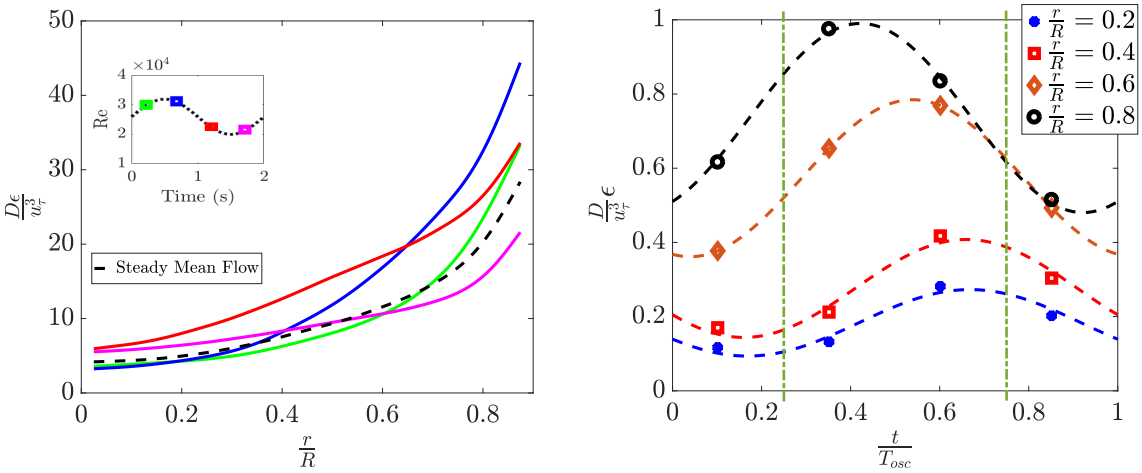


(a) Phase averaged dissipation rates at different phases. Inset shows phase points (shown in same colour) at which values measured.

(b) Curves fitted to dissipation rates measured.Bulk flow is decelerating between vertical lines.

Figure 3.12: Dissipation term

The phase difference in the response of the dissipation rates to the production rates at different locations are the same (See Fig. 3.13b). This implies that the difference between the time lag in the response of the large scales and the small scales at the present rate of oscillations are negligibly small. A difference is noticed at r=0.2R , however as towards the centre of the pipe the amplitude of the sinusoidal function is small, a small scatter of data around the true phase average may increase the error of the phase lag. Thus, data at more data points are required to reach a definitive conclusion. There is a difference in the response of the in-plane and axial dissipation rates (Fig. 3.14).

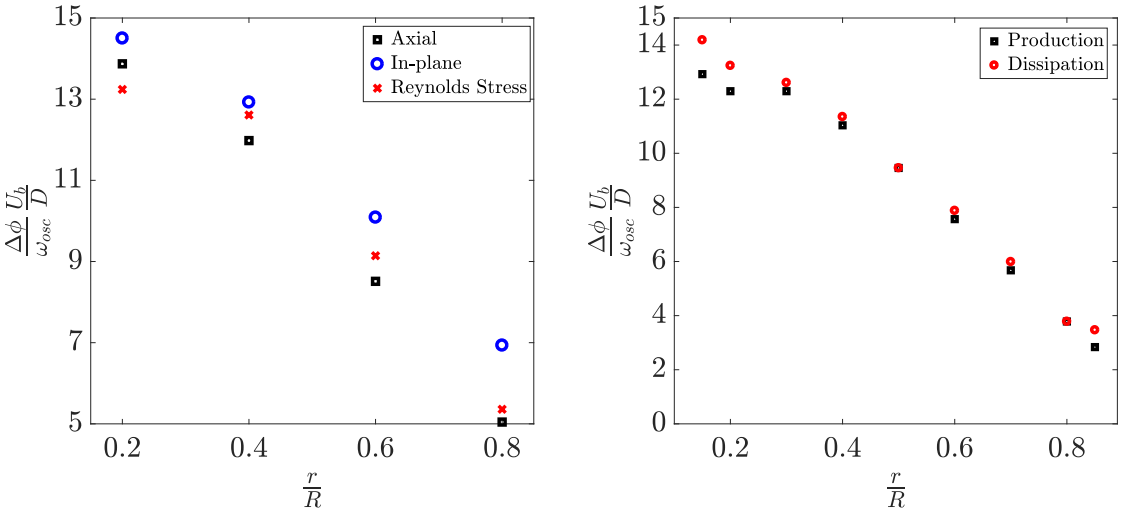


(a) Comparison in the delay of the response of axial turbulence intensity ($\langle \acute{u_z}^2 \rangle$) and in-plane turbulence intensities ($\langle \acute{u_r}^2 \rangle$ & $\langle \acute{u_\theta}^2 \rangle$).

(b) Comparison of the phase delay of the prodution term and dissipation terms in response to the imposed oscillations.

Figure 3.13: Delay in the response of different turbulence parameters.$\Delta\Phi$ denotes the phase lag with bulk flow oscillation. The time lag is scaled with $\frac{D}{U_b} = 0.0634s$

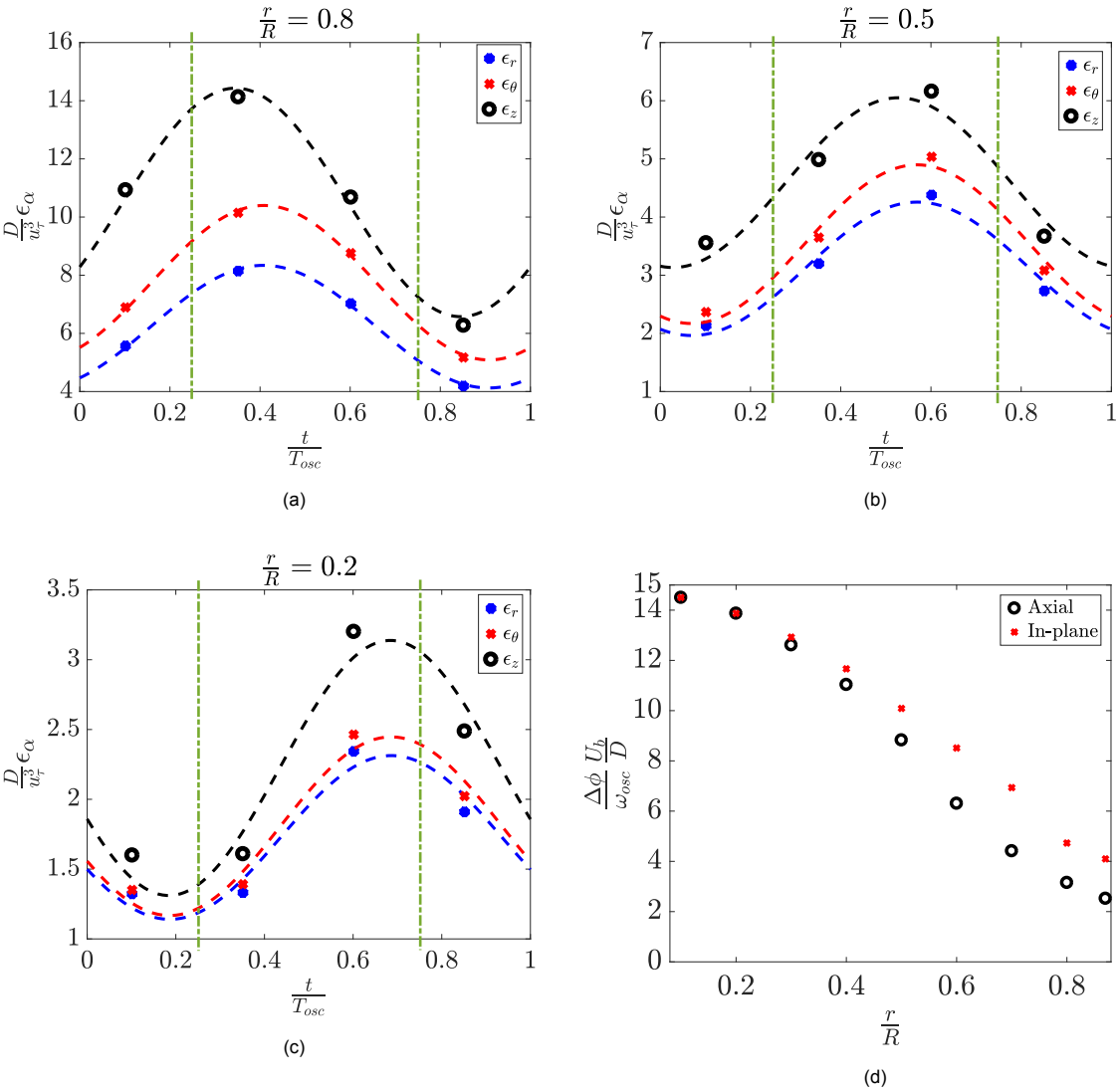


Figure 3.14: Delay in the response of in-plane dissipation rates and axial dissipation rate.Bulk flow is decelerating between vertical lines.

The delay in the response of the in-plane dissipation rates indicates that the delay in the distribution of turbulence from the axial components to the in-plane components, extends to the small scales. However at r=0.2R, it is seen that the axial and in-plane dissipation rates show the same delay. Though the magnitude of dissipation in the axial component remains higher, this can be seen as a tendency of the small scales to move towards isotropy towards the centre of the pipe.

### 3.5.4. Distribution of TKE at different radial points

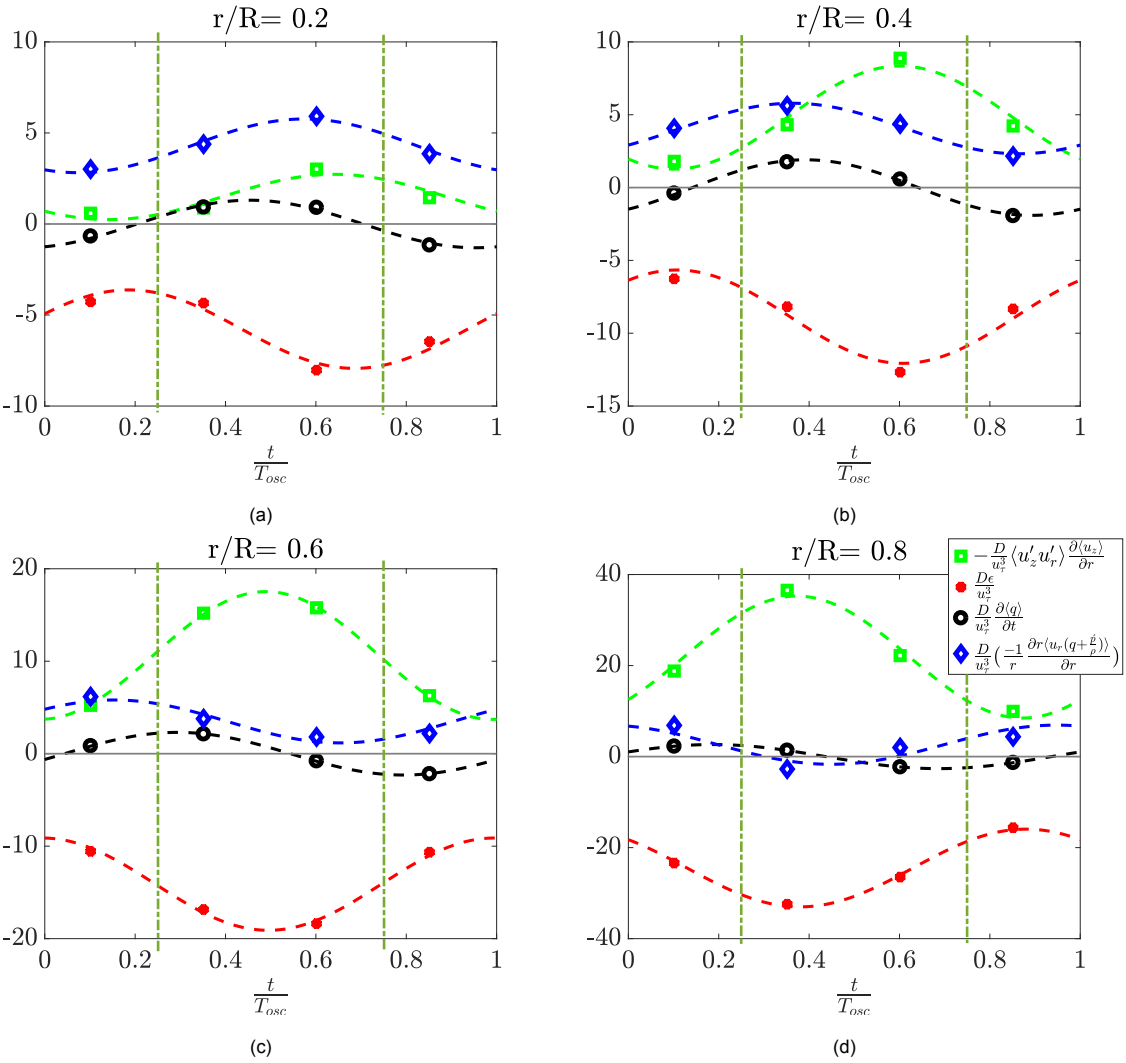


Figure 3.15: Comparison of the terms of the TKE at different radial points. Bulk flow is decelerating between vertical lines.

At r=0.8R (fig 3.15a) both production and dissipation are highest at the beginning of deceleration, while at r=0.2R (fig 3.15d) both these terms are highest towards the end of deceleration.

During deceleration, the diffusion term (which includes transport by both pressure fluctuations and velocity fluctuations) at r=0.8R tends to distribute turbulence from the region close to the wall to the region towards the centre.

The unsteady term is a measure of accumulation of TKE at a point. Hence at r=0.8R there is accumulation of TKE starting at $t \approx 0.9T_{osc}$ which is while the bulk flow is accelerating and continues to accumulate till $t \approx 0.45T_{osc}$ while the flow is deceleration, while towards the centre of the pipe r=0.2R the accumulation occurs during the beginning of deceleration and continues to do so till its end of deceleration. The accumulation of turbulence seen during deceleration of the bulk flow in the outer region of the pipe towards the end of deceleration ( See Fig 3.8), is a combination of excess production as

well as transport from the region towards the wall to the centre of the pipe. A drop in the magnitude of production is responsible for the decrease of turbulence during acceleration.

By definition, the transfer of energy from the mean flow field to the turbulent flow field in steady flow is same throughout all times. In pulsatile flows, the transfer of energy from the phase averaged flow field to the turbulent flow field has different magnitudes at different phase points of the oscillation. At **r=0.8R** the transfer of energy is highest in the beginning of deceleration and decreases while the bulk flow is decelerating, this implies that the magnitude of the gradient of Reynolds stress in the region towards the wall of the pipe has the highest magnitude around the end of acceleration (as shown in Fig. 3.5a). As the phase difference of the production term with respect to the bulk flow oscillation increases on moving closer to the centre, at **r=0.2R**, the transfer is maximum around the end of deceleration and decreases till the end of acceleration. This causes the magnitude of the gradient of the Reynolds stress near the centre of the pipe to be higher in magnitude towards the end of deceleration (Fig. 3.5d). This change in the gradient of the Reynolds stress at different regions, in turn deforms the phase averaged velocity (Fig. 3.5) to repeat the cycle in every oscillation.

Fig 3.16 shows the terms of the total TKE equations as well as those obtained for different components in a steady flow.

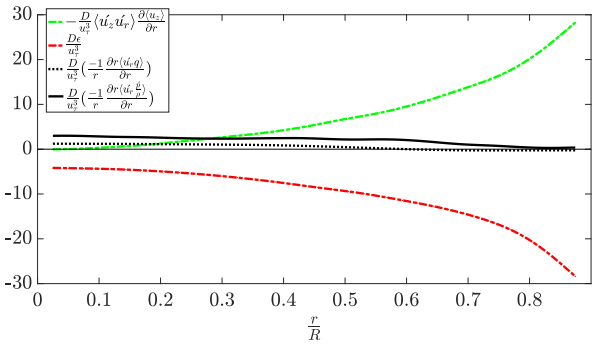


(a) TKE

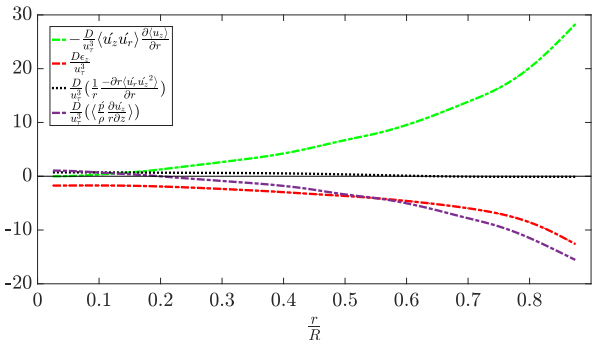


(b) Axial Kinetic Energy Budget

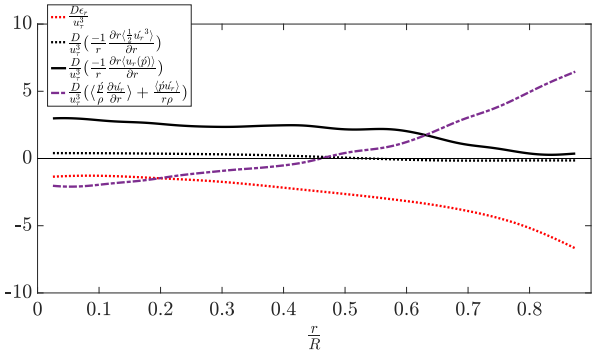


(c) Radial Kinetic Energy Budget

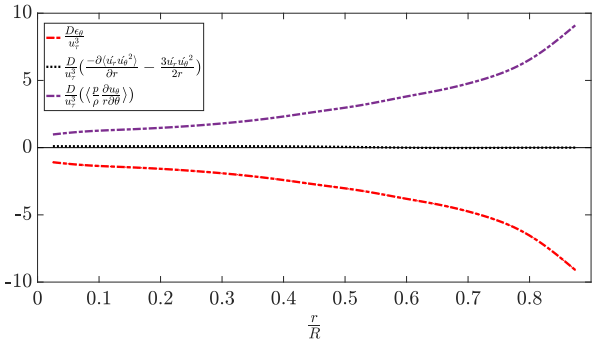


(d) Azimuthal Kinetic Energy Budget

Figure 3.16: Energy Budget Equations for steady flow (Re # 25,900) are shown for reference.

Fig 3.17 shows the terms of the total TKE equations for pulsatile flows.

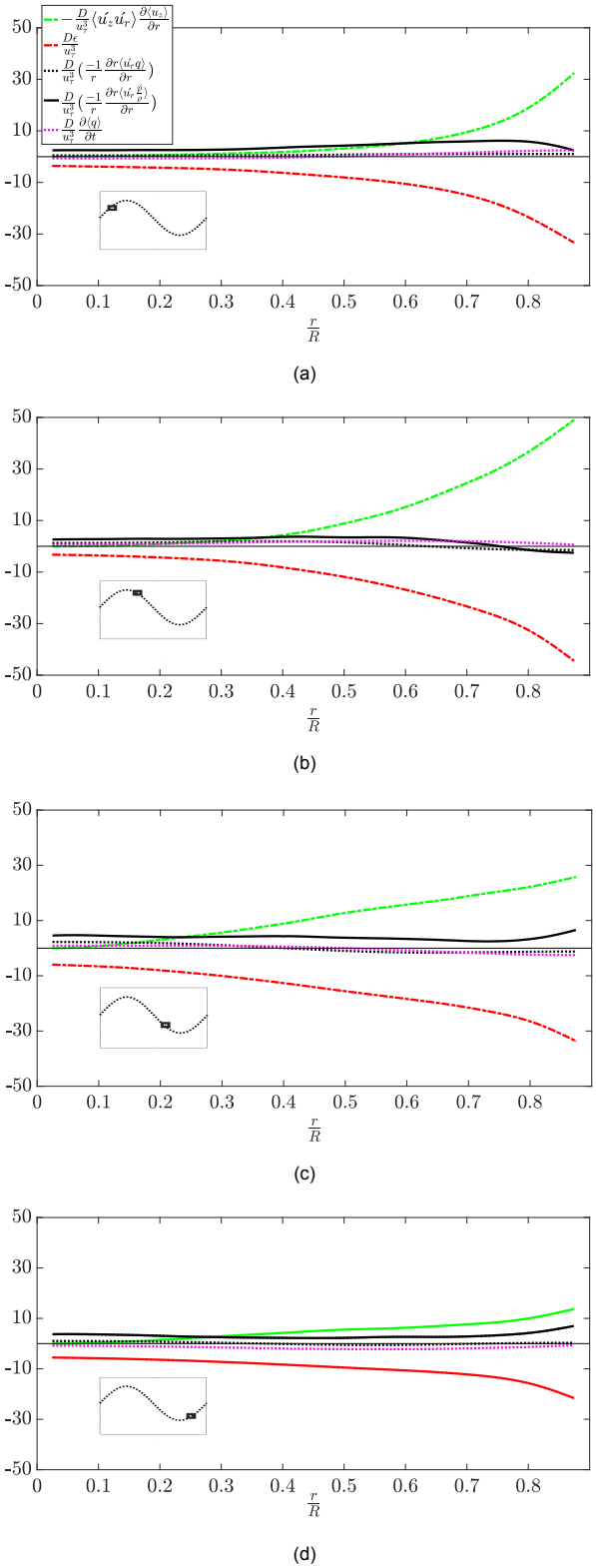


Figure 3.17: Comparison of the terms of the TKE at different phase points

Fig 3.18,Fig 3.19 and Fig 3.20, shows the terms of the total kinetic energy equations for the radial, axial and azimuthal components of pulsatile flows respectively.

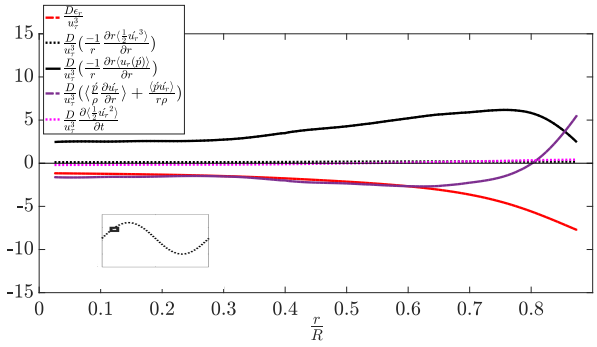


(a)

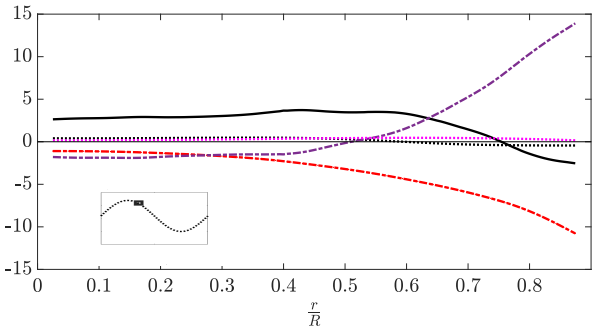


(b)

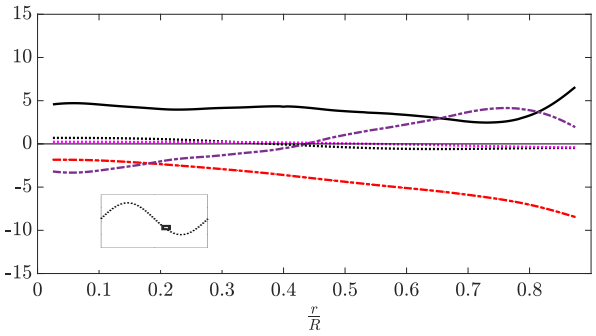


(c)

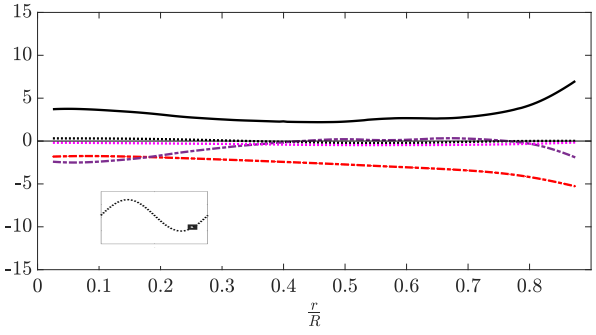


(d)

Figure 3.18: Comparison of the terms of the Radial Kinetic Energy Budget at different phase points

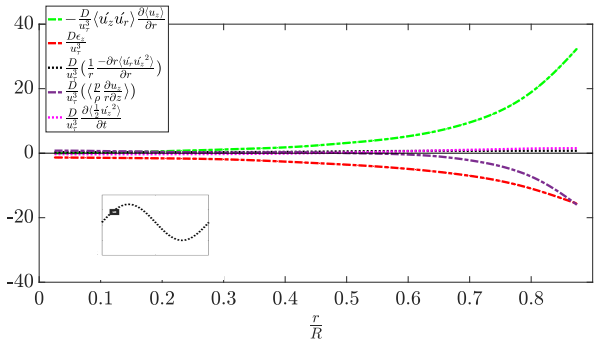


(a)

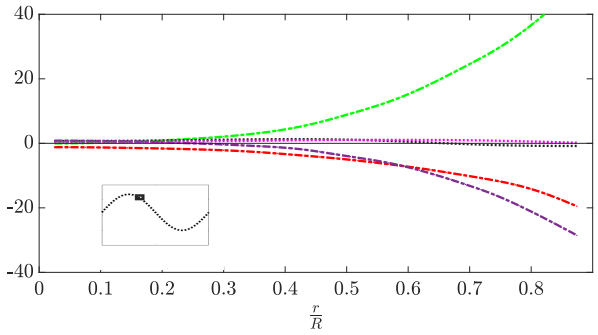


(b)

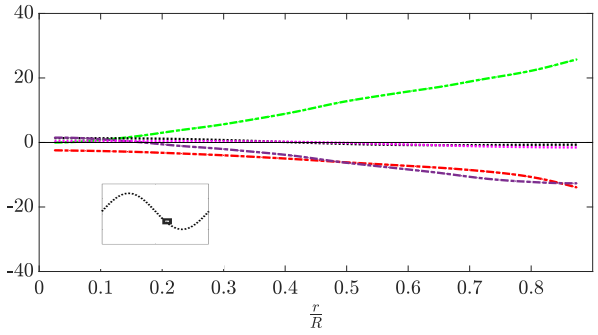


(c)

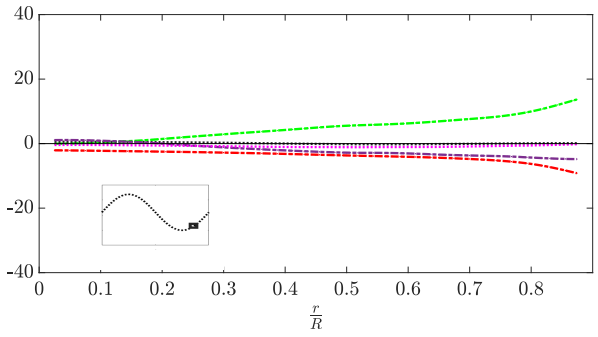


(d)

Figure 3.19: Comparison of the terms of the Axial Kinetic Energy Budget at different phase points

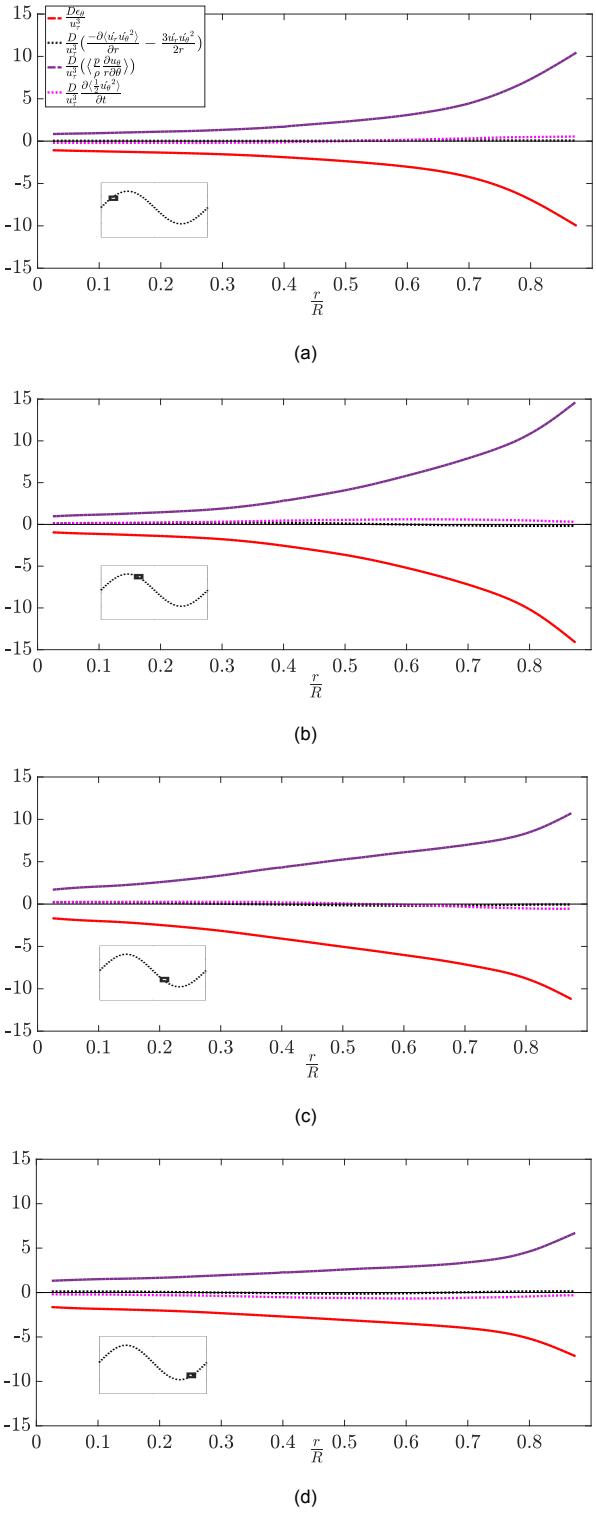


Figure 3.20: Comparison of the terms of the Azimuthal Kinetic Energy Budget at different phase points

The terms of all the components of the energy budget display a delay in the response to the oscillating flows, resulting in a phase shift in the response of the turbulence, which increases on moving from the wall to the centre.

## 3.6. Effect of oscillations azimuthal correlations

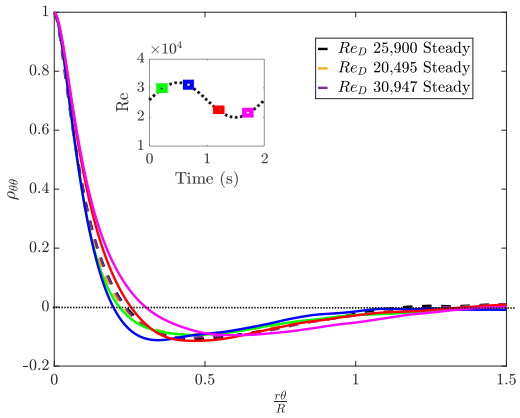


(a)

Figure 3.21: **Figure (a)** Azimuthal correlations at r=0.86R.

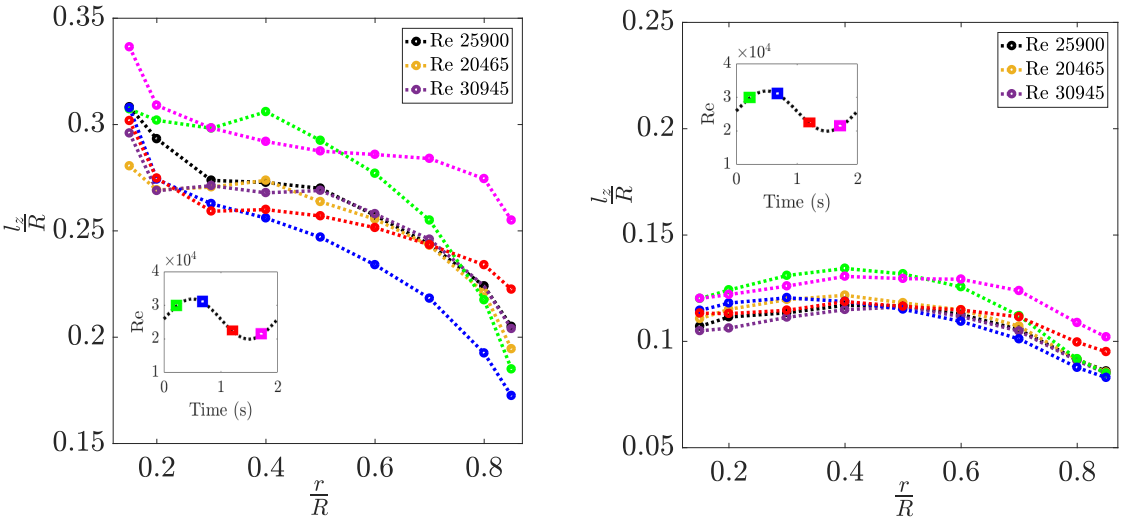


(a) (b)

Figure 3.22: Variation of azimuthal length scale ($l_z$) with distance from the center, for different correlation coefficient thresholds. **Figure (a)** $\rho_{\theta\theta} = 0.05$**Figure (b)**$\rho_{\theta\theta} = 0.5$

The azimuthal correlation coeffcient is defined as,

$$\rho_{\theta\theta} = \frac{\overline{\acute{u_z}(r,0,z)\acute{u_z}(r,\theta,z)}}{\sqrt{\overline{\acute{u_z}^2(r,0,z)}}\sqrt{\overline{\acute{u_z}^2(r,\theta,z)}}} \tag{3.15}$$

Here, the overline represents both ensemble and spatial averaging. The quantity $l_z$ is the distance at which the correlation coefficient is at a certain threshold value, it represents the average width of structures at a particular radial location [34]. Fig 3.22a and Fig 3.22b shows the value of $l_z$ at thresholds

of $\rho_{\theta\theta} = 0.05$ and $\rho_{\theta\theta} = 0.5$ respectively. Though a threshold of $\rho_{\theta\theta} = 0.05$ is closer to the true azimuthal length scale, the trend of the variations do not change at $\rho_{\theta\theta} = 0.5$. It is seen that $l_z$ for the threshold $\rho_{\theta\theta} = 0.05$ increases with increasing distance from the wall. This trend is consistent with the observations of Monty *et al.*[34], Bailey *et al.*[35],etc. for steady flows. Moreover, $l_z$ for steady flows shown are quantitatively similar to each other. As expected, the average width of structures in a pipe at a certain radial location changes with the phase of oscillation. In the logarithmic region (r=0.85R), $l_z$ is maximum at the trough of oscillation and minimum at the crest. On moving towards the center, this trend changes and for a major portion of the wake region, $l_z$ is higher when the flow is accelerating and lower when it is decelerating.

# 4

# Results (Time Series)

Low speed streaks are a characteristic feature in near-wall turbulence flows and in this chapter the implications of the imposed oscillations on these low speed streaks have been shown.

In order to detect regions of low momentum, the velocity field is traditionally compared to the local mean velocity. As 10 time series data sets were recorded, an averaging was done with these to obtain the local mean. However, PIV involves gathering a large amount of data, and it was not feasible to measure enough samples to obtain a statistically unbiased average velocity field from the time series data. In order to overcome this limitation, the ensemble averaged axial velocity of the pulsatile flow at each radial location is curve fitted with a sinusoidal function of time and the fitted velocity is used as a reference velocity ($U_{ref}$) (Fig 4.1b). A similar scheme is used for detecting regions of low momentum in steady flows, which are shown for comparison.

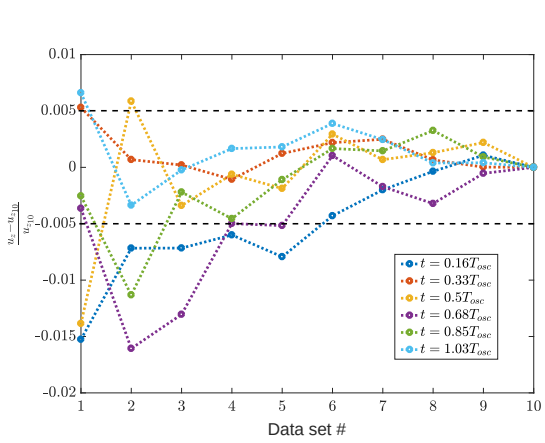


(a) Convergence of ensemble averaging at y+=104;r=0.85R

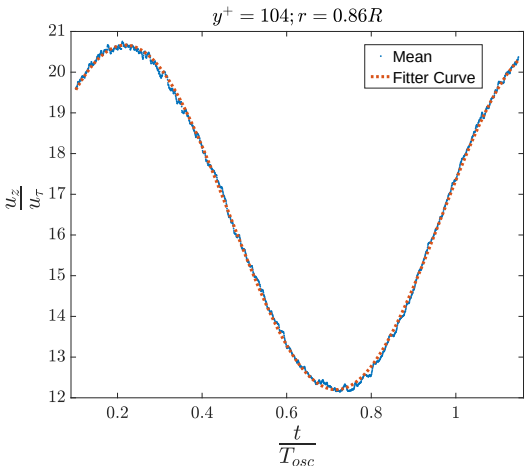


(b) For pulsatile flow

Figure 4.1: Cure fitting at y+=104; r=0.85R.

Let $v_z = u_z - U_{ref}$, $v_z$ is compared with $U_{ref}$ and regions with values less than $-0.05U_{ref}$ are shown as low momentum regions. Changing this criteria will cause changes in the regions defined, but that will not change the inference. At every radial location, the plane surrounding the pipe may be unwrapped in the azimuthal sense to visualize these regions. Moreover, many small 'patches' of low momentum regions are detected that do not fit the definition of a 'streak' (Fig 4.2b). Using an algorithm, these patches are removed for clarity and also for the purpose of facilitating further analysis (Fig 4.2). The algorithm fails to remove patches at the very beginning ($t < 0.0093T_{osc}$) and the extreme end of the time series ($t > 1.137T_{osc}$), leading to patches being present in these regions. In pulsatile flows, as the turbulence characteristics are changing throughout the time series, the Taylor hypothesis of 'frozen' turbulence has not been applied, and data is presented as a time series.

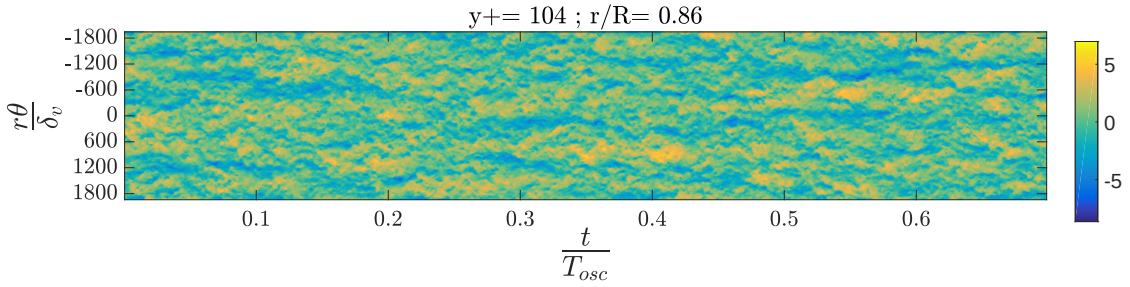


(a) Raw velocity field $v_z$. Velocities are scaled with the friction velocity $u_\tau$ of the mean flow rate.

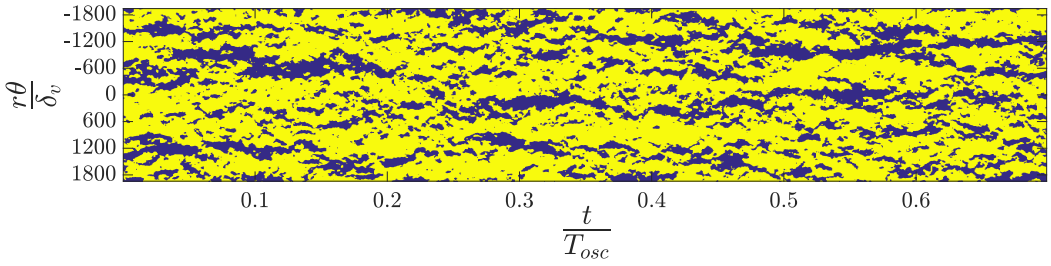


(b) $v_z < -0.05U_{ref}$ is shown in blue, otherwise the velocities are shown in yellow.

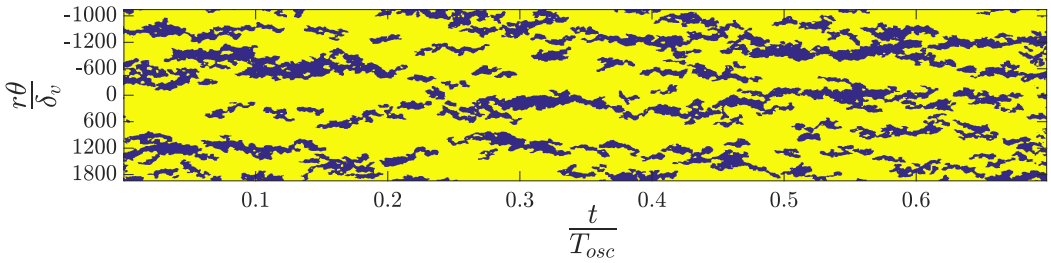


(c) Velocity field after removing small 'patches' of blue.

Figure 4.2: Velocity field for steady flow at y+=104. ($\delta_v = \frac{\nu}{u_\tau}$, depicts viscous wall units)

Fig 4.3 shows the different radial locations for steady flows for comparison with pulsatile flows shown in Fig 4.4. On moving away from the wall these low speed streaks are replaced by 'blobs' of low momentum.

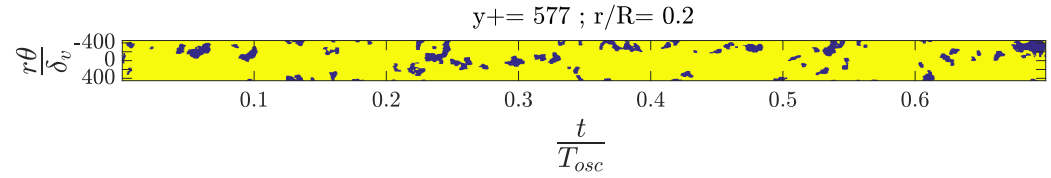


(a)

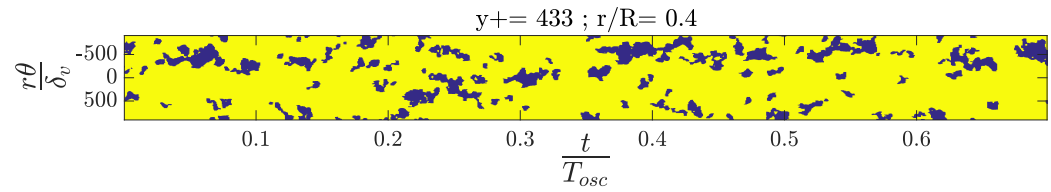


(b)

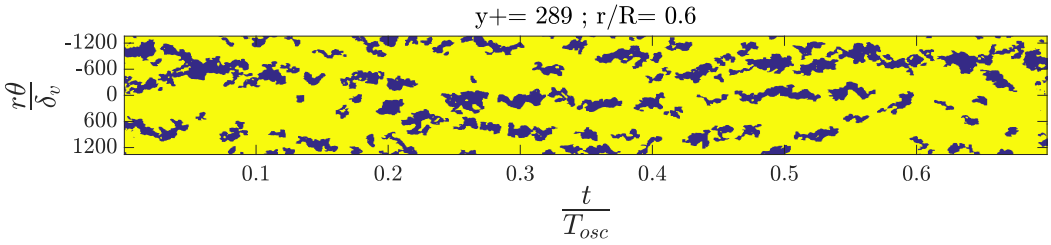


(c)

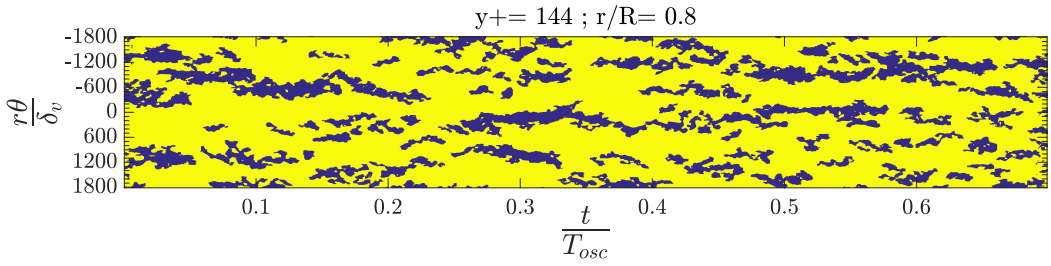


(d)

Figure 4.3: Velocity field for steady flow at different radial locations.

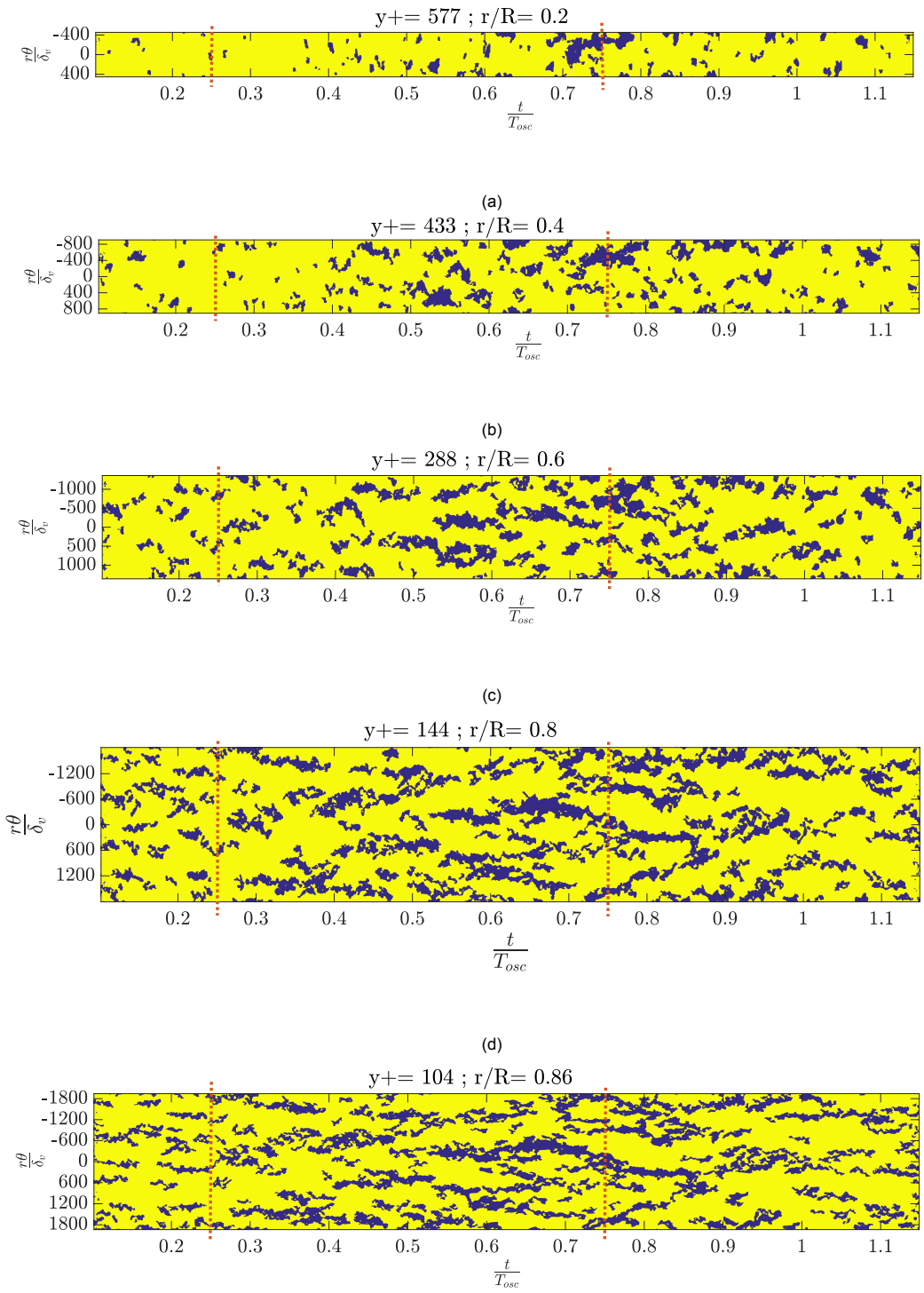


Figure 4.4: Velocity field for pulsatile flow at different radial locations. Bulk flow is decelerating between vertical lines

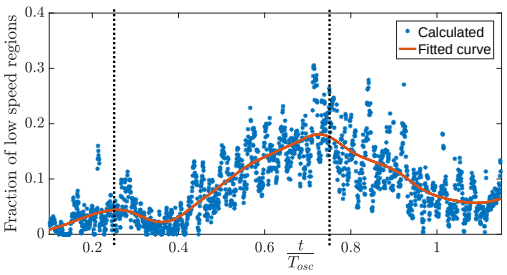


(a) Pulsatile flow; r=0.2R; y+=577

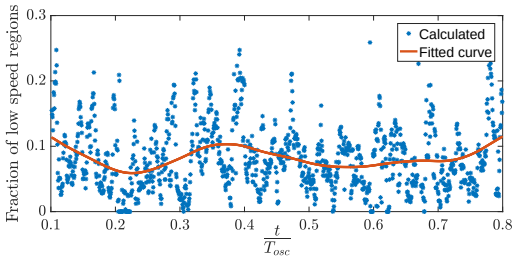


(b) Steady flow; r=0.2R; y+=577

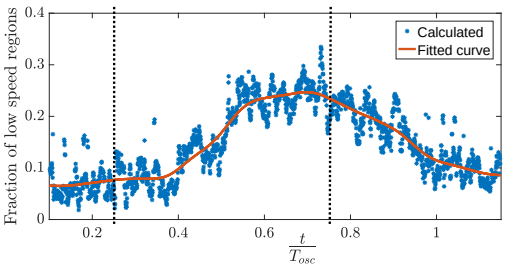


(c) Pulsatile flow; r=0.4R; y+=433

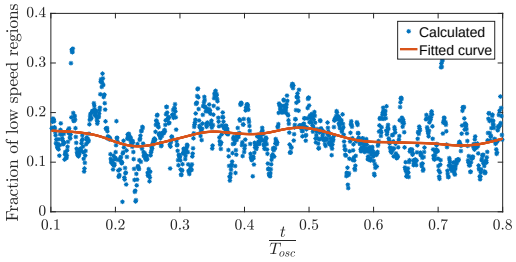


(d) Steady flow; r=0.4R; y+=433

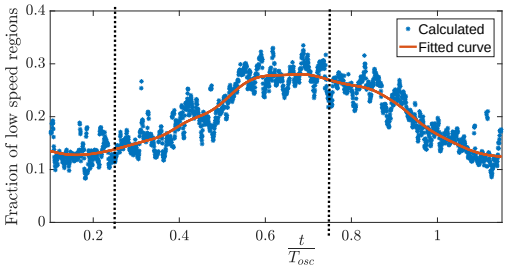


(e) Pulsatile flow; r=0.6R; y+=288

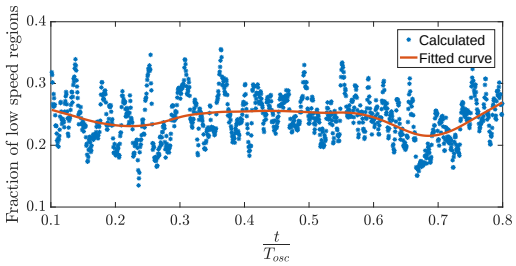


(f) Pulsatile flow; r=0.6R; y+=288

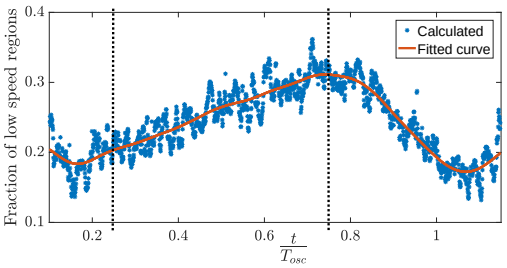


(g) Pulsatile flow; r=0.8R; y+=144

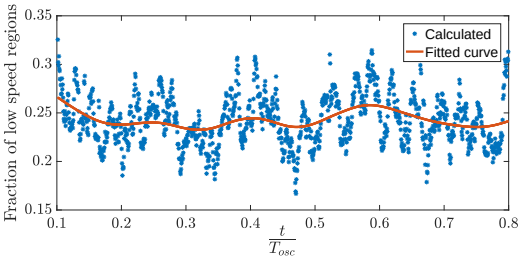


(h) Steady flow; r=0.8R; y+=144

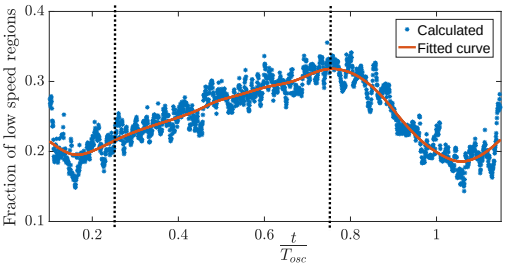


(i) Pulsatile flow; r=0.86R; y+=104

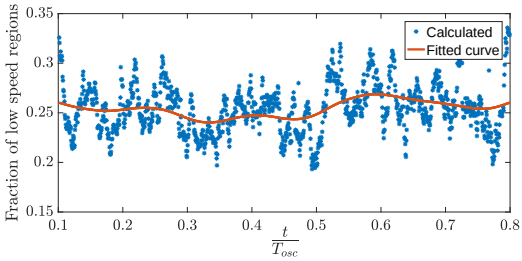


(j) Steady flow; r=0.86R; y+=104

Figure 4.5: Fraction of low momentum fluid at different radial locations. Steady flow measurements are shown in right for comparison with pulsatile flows in the left.

In Fig 4.5, the fraction of span wise length occupied by the low momentum is shown. The increase at the

extreme end and beginning of the time series is due to the patches not being removed in these regions. the plots were obtained by using the data from 10 data sets of the time series for pulsatile flow and 5 data sets for steady flow. As, the number of samples were low, these fractions are not mathematical averages but display a general trend. In pulsatile flows, when the bulk flow is decelerating the fraction of the span wise length occupied by the low speed momentum regions increases, while it decreases as the flow starts to accelerate. Visually from Fig. 4.4 it is seen that width of these low momentum zones decreases as the bulk flow accelerates and increases when the flow decelerates. It is also seen that the number of streaks increases when the flow decelerates and decreases when the flow accelerates. These low momentum regions are associated with the back induction caused by vortex packets . Adrian *et. al* [36] proposed that the burst phenomenon as depicted by Kline *et. al* [37] is a manifestation of the passage of a hairpin packet. Hence the resonance of the bursting frequency and the oscillating frequency as reported by Mizushina *et. al* [14] is likely to be due an increase in the frequency of appearance of low momentum regions during the deceleration of the flow and as such causing the mean bursting period to be that of the time period of oscillation.

The monotonic increase of the low momentum regions during deceleration/acceleration across all radial locations is different from the phase difference the parameters shown in Chapter 3. The increase/decrease in turbulence during oscillation is likely due to the effects of vortex stretching/compression. This would also explain the delay in the transfer of energy from the axial components to the in-plane components as a stretched non in-plane vortex would have more energy in the axial component of velocity. However, further analysis is required to reach a definitive conclusion.

In Fig 4.6 and Fig 4.7 the turbulence kinetic energies (TKE) at r=0.8R and r=0.2R respectively averaged over 10 data sets. The values are obtained are qualitatively similar to that shown in Chapter 3 which are calculated by ensemble averaging a large number of velocity fields. A notable feature from the velocity field at r=0.8R is that even though the fraction of span wise length occupied by the low momentum fluid is maximum at $t = 0.75T_{osc}$, the maximum turbulent kinetic energy is contained in the regions around $t = 0.35T_{osc}$, indicating that the turbulence generated towards the wall while the bulk flow is accelerating has a much higher intensity. However, at r=0.2R the 'blobs' of low momentum at $t = 0.35T_{osc}$ have a greater TKE, which contribute to the turbulence generated when the flow is decelerating. These regions are in turn visually different from that in steady flows indicating that the structural organization in unsteady flows will be different from that in steady flows. Further analysis of these structures are left for future work.

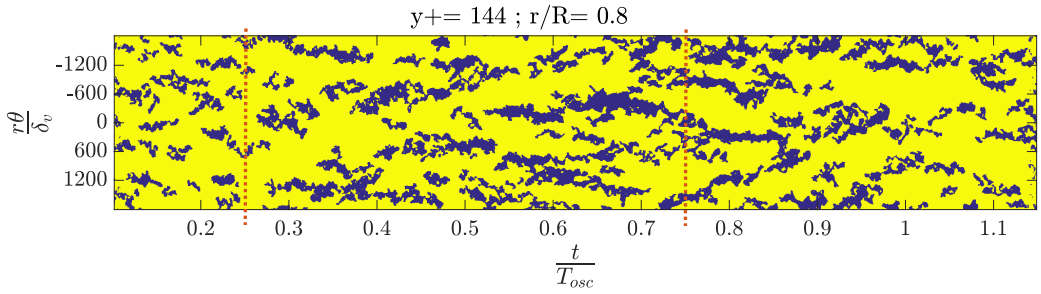


(a) Velocity field after removing patches

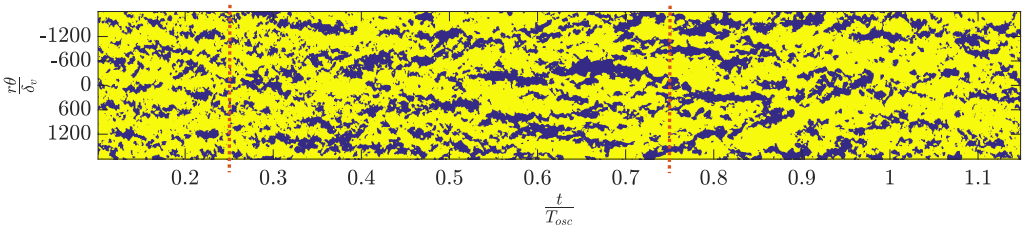


(b) Velocity field before removing patches

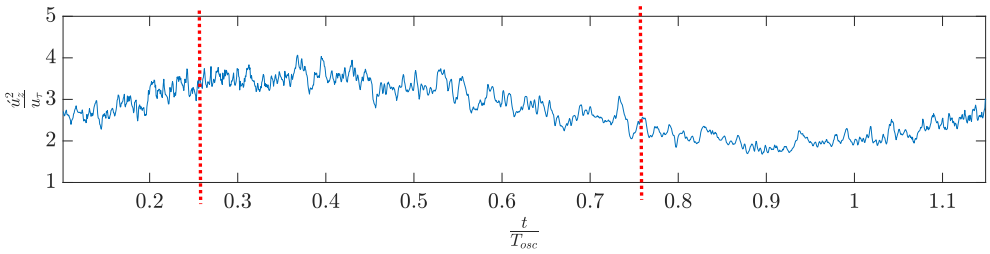


(c) Turbulent kinetic energy obtained by averaging 10 sets of time series

Figure 4.6: Turbulent kinetic energy (TKE) at r=0.8R

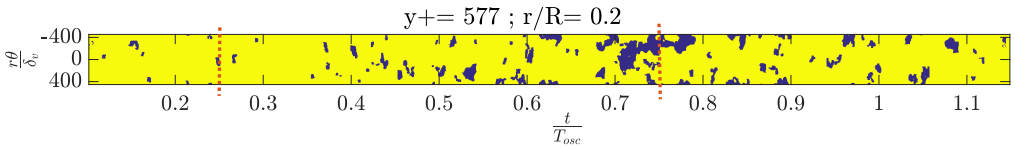


(a) Velocity field after removing patches

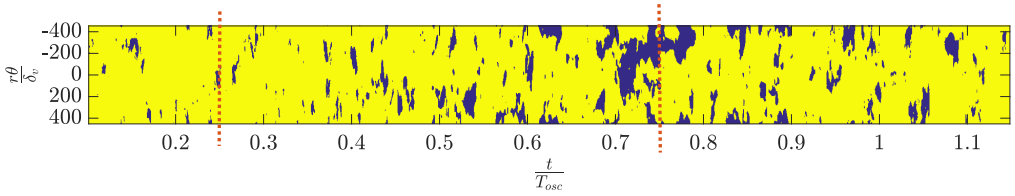


(b) Velocity field before removing patches

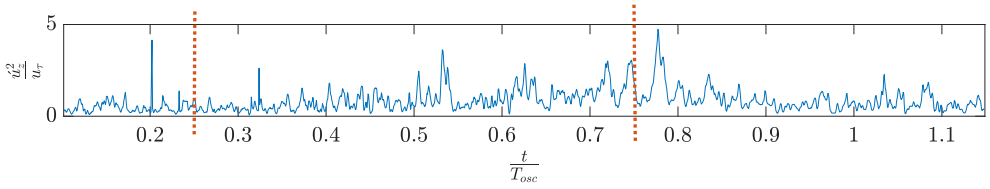


(c) Turbulent kinetic energy obtained from time series

Figure 4.7: Turbulent kinetic energy (TKE) at r=0.2R

# 5

# Conclusions and Recommendations

### 5.0.1. Conclusions

The main objective of this thesis was to experimentally analyze the terms of the turbulent kinetic energy budget equation in an unsteady flow using PIV. This was done to understand the cause of the increase/decrease of turbulence during the acceleration/deceleration of unsteady flows.

The turbulence parameters are seen to be oscillating in a sinusoidal manner with the same oscillating frequency as that of the bulk flow. The time delay in the response of these turbulence parameters increases with increasing distance from the pipe wall. This time delay is expressed as a phase difference between the sinusoidal functions describing these turbulence parameters and the bulk flow.

It has been observed that turbulence in the log region of the pipe increases during acceleration while it decreases during deceleration. On moving towards the centre, there is a time lag in the response of the turbulence, leading to the increase of turbulence during deceleration and decrease during acceleration. Due to the effects of the delayed response of the Reynolds stress, the mean velocity profiles deforms in unalike ways when the flow decelerates and accelerates, facilitating the transfer of energy to repeat the cycle in every oscillation.

The delay in the response of the production term and the dissipation term of the turbulent kinetic energy budget equation is the same, indicating that for the present rate of oscillation the large and small scales respond to the oscillations of the bulk flow in a similar way.

In the log region as the flow accelerates, the turbulence increases both due to increase in production as well as diffusion. The excess turbulence generated in the wake region of the pipe during deceleration is due to an increase in the production of turbulence as well as diffusing of turbulence transported from

the region towards the wall and the turbulence decreases due to the decrease of the production term during acceleration.

There is a greater delay in the response of the in-plane turbulence components as compared to the axial turbulence components, which decreases on moving away from the wall. This difference is also seen in the dissipation rates of these components indicating that the delay extends to the small scales. However, towards the centre the difference in the delays is not present indicating the tendency of the small scales to be isotropic.

The low momentum streaks in the outer log region of the pipe increase/decrease in frequency of occurrence during deceleration/acceleration of the bulk flow. Moreover, it was seen that the structural organization of unsteady flows will be different from steady flows.

### 5.0.2. Recommendations for future work

As there is a time delay in the response of the turbulence, the effects of varying the frequencies and amplitude of oscillations on the delay of the response of turbulence can be analyzed. This will also aid in characterizing the flows using a physical basis.

In the present rate of oscillation the large scale and the small scales are not decoupled. On using a higher frequency of oscillation the scales might be decoupled. Moreover, 'frozen' turbulence might be detected near the centre of the pipe. The dynamics of turbulence need to be analyzed in this state.

The role of vortex dynamics can be analyzed and the processes responsible for creating a difference in the delay of the response of the axial and in-plane turbulence need to be analyzed.

# Bibliography


[1] CH Sieverding, T Arts, R Dénos, and J-F Brouckaert. Measurement techniques for unsteady flows in turbomachines. *Experiments in fluids*, 28(4):285–321, 2000.

[2] LE Ericsson and JP Reding. Unsteady flow concepts for dynamic stall analysis. *Journal of aircraft*, 21(8):601–606, 1984.

[3] Ch Brücker, U Steinseifer, W Schröder, and H Reul. Unsteady flow through a new mechanical heart valve prosthesis analysed by digital particle image velocimetry. *Measurement Science and Technology*, 13(7):1043, 2002.

[4] Manosh C Paul, Md Mamun Molla, and Giles Roditi. Large–eddy simulation of pulsatile blood flow. *Medical engineering & physics*, 31(1):153–159, 2009.

[5] S He and JD Jackson. A study of turbulence under conditions of transient flow in a pipe. *Journal of Fluid Mechanics*, 408:1–38, 2000.

[6] Sébastien Candel. Combustion dynamics and control: Progress and challenges. *Proceedings of the combustion institute*, 29(1):1–28, 2002.

[7] RK Shah, MR Heikal, B Thonon, and P Tochon. Progress in the numerical analysis of compact heat exchanger surfaces. In *Advances in heat transfer*, volume 34, pages 363–I. Elsevier, 2001.

[8] Jian Jun Shu, Clifford R Burrows, and Kevin A Edge. Pressure pulsations in reciprocating pump piping systems part 1: modelling. *Proceedings of the Institution of Mechanical Engineers, Part I: Journal of Systems and Control Engineering*, 211(3):229–235, 1997.

[9] Majid Nabavi and Kamran Siddiqui. A critical review on advanced velocity measurement techniques in pulsating flows. *Measurement science and technology*, 21(4):042002, 2010.

[10] FT Brown, Donald L Margolis, and Rasiklal Punjalah Shah. Small-amplitude frequency behavior of fluid lines with turbulent flow. *Journal of Basic Engineering*, 91(4):678–693, 1969.

[11] Munekazu OHMI and Tateo USUI. Pressure and velocity distributions in pulsating turbulent pipe flow part 1 theoretical treatments. *Bulletin of JSME*, 19(129):307–313, 1976.

[12] Munekazu OHMI, Susumu KYOMEN, and Tateo USui. Analysis of velocity distribution in pulsating turbulent pipe flow with time-dependent friction velocity. *Bulletin of JSME*, 21(157):1137–1143, 1978.

[13] L Shemer, I Wygnanski, and E Kit. Pulsating flow in a pipe. *Journal of Fluid Mechanics*, 153:313–337, 1985.

[14] TOKURO MIZUSHINA, TOSHIRO MARUYAMA, and HIDEO HIRASAWA. Structure of the turbulence in pulsating pipe flows. *Journal of Chemical Engineering of Japan*, 8(3):210–216, 1975.

[15] L Shemer, I Wygnanski, and E Kit. Pulsating flow in a pipe. *Journal of Fluid Mechanics*, 153:313–337, 1985.

[16] SW Tu and BR Ramaprian. Fully developed periodic turbulent pipe flow. part 1. main experimental results and comparison with predictions. *Journal of Fluid Mechanics*, 137:31–58, 1983.

[17] BR Ramaprian and SW Tu. Fully developed periodic turbulent pipe flow. part 2. the detailed structure of the flow. *Journal of Fluid Mechanics*, 137:59–81, 1983.

[18] Zhuo-Xiong Mao and Thomas J Hanratty. Studies of the wall shear stress in a turbulent pulsating pipe flow. *Journal of Fluid Mechanics*, 170:545–564, 1986.

[19] F Sedat Tardu and Gilbert Binder. Wall shear stress modulation in unsteady turbulent channel flow with high imposed frequencies. *Physics of Fluids A: Fluid Dynamics*, 5(8):2028–2037, 1993.

[20] Alberto Scotti and Ugo Piomelli. Numerical simulation of pulsating turbulent channel flow. *Physics of Fluids*, 13(5):1367–1384, 2001.

[21] Melda Özdinç Çarpinlio□lu and Mehmet Yaşar Gündo□du. A critical review on pulsatile pipe flow studies directing towards future research topics. *Flow Measurement and Instrumentation*, 12(3):163–174, 2001.

[22] Ronald J Adrian and Jerry Westerweel. *Particle image velocimetry*. Number 30. Cambridge University Press, 2011.

[23] Ajay K Prasad. Stereoscopic particle image velocimetry. *Experiments in fluids*, 29(2):103–116, 2000.

[24] Steven M Soloff, Ronald J Adrian, and Zi-Chao Liu. Distortion compensation for generalized stereoscopic particle image velocimetry. *Measurement science and technology*, 8(12):1441, 1997.

[25] B Wieneke. Stereo-piv using self-calibration on particle images. *Experiments in fluids*, 39(2):267–280, 2005.

[26] JMJ Den Toonder and FTM Nieuwstadt. Reynolds number effects in a turbulent pipe flow for low to moderate re. *Physics of Fluids*, 9(11):3398–3409, 1997.

[27] Munsun Young Okiishi, B Munson, and D Young. Fundamentals of fluid mechanics. *John Wiley & Sons, Inc*, 2006.

[28] GJ Brereton, WC Reynolds, and R Jayaraman. Response of a turbulent boundary layer to sinusoidal free-stream unsteadiness. *Journal of fluid mechanics*, 221:131–159, 1990.

[29] Shuisheng He and JD Jackson. An experimental study of pulsating turbulent flow in a pipe. *European Journal of Mechanics-B/Fluids*, 28(2):309–320, 2009.

[30] J Sheng, H Meng, and RO Fox. A large eddy piv method for turbulence dissipation rate estimation. *Chemical engineering science*, 55(20):4423–4434, 2000.

[31] Guus Bertens, Dennis van der Voort, Humberto Bocanegra-Evans, and Willem van de Water. Large-eddy estimate of the turbulent dissipation rate using piv. *Experiments in Fluids*, 56(5):89, 2015.

[32] John Laufer. The structure of turbulence in fully developed pipe flow. 1954.

[33] CJ Lawn. The determination of the rate of dissipation in turbulent pipe flow. *Journal of Fluid Mechanics*, 48(3):477–505, 1971.

[34] JP Monty, JA Stewart, RC Williams, and MS Chong. Large-scale features in turbulent pipe and channel flows. *Journal of Fluid Mechanics*, 589:147–156, 2007.

[35] Sean CC Bailey, Marcus Hultmark, Alexander J Smits, and Michael P Schultz. Azimuthal structure of turbulence in high reynolds number pipe flow. *Journal of Fluid Mechanics*, 615:121–138, 2008.

[36] Ronald J Adrian, Carl D Meinhart, and Christopher D Tomkins. Vortex organization in the outer region of the turbulent boundary layer. *Journal of Fluid Mechanics*, 422:1–54, 2000.

[37] Stephen J Kline, William C Reynolds, FA Schraub, and PW Runstadler. The structure of turbulent boundary layers. *Journal of Fluid Mechanics*, 30(4):741–773, 1967.

# A

# Appendix 1

Let $u_z$,$u_r$ and $u_\theta$ be the projections of velocity in the axial, radial and tangential directions respectively, and $p$ be the pressure.$\upsilon$ is the kinematic viscosity of the fluid.

The continuity equation is given as,

$$\frac{\partial u_z}{\partial z} + \frac{\partial u_r}{\partial r} + \frac{1}{r}\frac{\partial u_\theta}{\partial \theta} = -\frac{u_r}{r} \tag{A.1}$$

The Navier Stokes equation for the three velocity components are as follows,

$$\frac{\partial u_z}{\partial t} + u_z\frac{\partial u_z}{\partial z} + u_r\frac{\partial u_z}{\partial r} + \frac{u_\theta}{r}\frac{\partial u_z}{\partial \theta} = -\frac{1}{\rho}\frac{\partial p}{\partial z} + 2\upsilon[\frac{\partial S_{zz}}{\partial z} + \frac{\partial (rS_{rz})}{r\partial r} + \frac{1}{r}\frac{\partial S_{z\theta}}{\partial \theta}] \tag{A.2}$$

$$\frac{\partial u_r}{\partial t} + u_z\frac{\partial u_r}{\partial z} + u_r\frac{\partial u_r}{\partial r} + \frac{u_\theta}{r}\frac{\partial u_r}{\partial \theta} - \frac{u_\theta^2}{r} = -\frac{1}{\rho}\frac{\partial p}{\partial r} + 2\upsilon[\frac{\partial S_{zr}}{\partial z} + \frac{\partial (rS_{rr})}{r\partial r} + \frac{1}{r}\frac{\partial S_{r\theta}}{\partial \theta} - \frac{S_{\theta\theta}}{r}] \tag{A.3}$$

$$\frac{\partial u_\theta}{\partial t} + u_z\frac{\partial u_\theta}{\partial z} + u_r\frac{\partial u_\theta}{\partial r} + \frac{u_\theta}{r}\frac{\partial u_\theta}{\partial \theta} + \frac{u_\theta u_r}{r} = -\frac{1}{\rho r}\frac{\partial p}{\partial \theta} + 2\upsilon[\frac{\partial S_{z\theta}}{\partial z} + \frac{\partial (rS_{r\theta})}{r\partial r} + \frac{1}{r}\frac{\partial S_{\theta\theta}}{\partial \theta} + \frac{S_{r\theta}}{r}] \tag{A.4}$$

On dividing the velocity components and pressure into their ensemble mean and fluctuating parts, we have $u_z = \overline{u_z} + \acute{u_z}$, $u_r = \overline{u_r} + \acute{u_r}$, $u_\theta = \overline{u_\theta} + \acute{u_\theta}$ and $p = \overline{p} + \acute{p}$. **Here the overline symbol is used to denote an ensemble mean. In the report brackets (⟨⟩) are used to denote a phase average.**

For the mean flow, the continuity equation is,

$$\frac{\partial \overline{u_z}}{\partial z} + \frac{\partial \overline{u_r}}{\partial r} + \frac{1}{r}\frac{\partial \overline{u_\theta}}{\partial \theta} = -\frac{\overline{u_r}}{r} \tag{A.5}$$

For the fluctuating component, the continuity equation is ,

$$\frac{\partial \acute{u_z}}{\partial z} + \frac{\partial \acute{u_r}}{\partial r} + \frac{1}{r}\frac{\partial \acute{u_\theta}}{\partial \theta} = -\frac{\acute{u_r}}{r} \tag{A.6}$$

Replacing the mean and fluctuating velocity components and pressure into equation (2) and averaging we have,

$$\begin{aligned}&\frac{\partial \overline{u_z}}{\partial t} + \overline{u_z}\frac{\partial \overline{u_z}}{\partial z} + \overline{\acute{u_z}\frac{\partial \acute{u_z}}{\partial z}} + \overline{u_r}\frac{\partial \overline{u_z}}{\partial r} + \overline{\acute{u_r}\frac{\partial \acute{u_z}}{\partial r}} + \overline{u_\theta}\frac{\partial \overline{u_z}}{r\partial \theta} + \overline{\acute{u_\theta}\frac{\partial \acute{u_z}}{r\partial \theta}} \\ &= -\frac{1}{\rho}\frac{\partial \overline{p}}{\partial z} + 2\upsilon\left(\frac{\partial \overline{S_{zz}}}{\partial z} + \frac{\partial r\overline{S_{rz}}}{r\partial r} + \frac{1}{r}\frac{\partial \overline{S_{z\theta}}}{\partial \theta}\right)\end{aligned} \tag{A.7}$$

Multiplying equation (7) with $\overline{u_z}$ we have,

$$\begin{aligned}&\overline{u_z}\frac{\partial \overline{u_z}}{\partial t} + \overline{u_z}^2\frac{\partial \overline{u_z}}{\partial z} + \overline{u_z}\cdot\overline{u_r}\frac{\partial \overline{u_z}}{\partial r} + \overline{u_z}\cdot\overline{u_\theta}\frac{\partial \overline{u_z}}{r\partial \theta} + \overline{u_z}\left(\overline{\acute{u_z}\frac{\partial \acute{u_z}}{\partial z}} + \overline{\acute{u_r}\frac{\partial \acute{u_z}}{\partial r}} + \overline{\frac{\acute{u_\theta}}{r}\frac{\partial \acute{u_z}}{\partial \theta}}\right) \\ &= -\frac{\overline{u_z}}{\rho}\frac{\partial \overline{p}}{\partial z} + 2\upsilon\left(\overline{u_z}\frac{\partial \overline{S_{zz}}}{\partial z} + \overline{u_z}\frac{\partial r\overline{S_{zr}}}{r\partial r} + \frac{\overline{u_z}}{r}\frac{\partial \overline{S_{z\theta}}}{\partial \theta}\right)\end{aligned}$$

The terms in red are expanded using the product rule of differentiation,

$$\begin{aligned}&\overline{u_z}\frac{\partial \overline{u_z}}{\partial t} + \overline{u_z}^2\frac{\partial \overline{u_z}}{\partial z} + \overline{u_z}\cdot\overline{u_r}\frac{\partial \overline{u_z}}{\partial r} + \overline{u_z}\cdot\overline{u_\theta}\frac{\partial \overline{u_z}}{r\partial \theta} + \frac{\partial \overline{u_z}\cdot\overline{\acute{u_z}\acute{u_z}}}{\partial z} - \overline{\acute{u_z}^2}\frac{\partial \overline{u_z}}{\partial z} - \overline{u_z}\overline{\acute{u_z}\frac{\partial \acute{u_z}}{\partial z}} \\ &+ \frac{\partial \overline{u_z}\overline{\acute{u_z}\acute{u_r}}}{\partial r} - \overline{\acute{u_z}\acute{u_r}}\frac{\partial \overline{u_z}}{\partial r} - \overline{u_z}\overline{\acute{u_z}\frac{\partial \acute{u_r}}{\partial r}} + \frac{1}{r}\frac{\partial \overline{u_z}\overline{\acute{u_z}\acute{u_\theta}}}{\partial \theta} - \frac{1}{r}\overline{\acute{u_z}\acute{u_\theta}}\frac{\partial \overline{u_z}}{\partial \theta} - \frac{1}{r}\overline{u_z}\overline{\acute{u_z}\frac{\partial \acute{u_\theta}}{\partial \theta}} \\ &= -\frac{\overline{u_z}}{\rho}\frac{\partial \overline{p}}{\partial z} + 2\upsilon\left(\frac{\partial \overline{u_z}\overline{S_{zz}}}{\partial z} + \frac{\partial r\overline{u_z}\overline{S_{zr}}}{r\partial r} + \frac{1}{r}\frac{\partial \overline{u_z}\overline{S_{z\theta}}}{\partial \theta} - \overline{S_{zz}}\frac{\partial \overline{u_z}}{\partial z} - \overline{S_{zr}}\frac{\partial \overline{u_z}}{\partial r} - \frac{\overline{S_{z\theta}}}{r}\frac{\partial \overline{u_z}}{\partial \theta}\right)\end{aligned} \tag{A.8}$$

The terms in green can be changed into the following using the continuity equation,

$$\begin{aligned}&\overline{u_z}\frac{\partial \overline{u_z}}{\partial t} + \overline{u_z}^2\frac{\partial \overline{u_z}}{\partial z} + \overline{u_z}\cdot\overline{u_r}\frac{\partial \overline{u_z}}{\partial r} + \overline{u_z}\cdot\overline{u_\theta}\frac{\partial \overline{u_z}}{r\partial \theta} + \frac{\partial \overline{u_z}\cdot\overline{\acute{u_z}\acute{u_z}}}{\partial z} - \overline{\acute{u_z}^2}\frac{\partial \overline{u_z}}{\partial z} + \overline{u_z}\overline{\acute{u_z}\frac{\acute{u_r}}{r}} \\ &+ \frac{\partial \overline{u_z}\overline{\acute{u_z}\acute{u_r}}}{\partial r} - \overline{\acute{u_z}\acute{u_r}}\frac{\partial \overline{u_z}}{\partial r} + \frac{1}{r}\frac{\partial \overline{u_z}\overline{\acute{u_z}\acute{u_\theta}}}{\partial \theta} - \frac{1}{r}\overline{\acute{u_z}\acute{u_\theta}}\frac{\partial \overline{u_z}}{\partial \theta} = -\frac{\overline{u_z}}{\rho}\frac{\partial \overline{p}}{\partial z} + 2\upsilon\left(\frac{\partial \overline{u_z}\overline{S_{zz}}}{\partial z} + \frac{\partial r\overline{u_z}\overline{S_{zr}}}{r\partial r} + \right. \\ &\left.\frac{1}{r}\frac{\partial \overline{u_z}\overline{S_{z\theta}}}{\partial \theta} - \overline{S_{zz}}\frac{\partial \overline{u_z}}{\partial z} - \overline{S_{zr}}\frac{\partial \overline{u_z}}{\partial r} - \frac{\overline{S_{z\theta}}}{r}\frac{\partial \overline{u_z}}{\partial \theta}\right)\end{aligned} \tag{A.9}$$

$$\begin{aligned}&\overline{u_z}\frac{\partial \overline{u_z}}{\partial t} + \overline{u_z}^2\frac{\partial \overline{u_z}}{\partial z} + \overline{u_z}\cdot\overline{u_r}\frac{\partial \overline{u_z}}{\partial r} + \overline{u_z}\cdot\overline{u_\theta}\frac{\partial \overline{u_z}}{r\partial \theta} + \frac{\partial \overline{u_z}\cdot\overline{\acute{u_z}\acute{u_z}}}{\partial z} - \overline{\acute{u_z}^2}\frac{\partial \overline{u_z}}{\partial z} + \frac{1}{r}\frac{\partial r(\overline{u_z}\overline{\acute{u_z}\acute{u_r}})}{\partial r} \\ &- \overline{\acute{u_z}\acute{u_r}}\frac{\partial \overline{u_z}}{\partial r} + \frac{1}{r}\frac{\partial \overline{u_z}\overline{\acute{u_z}\acute{u_\theta}}}{\partial \theta} - \frac{1}{r}\overline{\acute{u_z}\acute{u_\theta}}\frac{\partial \overline{u_z}}{\partial \theta} = -\frac{\overline{u_z}}{\rho}\frac{\partial \overline{p}}{\partial z} + 2\upsilon\left(\frac{\partial \overline{u_z}\overline{S_{zz}}}{\partial z} + \frac{\partial r\overline{u_z}\overline{S_{zr}}}{r\partial r} + \right. \\ &\left.\frac{1}{r}\frac{\partial \overline{u_z}\overline{S_{z\theta}}}{\partial \theta} - \overline{S_{zz}}\frac{\partial \overline{u_z}}{\partial z} - \overline{S_{zr}}\frac{\partial \overline{u_z}}{\partial r} - \frac{\overline{S_{z\theta}}}{r}\frac{\partial \overline{u_z}}{\partial \theta}\right)\end{aligned} \tag{A.10}$$

Replacing the velocity components and pressure into equation (3) and averaging we have,

$$\frac{\partial \overline{u_r}}{\partial t} + \overline{u_z}\frac{\partial \overline{u_r}}{\partial z} + \overline{\acute{u}_z\frac{\partial \acute{u}_r}{\partial z}} + \overline{u_r}\frac{\partial \overline{u_r}}{\partial r} + \overline{\acute{u}_r\frac{\partial \acute{u}_r}{\partial r}} + \overline{u_\theta}\frac{\partial \overline{u_r}}{r\partial \theta} + \overline{\acute{u}_\theta\frac{\partial \acute{u}_r}{r\partial \theta}} - \frac{\overline{u_\theta}^2}{r} - \frac{\overline{\acute{u}_\theta}^2}{r} = -\frac{1}{\rho}\frac{\partial \overline{p}}{\partial r} + 2\upsilon\left(\frac{\partial \overline{S_{rz}}}{\partial z} + \frac{\partial r\overline{S_{rr}}}{r\partial r} + \frac{1}{r}\frac{\partial \overline{S_{r\theta}}}{\partial \theta} - \frac{\overline{S_{\theta\theta}}}{r}\right) \quad \text{(A.11)}$$

Multiplying equation (11) with $\overline{u_r}$ we have,

$$\overline{u_r}\frac{\partial \overline{u_r}}{\partial t} + \overline{u_r}\cdot\overline{u_z}\frac{\partial \overline{u_r}}{\partial z} + \overline{u_r}^2\frac{\partial \overline{u_r}}{\partial r} + \overline{u_r}\cdot\overline{u_\theta}\frac{\partial \overline{u_z}}{r\partial \theta} + \overline{u_r}\overline{\left(\acute{u}_z\frac{\partial \acute{u}_r}{\partial z} + \acute{u}_r\frac{\partial \acute{u}_r}{\partial r} + \frac{\acute{u}_\theta}{r}\frac{\partial \acute{u}_r}{\partial \theta}\right)} - \frac{\overline{u_r}\cdot\overline{u_\theta}^2}{r} - \frac{\overline{u_r}\overline{\acute{u}_\theta}^2}{r}$$
$$= -\frac{\overline{u_r}}{\rho}\frac{\partial \overline{p}}{\partial r} + 2\upsilon\left(\overline{u_r}\frac{\partial \overline{S_{rz}}}{\partial z} + \overline{u_r}\frac{\partial r\overline{S_{rr}}}{r\partial r} + \frac{\overline{u_r}}{r}\frac{\partial \overline{S_{r\theta}}}{\partial \theta} - \frac{\overline{u_r}\overline{S_{\theta\theta}}}{r}\right)$$

$$\overline{u_r}\frac{\partial \overline{u_r}}{\partial t} + \overline{u_r}\cdot\overline{u_z}\frac{\partial \overline{u_r}}{\partial z} + \overline{u_r}^2\frac{\partial \overline{u_r}}{\partial r} + \overline{u_r}\cdot\overline{u_\theta}\frac{\partial \overline{u_z}}{r\partial \theta} + \frac{\partial \overline{u_r}\cdot\overline{\acute{u}_z\acute{u}_r}}{\partial z} - \overline{\acute{u}_z\acute{u}_r}\frac{\partial \overline{u_r}}{\partial z} - \overline{u_r}\overline{\acute{u}_r\frac{\partial \acute{u}_z}{\partial z}}$$
$$+ \frac{\partial \overline{u_r}\overline{\acute{u}_r\acute{u}_r}}{\partial r} - \overline{\acute{u}_r\acute{u}_r}\frac{\partial \overline{u_r}}{\partial r} - \overline{u_r}\overline{\acute{u}_r\frac{\partial \acute{u}_r}{\partial r}} + \frac{1}{r}\frac{\partial \overline{u_r}\overline{\acute{u}_r\acute{u}_\theta}}{\partial \theta} - \frac{1}{r}\overline{\acute{u}_r\acute{u}_\theta}\frac{\partial \overline{u_r}}{\partial \theta} - \frac{1}{r}\overline{u_r}\overline{\acute{u}_r\frac{\partial \acute{u}_\theta}{\partial \theta}} - \frac{\overline{u_r}\cdot\overline{u_\theta}^2}{r} - \frac{\overline{u_r}\overline{\acute{u}_\theta}^2}{r}$$
$$= -\frac{\overline{u_r}}{\rho}\frac{\partial \overline{p}}{\partial r} + 2\upsilon\left(\frac{\partial \overline{u_r}\overline{S_{rz}}}{\partial z} + \frac{\partial r\overline{u_r}\overline{S_{rr}}}{r\partial r} + \frac{1}{r}\frac{\partial \overline{u_r}\overline{S_{r\theta}}}{\partial \theta} - \overline{S_{rz}}\frac{\partial \overline{u_r}}{\partial z} - \overline{S_{rr}}\frac{\partial \overline{u_r}}{\partial r} - \frac{\overline{S_{r\theta}}}{r}\frac{\partial \overline{u_r}}{\partial \theta} - \frac{\overline{u_r}\overline{S_{\theta\theta}}}{r}\right) \quad \text{(A.12)}$$

$$\overline{u_r}\frac{\partial \overline{u_r}}{\partial t} + \overline{u_r}\cdot\overline{u_z}\frac{\partial \overline{u_r}}{\partial z} + \overline{u_r}^2\frac{\partial \overline{u_r}}{\partial r} + \overline{u_r}\cdot\overline{u_\theta}\frac{\partial \overline{u_z}}{r\partial \theta} + \frac{\partial \overline{u_r}\cdot\overline{\acute{u}_z\acute{u}_r}}{\partial z} - \overline{\acute{u}_z\acute{u}_r}\frac{\partial \overline{u_r}}{\partial z} + \overline{u_r}\overline{\acute{u}_r\frac{\acute{u}_r}{r}}$$
$$+ \frac{\partial \overline{u_r}\overline{\acute{u}_r\acute{u}_r}}{\partial r} - \overline{\acute{u}_r\acute{u}_r}\frac{\partial \overline{u_r}}{\partial r} + \frac{1}{r}\frac{\partial \overline{u_r}\overline{\acute{u}_r\acute{u}_\theta}}{\partial \theta} - \frac{1}{r}\overline{\acute{u}_r\acute{u}_\theta}\frac{\partial \overline{u_r}}{\partial \theta} - \frac{\overline{u_r}\cdot\overline{u_\theta}^2}{r} - \frac{\overline{u_r}\overline{\acute{u}_\theta}^2}{r} \quad \text{(A.13)}$$
$$= -\frac{\overline{u_r}}{\rho}\frac{\partial \overline{p}}{\partial r} + 2\upsilon\left(\frac{\partial \overline{u_r}\overline{S_{rz}}}{\partial z} + \frac{\partial r\overline{u_r}\overline{S_{rr}}}{r\partial r} + \frac{1}{r}\frac{\partial \overline{u_r}\overline{S_{r\theta}}}{\partial \theta} - \overline{S_{rz}}\frac{\partial \overline{u_r}}{\partial z} - \overline{S_{rr}}\frac{\partial \overline{u_r}}{\partial r} - \frac{\overline{S_{r\theta}}}{r}\frac{\partial \overline{u_r}}{\partial \theta} - \frac{\overline{u_r}\overline{S_{\theta\theta}}}{r}\right)$$

$$\overline{u_r}\frac{\partial \overline{u_r}}{\partial t} + \overline{u_r}\cdot\overline{u_z}\frac{\partial \overline{u_r}}{\partial z} + \overline{u_r}^2\frac{\partial \overline{u_r}}{\partial r} + \overline{u_r}\cdot\overline{u_\theta}\frac{\partial \overline{u_z}}{r\partial \theta} + \frac{\partial \overline{u_r}\cdot\overline{\acute{u}_z\acute{u}_r}}{\partial z} - \overline{\acute{u}_z\acute{u}_r}\frac{\partial \overline{u_r}}{\partial z}$$
$$+ \frac{1}{r}\frac{\partial r(\overline{u_r}\overline{\acute{u}_r\acute{u}_r})}{\partial r} - \overline{\acute{u}_r\acute{u}_r}\frac{\partial \overline{u_r}}{\partial r} + \frac{1}{r}\frac{\partial \overline{u_r}\overline{\acute{u}_r\acute{u}_\theta}}{\partial \theta} - \frac{1}{r}\overline{\acute{u}_r\acute{u}_\theta}\frac{\partial \overline{u_r}}{\partial \theta} - \frac{\overline{u_r}\cdot\overline{u_\theta}^2}{r} - \frac{\overline{u_r}\overline{\acute{u}_\theta}^2}{r} = -\frac{\overline{u_r}}{\rho}\frac{\partial \overline{p}}{\partial r} \quad \text{(A.14)}$$
$$+ 2\upsilon\left(\frac{\partial \overline{u_r}\overline{S_{rz}}}{\partial z} + \frac{\partial r\overline{u_r}\overline{S_{rr}}}{r\partial r} + \frac{1}{r}\frac{\partial \overline{u_r}\overline{S_{r\theta}}}{\partial \theta} - \overline{S_{rz}}\frac{\partial \overline{u_r}}{\partial z} - \overline{S_{rr}}\frac{\partial \overline{u_r}}{\partial r} - \frac{\overline{S_{r\theta}}}{r}\frac{\partial \overline{u_r}}{\partial \theta} - \frac{\overline{u_r}\overline{S_{\theta\theta}}}{r}\right)$$

Replacing the velocity components and pressure into equation (3) and averaging we have,

$$\frac{\partial \overline{u_\theta}}{\partial t} + \overline{u_z}\frac{\partial \overline{u_\theta}}{\partial z} + \overline{\acute{u}_z\frac{\partial \acute{u}_\theta}{\partial z}} + \overline{u_r}\frac{\partial \overline{u_\theta}}{\partial r} + \overline{\acute{u}_r\frac{\partial \acute{u}_\theta}{\partial r}} + \overline{u_\theta}\frac{\partial \overline{u_\theta}}{r\partial \theta} + \overline{\acute{u}_\theta\frac{\partial \acute{u}_\theta}{r\partial \theta}} + \frac{\overline{u_\theta}\cdot\overline{u_r}}{r} + \frac{\overline{\acute{u}_\theta\acute{u}_r}}{r} = -\frac{1}{r\rho}\frac{\partial \overline{p}}{\partial \theta} + 2\upsilon\left(\frac{\partial \overline{S_{\theta z}}}{\partial z} + \frac{\partial r\overline{S_{r\theta}}}{r\partial r} + \frac{1}{r}\frac{\partial \overline{S_{\theta\theta}}}{\partial \theta} + \frac{\overline{S_{r\theta}}}{r}\right) \quad \text{(A.15)}$$

Multiplying equation (12) with $\overline{u_\theta}$ we have,

$$\overline{u_\theta}\frac{\partial\overline{u_\theta}}{\partial t}+\overline{u_\theta}\cdot\overline{u_z}\frac{\partial\overline{u_\theta}}{\partial z}+\overline{u_\theta}\cdot\overline{u_r}\frac{\partial\overline{u_\theta}}{\partial r}+\overline{u_\theta}^2\frac{\partial\overline{u_z}}{r\partial\theta}+\overline{u_\theta}(\overline{\acute{u}_z\frac{\partial\acute{u}_\theta}{\partial z}}+\overline{\acute{u}_r\frac{\partial\acute{u}_\theta}{\partial r}}+\overline{\frac{\acute{u}_\theta}{r}\frac{\partial\acute{u}_\theta}{\partial\theta}})+\frac{\overline{u_r}\cdot\overline{u_\theta}^2}{r}+\frac{\overline{u_\theta}\overline{\acute{u}_\theta\acute{u}_r}}{r}$$
$$=-\frac{\overline{u_\theta}}{r\rho}\frac{\partial\overline{p}}{\partial\theta}+2\upsilon(\overline{u_\theta}\frac{\partial\overline{S_{\theta z}}}{\partial z}+\overline{u_\theta}\frac{\partial r\overline{S_{r\theta}}}{r\partial r}+\frac{\overline{u_\theta}}{r}\frac{\partial\overline{S_{\theta\theta}}}{\partial\theta}+\frac{\overline{u_\theta}\overline{S_{r\theta}}}{r})$$

$$\overline{u_\theta}\frac{\partial\overline{u_\theta}}{\partial t}+\overline{u_\theta}\cdot\overline{u_z}\frac{\partial\overline{u_\theta}}{\partial z}+\overline{u_\theta}\cdot\overline{u_r}\frac{\partial\overline{u_\theta}}{\partial r}+\overline{u_\theta}^2\frac{\partial\overline{u_z}}{r\partial\theta}+\frac{\partial\overline{u_\theta}\cdot\overline{\acute{u}_z\acute{u}_\theta}}{\partial z}-\overline{\acute{u}_z\acute{u}_\theta}\frac{\partial\overline{u_\theta}}{\partial z}-\overline{u_\theta}\overline{\acute{u}_\theta\frac{\partial\acute{u}_z}{\partial z}}$$
$$+\frac{\partial\overline{u_\theta}\overline{\acute{u}_r\acute{u}_\theta}}{\partial r}-\overline{\acute{u}_r\acute{u}_\theta}\frac{\partial\overline{u_\theta}}{\partial r}-\overline{u_\theta}\overline{\acute{u}_\theta\frac{\partial\acute{u}_r}{\partial r}}+\frac{1}{r}\frac{\partial\overline{u_\theta}\overline{\acute{u}_\theta\acute{u}_\theta}}{\partial\theta}-\frac{1}{r}\overline{\acute{u}_\theta\acute{u}_\theta}\frac{\partial\overline{u_\theta}}{\partial\theta}-\frac{1}{r}\overline{u_\theta}\overline{\acute{u}_\theta\frac{\partial\acute{u}_\theta}{\partial\theta}}+\frac{\overline{u_r}\cdot\overline{u_\theta}^2}{r}+\frac{\overline{u_\theta}\overline{\acute{u}_\theta\acute{u}_r}}{r}$$
$$=-\frac{\overline{u_\theta}}{r\rho}\frac{\partial\overline{p}}{\partial\theta}+2\upsilon(\frac{\partial\overline{u_\theta}\overline{S_{\theta z}}}{\partial z}+\frac{\partial r\overline{u_\theta}\overline{S_{r\theta}}}{r\partial r}+\frac{1}{r}\frac{\partial\overline{u_\theta}\overline{S_{\theta\theta}}}{\partial\theta}-\overline{S_{\theta z}}\frac{\partial\overline{u_\theta}}{\partial z}-\overline{S_{r\theta}}\frac{\partial\overline{u_\theta}}{\partial r}-\frac{\overline{S_{\theta\theta}}}{r}\frac{\partial\overline{u_\theta}}{\partial\theta}+\frac{\overline{u_\theta}\overline{S_{r\theta}}}{r}) \quad \text{(A.16)}$$

$$\overline{u_\theta}\frac{\partial\overline{u_\theta}}{\partial t}+\overline{u_\theta}\cdot\overline{u_z}\frac{\partial\overline{u_\theta}}{\partial z}+\overline{u_\theta}\cdot\overline{u_r}\frac{\partial\overline{u_\theta}}{\partial r}+\overline{u_\theta}^2\frac{\partial\overline{u_z}}{r\partial\theta}+\frac{\partial\overline{u_\theta}\cdot\overline{\acute{u}_z\acute{u}_\theta}}{\partial z}-\overline{\acute{u}_z\acute{u}_\theta}\frac{\partial\overline{u_\theta}}{\partial z}+\overline{u_\theta}\overline{\acute{u}_\theta\frac{\acute{u}_r}{r}}$$
$$+\frac{\partial\overline{u_\theta}\overline{\acute{u}_r\acute{u}_\theta}}{\partial r}-\overline{\acute{u}_r\acute{u}_\theta}\frac{\partial\overline{u_\theta}}{\partial r}+\frac{1}{r}\frac{\partial\overline{u_\theta}\overline{\acute{u}_\theta\acute{u}_\theta}}{\partial\theta}-\frac{1}{r}\overline{\acute{u}_\theta\acute{u}_\theta}\frac{\partial\overline{u_\theta}}{\partial\theta}+\frac{\overline{u_r}\cdot\overline{u_\theta}^2}{r}+\frac{\overline{u_\theta}\overline{\acute{u}_\theta\acute{u}_r}}{r} \quad \text{(A.17)}$$
$$=-\frac{\overline{u_\theta}}{r\rho}\frac{\partial\overline{p}}{\partial\theta}+2\upsilon(\frac{\partial\overline{u_\theta}\overline{S_{\theta z}}}{\partial z}+\frac{\partial r\overline{u_\theta}\overline{S_{r\theta}}}{r\partial r}+\frac{1}{r}\frac{\partial\overline{u_\theta}\overline{S_{\theta\theta}}}{\partial\theta}-\overline{S_{\theta z}}\frac{\partial\overline{u_\theta}}{\partial z}-\overline{S_{r\theta}}\frac{\partial\overline{u_\theta}}{\partial r}-\frac{\overline{S_{\theta\theta}}}{r}\frac{\partial\overline{u_\theta}}{\partial\theta}+\frac{\overline{u_\theta}\overline{S_{r\theta}}}{r})$$

$$\overline{u_\theta}\frac{\partial\overline{u_\theta}}{\partial t}+\overline{u_\theta}\cdot\overline{u_z}\frac{\partial\overline{u_\theta}}{\partial z}+\overline{u_\theta}\cdot\overline{u_r}\frac{\partial\overline{u_\theta}}{\partial r}+\overline{u_\theta}^2\frac{\partial\overline{u_z}}{r\partial\theta}+\frac{\partial\overline{u_\theta}\cdot\overline{\acute{u}_z\acute{u}_\theta}}{\partial z}-\overline{\acute{u}_z\acute{u}_\theta}\frac{\partial\overline{u_\theta}}{\partial z}$$
$$+\frac{1}{r}\frac{\partial r(\overline{u_\theta}\overline{\acute{u}_r\acute{u}_\theta})}{\partial r}-\overline{\acute{u}_r\acute{u}_\theta}\frac{\partial\overline{u_\theta}}{\partial r}+\frac{1}{r}\frac{\partial\overline{u_\theta}\overline{\acute{u}_\theta\acute{u}_\theta}}{\partial\theta}-\frac{1}{r}\overline{\acute{u}_\theta\acute{u}_\theta}\frac{\partial\overline{u_\theta}}{\partial\theta}+\frac{\overline{u_r}\cdot\overline{u_\theta}^2}{r}+\frac{\overline{u_\theta}\overline{\acute{u}_\theta\acute{u}_r}}{r} \quad \text{(A.18)}$$
$$=-\frac{\overline{u_\theta}}{r\rho}\frac{\partial\overline{p}}{\partial\theta}+2\upsilon(\frac{\partial\overline{u_\theta}\overline{S_{\theta z}}}{\partial z}+\frac{\partial r\overline{u_\theta}\overline{S_{r\theta}}}{r\partial r}+\frac{1}{r}\frac{\partial\overline{u_\theta}\overline{S_{\theta\theta}}}{\partial\theta}-\overline{S_{\theta z}}\frac{\partial\overline{u_\theta}}{\partial z}-\overline{S_{r\theta}}\frac{\partial\overline{u_\theta}}{\partial r}-\frac{\overline{S_{\theta\theta}}}{r}\frac{\partial\overline{u_\theta}}{\partial\theta}+\frac{\overline{u_\theta}\overline{S_{r\theta}}}{r})$$

Adding equation (10), (14) and (18) we have,

(1st terms of LHS)

$$\overline{u_z}\frac{\partial\overline{u_z}}{\partial t}+\overline{u_r}\frac{\partial\overline{u_r}}{\partial t}+\overline{u_\theta}\frac{\partial\overline{u_\theta}}{\partial t}$$

(2nd terms of LHS)

$$+\overline{u_z}(\overline{u_z}\frac{\partial\overline{u_z}}{\partial z}+\overline{u_r}\frac{\partial\overline{u_r}}{\partial z}+\overline{u_\theta}\frac{\partial\overline{u_\theta}}{\partial z})$$

(3rd terms of LHS)

$$+\overline{u_r}(\overline{u_z}\frac{\partial\overline{u_z}}{\partial r}+\overline{u_r}\frac{\partial\overline{u_r}}{\partial r}+\overline{u_\theta}\frac{\partial\overline{u_\theta}}{\partial r})$$

(4th terms of LHS)

$$+\overline{u_\theta}\left(\overline{u_z}\frac{\partial\overline{u_z}}{r\partial\theta}+\overline{u_r}\frac{\partial\overline{u_z}}{r\partial\theta}+\overline{u_\theta}\frac{\partial\overline{u_z}}{r\partial\theta}\right)$$

(5th terms of LHS)

$$+\frac{\partial\left(\overline{u_z}\cdot\overline{\acute{u}_z\acute{u}_z}+\overline{u_r}\cdot\overline{\acute{u}_z\acute{u}_r}+\overline{u_\theta}\cdot\overline{\acute{u}_z\acute{u}_\theta}\right)}{\partial z}$$

(6th terms of LHS)

$$-\overline{\acute{u}_z^{\,2}}\frac{\partial\overline{u_z}}{\partial z}-\overline{\acute{u}_z\acute{u}_r}\frac{\partial\overline{u_r}}{\partial z}-\overline{\acute{u}_z\acute{u}_\theta}\frac{\partial\overline{u_\theta}}{\partial z}$$

(7th terms of LHS)

$$+\frac{1}{r}\frac{\partial\left[r\left(\overline{u_z}\overline{\acute{u}_z\acute{u}_r}+\overline{u_r}\overline{\acute{u}_r\acute{u}_r}+\overline{u_\theta}\overline{\acute{u}_r\acute{u}_\theta}\right)\right]}{\partial r}$$

(8th terms of LHS)

$$-\overline{\acute{u}_z\acute{u}_r}\frac{\partial\overline{u_z}}{\partial r}-\overline{\acute{u}_r\acute{u}_r}\frac{\partial\overline{u_r}}{\partial r}-\overline{\acute{u}_r\acute{u}_\theta}\frac{\partial\overline{u_\theta}}{\partial r}$$

(9th terms of LHS)

$$+\frac{1}{r}\frac{\partial\left(\overline{u_z}\overline{\acute{u}_z\acute{u}_\theta}+\overline{u_r}\overline{\acute{u}_r\acute{u}_\theta}+\overline{u_\theta}\overline{\acute{u}_\theta\acute{u}_\theta}\right)}{\partial\theta}$$

(10th terms of LHS of eqn 2 and 3)

$$-\frac{1}{r}\overline{\acute{u}_z\acute{u}_\theta}\frac{\partial\overline{u_z}}{\partial\theta}-\frac{1}{r}\overline{\acute{u}_r\acute{u}_\theta}\frac{\partial\overline{u_r}}{\partial\theta}-\frac{1}{r}\overline{\acute{u}_\theta\acute{u}_\theta}\frac{\partial\overline{u_\theta}}{\partial\theta}$$

(Last terms from LHS of equations)

$$-\frac{\overline{u_r}\overline{\acute{u}_\theta^{\,2}}}{r}+\frac{\overline{u_\theta}\overline{\acute{u}_\theta\acute{u}_r}}{r}=$$

(1st terms of RHS)

$$-\frac{1}{\rho}\left(\frac{\partial\overline{u_z}\cdot\overline{p}}{\partial z}+\frac{1}{r}\frac{\partial\left(r\overline{u_r}\cdot\overline{p}\right)}{\partial r}+\frac{1}{r}\frac{\partial\overline{u_\theta}\cdot\overline{p}}{\partial\theta}\right)$$

(2nd terms of RHS)

$$+2\upsilon\left(\frac{\partial\overline{u_z}\overline{S_{zz}}}{\partial z}+\frac{\partial\overline{u_r}\overline{S_{rz}}}{\partial z}+\frac{\partial\overline{u_\theta}\overline{S_{\theta z}}}{\partial z}\right.$$

(3rd terms of RHS)

$$+\frac{\partial r\overline{u_z}\overline{S_{zr}}}{r\partial r}+\frac{\partial r\overline{u_r}\overline{S_{rr}}}{r\partial r}+\frac{\partial r\overline{u_\theta}\overline{S_{\theta r}}}{r\partial r}$$

(4th terms of RHS)

$$+\frac{1}{r}\frac{\partial\overline{u_z}\overline{S_{z\theta}}}{\partial\theta}+\frac{1}{r}\frac{\partial\overline{u_r}\overline{S_{r\theta}}}{\partial\theta}+\frac{1}{r}\frac{\partial\overline{u_\theta}\overline{S_{\theta\theta}}}{\partial\theta}$$

(5th terms of RHS)

$$-\overline{S_{zz}}\frac{\partial\overline{u_z}}{\partial z}-\overline{S_{rz}}\frac{\partial\overline{u_r}}{\partial z}-\overline{S_{z\theta}}\frac{\partial\overline{u_\theta}}{\partial z}$$

(6th terms of RHS)

$$-\overline{S_{zr}}\frac{\partial\overline{u_z}}{\partial r}-\overline{S_{rr}}\frac{\partial\overline{u_r}}{\partial r}-\overline{S_{r\theta}}\frac{\partial\overline{u_\theta}}{\partial r}$$

(7th terms of RHS)

$$-\frac{\overline{S_{z\theta}}}{r}\frac{\partial\overline{u_z}}{\partial\theta}-\frac{\overline{S_{r\theta}}}{r}\frac{\partial\overline{u_r}}{\partial\theta}-\frac{\overline{S_{\theta\theta}}}{r}\frac{\partial\overline{u_\theta}}{\partial\theta})$$

(8th terms of RHS) (A.19)

$$-\frac{\overline{u_r}\overline{S_{\theta\theta}}}{r}+\frac{\overline{u_\theta}\overline{S_{r\theta}}}{r}$$

Rearranging the terms we have,

$$\begin{aligned}
&\frac{\partial Q}{\partial t}+\overline{u_z}\frac{\partial Q}{\partial z}+\overline{u_r}\frac{\partial Q}{\partial r}+\frac{\overline{u_\theta}}{r}\frac{\partial Q}{\partial\theta}\\
&=-\frac{1}{\rho}(\frac{\partial\overline{u_z}\cdot\overline{p}}{\partial z}+\frac{1}{r}\frac{\partial(r\overline{u_r}\cdot\overline{p})}{\partial r}+\frac{1}{r}\frac{\partial\overline{u_\theta}\cdot\overline{p}}{\partial\theta})\\
&-\frac{\partial(\overline{u_z}\cdot\overline{u_z'u_z'}+\overline{u_r}\cdot\overline{u_z'u_r'}+\overline{u_\theta}\cdot\overline{u_z'u_\theta'})}{\partial z}\\
&+\overline{u_z'^2}\frac{\partial\overline{u_z}}{\partial z}+\overline{u_z'u_r'}\frac{\partial\overline{u_r}}{\partial z}+\overline{u_z'u_\theta'}\frac{\partial\overline{u_\theta}}{\partial z}\\
&-\frac{1}{r}\frac{\partial[r(\overline{u_z}\overline{u_z'u_r'}+\overline{u_r}\overline{u_r'u_r'}+\overline{u_\theta}\overline{u_r'u_\theta'})]}{\partial r}\\
&+\overline{u_z'u_r'}\frac{\partial\overline{u_z}}{\partial r}+\overline{u_r'u_r'}\frac{\partial\overline{u_r}}{\partial r}+\overline{u_r'u_\theta'}\frac{\partial\overline{u_\theta}}{\partial r}\\
&-\frac{1}{r}\frac{\partial(\overline{u_z}\overline{u_z'u_\theta'}+\overline{u_r}\overline{u_r'u_\theta'}+\overline{u_\theta}\overline{u_\theta'u_\theta'})}{\partial\theta}\\
&+\frac{1}{r}\overline{u_z'u_\theta'}\frac{\partial\overline{u_z}}{\partial\theta}+\frac{1}{r}\overline{u_r'u_\theta'}\frac{\partial\overline{u_r}}{\partial\theta}+\frac{1}{r}\overline{u_\theta'u_\theta'}\frac{\partial\overline{u_\theta}}{\partial\theta}\\
&+\frac{\overline{u_r}\overline{u_\theta'^2}}{r}-\frac{\overline{u_\theta}\overline{u_\theta'u_r'}}{r}\\
&+2\upsilon(\frac{\partial\overline{u_z}\overline{S_{zz}}}{\partial z}+\frac{\partial\overline{u_r}\overline{S_{rz}}}{\partial z}+\frac{\partial\overline{u_\theta}\overline{S_{\theta z}}}{\partial z}\\
&+\frac{\partial r\overline{u_z}\overline{S_{zr}}}{r\partial r}+\frac{\partial r\overline{u_r}\overline{S_{rr}}}{r\partial r}+\frac{\partial r\overline{u_\theta}\overline{S_{\theta r}}}{r\partial r}\\
&+\frac{1}{r}\frac{\partial\overline{u_z}\overline{S_{z\theta}}}{\partial\theta}+\frac{1}{r}\frac{\partial\overline{u_r}\overline{S_{r\theta}}}{\partial\theta}+\frac{1}{r}\frac{\partial\overline{u_\theta}\overline{S_{\theta\theta}}}{\partial\theta}\\
&-\overline{S_{zz}}\frac{\partial\overline{u_z}}{\partial z}-\overline{S_{rz}}\frac{\partial\overline{u_r}}{\partial z}-\overline{S_{z\theta}}\frac{\partial\overline{u_\theta}}{\partial z}\\
&-\overline{S_{zr}}\frac{\partial\overline{u_z}}{\partial r}-\overline{S_{rr}}\frac{\partial\overline{u_r}}{\partial r}-\overline{S_{r\theta}}\frac{\partial\overline{u_\theta}}{\partial r}\\
&-\frac{\overline{S_{z\theta}}}{r}\frac{\partial\overline{u_z}}{\partial\theta}-\frac{\overline{S_{r\theta}}}{r}\frac{\partial\overline{u_r}}{\partial\theta}-\frac{\overline{S_{\theta\theta}}}{r}\frac{\partial\overline{u_\theta}}{\partial\theta}\\
&-\frac{\overline{u_r}\overline{S_{\theta\theta}}}{r}+\frac{\overline{u_\theta}\overline{S_{r\theta}}}{r})
\end{aligned}$$

where, $Q=(\overline{u_z}^2+\overline{u_r}^2+\overline{u_\theta}^2)/2$

Multiplying equations (2),(3) and (4) with $u_z$,$u_r$ and $u_\theta$ respectively, we have

Along the 3 directions-

**Axial direction**

$$u_z\frac{\partial u_z}{\partial t}+u_z u_z\frac{\partial u_z}{\partial z}+u_z u_r\frac{\partial u_z}{\partial r}+\frac{u_z u_\theta}{r}\frac{\partial u_z}{\partial \theta}=-u_z\frac{1}{\rho}\frac{\partial p}{\partial z}+$$
$$2v[u_z\frac{\partial S_{zz}}{\partial z}+u_z\frac{\partial (rS_{rz})}{r\partial r}+\frac{u_z}{r}\frac{\partial S_{z\theta}}{\partial \theta}]$$

The terms in red add to 0 due to the continuity equation,

$$u_z\frac{\partial u_z}{\partial t}+\frac{1}{2}(2u_z u_z\frac{\partial u_z}{\partial z}+2u_z u_r\frac{\partial u_z}{\partial r}+\frac{2u_z u_\theta}{r}\frac{\partial u_z}{\partial \theta})$$
$$+\frac{u_z^2}{2}(\frac{\partial u_z}{\partial z}+\frac{\partial u_r}{\partial r}+\frac{1}{r}\frac{\partial u_\theta}{\partial \theta}+\frac{u_r}{r})=-u_z\frac{1}{\rho}\frac{\partial p}{\partial z}$$
$$2v[\frac{\partial u_z S_{zz}}{\partial z}+\frac{\partial (ru_z S_{rz})}{r\partial r}+\frac{1}{r}\frac{\partial u_z S_{z\theta}}{\partial \theta}-S_{zz}\frac{\partial u_z}{\partial z}-S_{zr}\frac{\partial u_z}{\partial r}-\frac{S_{z\theta}}{r}\frac{\partial u_z}{\partial \theta}]$$

$$u_z\frac{\partial u_z}{\partial t}+\frac{1}{2}(2u_z u_z\frac{\partial u_z}{\partial z}+u_z^2\frac{\partial u_z}{\partial z}+2u_z u_r\frac{\partial u_z}{\partial r}+u_z^2\frac{\partial u_r}{\partial r}+\frac{2u_z u_\theta}{r}\frac{\partial u_z}{\partial \theta}+\frac{u_z^2}{r}\frac{\partial u_\theta}{\partial \theta}+u_z^2\frac{u_r}{r})=$$
$$-u_z\frac{1}{\rho}\frac{\partial p}{\partial z}+2v[\frac{\partial u_z S_{zz}}{\partial z}+\frac{\partial (ru_z S_{rz})}{r\partial r}+\frac{1}{r}\frac{\partial u_z S_{z\theta}}{\partial \theta}-S_{zz}\frac{\partial u_z}{\partial z}-S_{zr}\frac{\partial u_z}{\partial r}-\frac{S_{z\theta}}{r}\frac{\partial u_z}{\partial \theta}]$$

$$\frac{1}{2}(\frac{\partial u_z^2}{\partial t}+\frac{\partial u_z^2 u_z}{\partial z}+\frac{\partial u_z^2 u_r}{\partial r}+\frac{1}{r}\frac{\partial u_z^2 u_\theta}{\partial \theta}+u_z^2\frac{u_r}{r})=-u_z\frac{1}{\rho}\frac{\partial p}{\partial z}+$$
$$2v[\frac{\partial u_z S_{zz}}{\partial z}+\frac{\partial (ru_z S_{rz})}{r\partial r}+\frac{1}{r}\frac{\partial u_z S_{z\theta}}{\partial \theta}-S_{zz}\frac{\partial u_z}{\partial z}-S_{zr}\frac{\partial u_z}{\partial r}-\frac{S_{z\theta}}{r}\frac{\partial u_z}{\partial \theta}] \quad \text{(A.20)}$$

**Radial Direction**

$$u_r\frac{\partial u_r}{\partial t}+u_r u_z\frac{\partial u_r}{\partial x}+u_r u_r\frac{\partial u_r}{\partial r}+\frac{u_r u_\theta}{r}\frac{\partial u_r}{\partial \theta}-\frac{u_r u_\theta^2}{r}=-\frac{u_r}{\rho}\frac{\partial p}{\partial r}+$$
$$2v[u_r\frac{\partial S_{zr}}{\partial z}+u_r\frac{\partial (rS_{rr})}{r\partial r}+\frac{u_r}{r}\frac{\partial S_{r\theta}}{\partial \theta}-u_r\frac{S_{\theta\theta}}{r}]$$

$$u_r\frac{\partial u_r}{\partial t}+\frac{1}{2}(2u_r u_z\frac{\partial u_r}{\partial x}+2u_r u_r\frac{\partial u_r}{\partial r}+\frac{2u_r u_\theta}{r}\frac{\partial u_r}{\partial \theta}-\frac{2u_r u_\theta^2}{r})+\frac{u_r^2}{2}(\frac{\partial u_z}{\partial z}+\frac{\partial u_r}{\partial r}+\frac{1}{r}\frac{\partial u_\theta}{\partial \theta}+\frac{u_r}{r})$$
$$=-\frac{u_r}{\rho}\frac{\partial p}{\partial r}+2v[\frac{\partial u_r S_{rz}}{\partial z}+\frac{\partial r u_r S_{rr}}{r\partial r}+\frac{1}{r}\frac{\partial u_r S_{r\theta}}{\partial \theta}-S_{rz}\frac{\partial u_r}{\partial z}-S_{rr}\frac{\partial u_r}{\partial r}-\frac{S_{r\theta}}{r}\frac{\partial u_r}{\partial \theta}-\frac{u_r S_{\theta\theta}}{r}]$$

$$u_r\frac{\partial u_r}{\partial t}+\frac{1}{2}(2u_r u_z\frac{\partial u_r}{\partial z}+u_r^2\frac{\partial u_z}{\partial z}+2u_r u_r\frac{\partial u_r}{\partial r}+u_r^2\frac{\partial u_r}{\partial r}+\frac{2u_r u_\theta}{r}\frac{\partial u_r}{\partial \theta}+\frac{u_r^2}{r}\frac{\partial u_\theta}{\partial \theta}-\frac{2u_r u_\theta^2}{r}+u_r^2\frac{u_r}{r})$$
$$=-\frac{u_r}{\rho}\frac{\partial p}{\partial r}+2v[\frac{\partial u_r S_{rz}}{\partial z}+\frac{\partial r u_r S_{rr}}{r\partial r}+\frac{1}{r}\frac{\partial u_r S_{r\theta}}{\partial \theta}-S_{rz}\frac{\partial u_r}{\partial z}-S_{rr}\frac{\partial u_r}{\partial r}-\frac{S_{r\theta}}{r}\frac{\partial u_r}{\partial \theta}-\frac{u_r S_{\theta\theta}}{r}]$$

$$\frac{1}{2}(\frac{\partial u_r^2}{\partial t}+\frac{\partial u_r^2 u_z}{\partial z}+\frac{\partial u_z^2 u_2}{\partial r}+\frac{1}{r}\frac{\partial u_r^2 u_\theta}{\partial \theta}+\frac{u_r(u_r^2-2u_\theta^2)}{r})=-\frac{u_r}{\rho}\frac{\partial p}{\partial r}+$$
$$2v[\frac{\partial u_r S_{rz}}{\partial z}+\frac{\partial r u_r S_{rr}}{r\partial r}+\frac{1}{r}\frac{\partial u_r S_{r\theta}}{\partial \theta}-S_{rz}\frac{\partial u_r}{\partial z}-S_{rr}\frac{\partial u_r}{\partial r}-\frac{S_{r\theta}}{r}\frac{\partial u_r}{\partial \theta}-\frac{u_r S_{\theta\theta}}{r}] \quad \text{(A.21)}$$

**Tangential Direction**

$$u_\theta\frac{\partial u_\theta}{\partial t}+u_\theta u_z\frac{\partial u_\theta}{\partial z}+u_\theta u_r\frac{\partial u_\theta}{\partial r}+\frac{u_\theta u_\theta}{r}\frac{\partial u_\theta}{\partial \theta}+\frac{u_r u_\theta^2}{r}=-\frac{u_\theta}{\rho r}\frac{\partial p}{\partial \theta}+$$
$$2\upsilon[u_\theta\frac{\partial S_{z\theta}}{\partial z}+u_\theta\frac{\partial(rS_{r\theta})}{r\partial r}+\frac{u_\theta}{r}\frac{\partial S_{\theta\theta}}{\partial \theta}+u_\theta\frac{S_{r\theta}}{r}]$$

$$u_\theta\frac{\partial u_\theta}{\partial t}+\frac{1}{2}(2u_\theta u_z\frac{\partial u_\theta}{\partial z}+2u_\theta u_r\frac{\partial u_\theta}{\partial r}+\frac{2u_\theta u_\theta}{r}\frac{\partial u_\theta}{\partial \theta}+\frac{2u_r u_\theta^2}{r})+\frac{u_\theta^2}{2}(\frac{\partial u_z}{\partial z}+\frac{\partial u_r}{\partial r}+\frac{1}{r}\frac{\partial u_\theta}{\partial \theta}+\frac{u_r}{r})$$
$$=-\frac{u_\theta}{\rho r}\frac{\partial p}{\partial \theta}+2\upsilon[\frac{\partial u_\theta S_{\theta z}}{\partial z}+\frac{\partial r u_\theta S_{r\theta}}{r\partial r}+\frac{1}{r}\frac{\partial u_\theta S_{\theta\theta}}{\partial \theta}-S_{\theta z}\frac{\partial u_\theta}{\partial z}-S_{r\theta}\frac{\partial u_\theta}{\partial r}-\frac{S_{\theta\theta}}{r}\frac{\partial u_\theta}{\partial \theta}+\frac{u_\theta S_{r\theta}}{r}]$$

$$u_\theta\frac{\partial u_\theta}{\partial t}+\frac{1}{2}(2u_\theta u_z\frac{\partial u_\theta}{\partial z}+u_\theta^2\frac{\partial u_z}{\partial z}+2u_\theta u_r\frac{\partial u_\theta}{\partial r}+u_\theta^2\frac{\partial u_r}{\partial r}+\frac{2u_\theta u_\theta}{r}\frac{\partial u_\theta}{\partial \theta}+\frac{u_\theta^2}{r}\frac{\partial u_\theta}{\partial \theta}+\frac{3u_r u_\theta^2}{r})=$$
$$-\frac{u_\theta}{\rho r}\frac{\partial p}{\partial \theta}+2\upsilon[\frac{\partial u_\theta S_{\theta z}}{\partial z}+\frac{\partial r u_\theta S_{r\theta}}{r\partial r}+\frac{1}{r}\frac{\partial u_\theta S_{\theta\theta}}{\partial \theta}-S_{\theta z}\frac{\partial u_\theta}{\partial z}-S_{r\theta}\frac{\partial u_\theta}{\partial r}-\frac{S_{\theta\theta}}{r}\frac{\partial u_\theta}{\partial \theta}+\frac{u_\theta S_{r\theta}}{r}]$$

$$\frac{1}{2}(\frac{\partial u_\theta^2}{\partial t}+\frac{\partial u_z u_\theta^2}{\partial z}+\frac{\partial u_r u_\theta^2}{\partial r}+\frac{1}{r}\frac{\partial u_\theta u_\theta^2}{\partial \theta}+\frac{3u_r u_\theta^2}{r})=-\frac{u_\theta}{\rho r}\frac{\partial p}{\partial \theta}+$$
$$2\upsilon[\frac{\partial u_\theta S_{\theta z}}{\partial z}+\frac{\partial r u_\theta S_{r\theta}}{r\partial r}+\frac{1}{r}\frac{\partial u_\theta S_{\theta\theta}}{\partial \theta}-S_{\theta z}\frac{\partial u_\theta}{\partial z}-S_{r\theta}\frac{\partial u_\theta}{\partial r}-\frac{S_{\theta\theta}}{r}\frac{\partial u_\theta}{\partial \theta}+\frac{u_\theta S_{r\theta}}{r}] \quad (A.22)$$

Replacing the mean and fluctuating velocity components and pressure into equation (20),(21) and (22) and averaging we have,

The total energy equation in the axial direction is,

$$\frac{1}{2}\frac{\partial\overline{u_z}^2}{\partial t}+\frac{1}{2}\frac{\partial\overline{u\acute{}_z^{\,2}}}{\partial t}+\frac{3\overline{u_z}^2}{2}\frac{\partial\overline{u_z}}{\partial z}+\frac{3}{2}\frac{\partial\overline{u\acute{}_z^{\,2}}\,\overline{u_z}}{\partial z}+\frac{1}{2}\frac{\partial\overline{u\acute{}_z^{\,3}}}{\partial z}+\overline{u_z}\cdot\overline{u_r}\frac{\partial\overline{u_z}}{\partial r}+\frac{\overline{u_z}^2}{2}\frac{\partial\overline{u_r}}{\partial r}+\frac{1}{2}\frac{\partial\overline{u\acute{}_z^{\,2}}\,\overline{u_r}}{\partial r}$$
$$+\frac{\partial\overline{u_z}\,\overline{u\acute{}_z u\acute{}_r}}{\partial r}+\frac{1}{2}\frac{\partial\overline{u\acute{}_z^{\,2}u\acute{}_r}}{\partial r}+\frac{\overline{u_z}\cdot\overline{u_\theta}}{r}\frac{\partial\overline{u_z}}{\partial\theta}+\frac{\overline{u_z}^2}{2r}\frac{\partial\overline{u_\theta}}{\partial\theta}+\frac{1}{2}\frac{\partial\overline{u\acute{}_z^{\,2}}\,\overline{u_\theta}}{r\partial\theta}+\frac{\partial\overline{u_z}\,\overline{u\acute{}_z u\acute{}_\theta}}{r\partial\theta}+\frac{1}{2}\frac{\partial\overline{u\acute{}_z^{\,2}u\acute{}_\theta}}{r\partial\theta}$$
$$+\frac{\overline{u_z}^2\overline{u_r}}{2r}+\frac{\overline{u\acute{}_z^{\,2}u_r}}{2r}+\frac{\overline{u_z}\,\overline{u\acute{}_z u\acute{}_r}}{r}+\frac{\overline{u\acute{}_z^{\,2}u\acute{}_r}}{2r}=-\frac{\overline{u_z}}{\rho}\frac{\partial\overline{p}}{\partial z}-\frac{\overline{u\acute{}_z}}{\rho}\frac{\partial\overline{p\acute{}}}{\partial z}+2\upsilon[\frac{\partial\overline{u_z}\,\overline{S_{zz}}}{\partial z}+\frac{\partial r\overline{u_z}\,\overline{S_{zr}}}{r\partial r}+ \quad (A.23)$$
$$\frac{1}{r}\frac{\partial\overline{u_z}\,\overline{S_{z\theta}}}{\partial\theta}-\overline{S_{zz}}\frac{\partial\overline{u_z}}{\partial z}-\overline{S_{zr}}\frac{\partial\overline{u_z}}{\partial r}-\frac{\overline{S_{z\theta}}}{r}\frac{\partial\overline{u_z}}{\partial\theta}+\frac{\partial\overline{u\acute{}_z S\acute{}_{zz}}}{\partial z}+\frac{\partial r\overline{u\acute{}_z S\acute{}_{zr}}}{r\partial r}+$$
$$\frac{1}{r}\frac{\partial\overline{u\acute{}_z S\acute{}_{z\theta}}}{\partial\theta}-\overline{S\acute{}_{zz}}\frac{\partial\overline{u\acute{}_z}}{\partial z}-\overline{S\acute{}_{zr}}\frac{\partial\overline{u\acute{}_z}}{\partial r}-\frac{\overline{S\acute{}_{z\theta}}}{r}\frac{\partial\overline{u\acute{}_z}}{\partial\theta}]$$

From equation (8), we have

$$\overline{u_z}\frac{\partial\overline{u_z}}{\partial t}+\overline{u_z}^2\frac{\partial\overline{u_z}}{\partial z}+\overline{u_z}\cdot\overline{u_r}\frac{\partial\overline{u_z}}{\partial r}+\overline{u_z}\cdot\overline{u_\theta}\frac{\partial\overline{u_z}}{r\partial\theta}+\frac{\partial\overline{u_z}\cdot\overline{u\acute{}_z u\acute{}_z}}{\partial z}-\overline{u\acute{}_z^{\,2}}\frac{\partial\overline{u_z}}{\partial z}-\overline{u_z}\overline{u\acute{}_z}\frac{\partial\overline{u\acute{}_z}}{\partial z}$$
$$+\frac{\partial\overline{u_z}\,\overline{u\acute{}_z u\acute{}_r}}{\partial r}-\overline{u\acute{}_z u\acute{}_r}\frac{\partial\overline{u_z}}{\partial r}-\overline{u_z}\overline{u\acute{}_z}\frac{\partial\overline{u\acute{}_r}}{\partial r}+\frac{1}{r}\frac{\partial\overline{u_z}\,\overline{u\acute{}_z u\acute{}_\theta}}{\partial\theta}-\frac{1}{r}\overline{u\acute{}_z u\acute{}_\theta}\frac{\partial\overline{u_z}}{\partial\theta}-\frac{1}{r}\overline{u_z}\overline{u\acute{}_z}\frac{\partial\overline{u\acute{}_\theta}}{\partial\theta}$$
$$=-\frac{\overline{u_z}}{\rho}\frac{\partial\overline{p}}{\partial z}+2\upsilon(\frac{\partial\overline{u_z}\,\overline{S_{zz}}}{\partial z}+\frac{\partial r\overline{u_z}\,\overline{S_{zr}}}{r\partial r}+\frac{1}{r}\frac{\partial\overline{u_z}\,\overline{S_{z\theta}}}{\partial\theta}-\overline{S_{zz}}\frac{\partial\overline{u_z}}{\partial z}-\overline{S_{zr}}\frac{\partial\overline{u_z}}{\partial r}-\frac{\overline{S_{z\theta}}}{r}\frac{\partial\overline{u_z}}{\partial\theta})$$

On subtracting eqn (8) from (23), we have

( The terms in red, green and blue each add to 0 due to the continuity equation)

$$\frac{1}{2}\frac{\partial\overline{u_z'^2}}{\partial t}+\frac{\overline{u_z}^2}{2}\frac{\partial\overline{u_z}}{\partial z}+\frac{\overline{u_z'^2}}{2}\frac{\partial\overline{u_z}}{\partial z}+\frac{\overline{u_z}}{2}\frac{\partial\overline{u_z'^2}}{\partial z}+\frac{1}{2}\frac{\partial\overline{u_z'^3}}{\partial z}+\overline{u_z'^2}\frac{\partial\overline{u_z}}{\partial z}+\overline{u_z}\overline{u_z'\frac{\partial u_z'}{\partial z}}+\frac{\overline{u_z}^2}{2}\frac{\partial\overline{u_r}}{\partial r}+\frac{\overline{u_z'^2}}{2}\frac{\partial\overline{u_r}}{\partial r}+\frac{\overline{u_r}}{2}\frac{\partial\overline{u_z'^2}}{\partial r}$$
$$+\frac{1}{2}\frac{\partial\overline{u_z'^2u_r'}}{\partial r}+\overline{u_z'u_r'}\frac{\partial\overline{u_z}}{\partial r}+\overline{u_z}\overline{u_z'\frac{\partial u_r'}{\partial r}}+\frac{\overline{u_z}^2}{2r}\frac{\partial\overline{u_\theta}}{\partial\theta}+\frac{\overline{u_z'^2}}{2}\frac{\partial\overline{u_\theta}}{r\partial\theta}+\frac{\overline{u_\theta}}{2}\frac{\partial\overline{u_z'^2}}{r\partial\theta}+\frac{1}{2}\frac{\partial\overline{u_z'^2u_\theta'}}{r\partial\theta}+\frac{1}{r}\overline{u_z'u_\theta'}\frac{\partial\overline{u_z}}{\partial\theta}$$
$$+\frac{1}{r}\overline{u_z}\overline{u_z'\frac{\partial u_\theta'}{\partial\theta}}+\frac{\overline{u_z}^2\overline{u_r}}{2r}+\frac{\overline{u_z'^2}\overline{u_r}}{2r}+\frac{\overline{u_z}\overline{u_z'u_r'}}{r}+\frac{\overline{u_z'^2u_r'}}{2r}=-\overline{\frac{u_z'}{\rho}\frac{\partial p'}{\partial z}}+2\upsilon[\frac{\partial\overline{u_z'S_{zz}'}}{\partial z}+\frac{\partial r\overline{u_z'S_{zr}'}}{r\partial r}+$$
$$\frac{1}{r}\frac{\partial\overline{u_z'S_{z\theta}'}}{\partial\theta}-\overline{S_{zz}'\frac{\partial u_z'}{\partial z}}-\overline{S_{zr}'\frac{\partial u_z'}{\partial r}}-\overline{\frac{S_{z\theta}'}{r}\frac{\partial u_z'}{\partial\theta}}]$$

(A.24)

$$\frac{1}{2}\frac{\partial\overline{u_z'^2}}{\partial t}+\frac{\overline{u_z}}{2}\frac{\partial\overline{u_z'^2}}{\partial z}+\frac{1}{2}\frac{\partial\overline{u_z'^3}}{\partial z}+\overline{u_z'^2}\frac{\partial\overline{u_z}}{\partial z}+\frac{\overline{u_r}}{2}\frac{\partial\overline{u_z'^2}}{\partial r}+\frac{1}{2}\frac{\partial\overline{u_z'^2u_r'}}{\partial r}+\overline{u_z'u_r'}\frac{\partial\overline{u_z}}{\partial r}$$
$$+\frac{\overline{u_\theta}}{2}\frac{\partial\overline{u_z'^2}}{r\partial\theta}+\frac{1}{2}\frac{\partial\overline{u_z'^2u_\theta'}}{r\partial\theta}+\frac{1}{r}\overline{u_z'u_\theta'}\frac{\partial\overline{u_z}}{\partial\theta}+\frac{\overline{u_z'^2u_r'}}{2r}=\overline{\frac{p'}{\rho}\frac{\partial u_z'}{\partial z}}-\overline{\frac{1}{\rho}\frac{\partial u_z'p'}{\partial z}}+2\upsilon[\frac{\partial\overline{u_z'S_{zz}'}}{\partial z}+\frac{\partial r\overline{u_z'S_{zr}'}}{r\partial r}+$$
$$\frac{1}{r}\frac{\partial\overline{u_z'S_{z\theta}'}}{\partial\theta}-\overline{S_{zz}'\frac{\partial u_z'}{\partial z}}-\overline{S_{zr}'\frac{\partial u_z'}{\partial r}}-\overline{\frac{S_{z\theta}'}{r}\frac{\partial u_z'}{\partial\theta}}]$$

(A.25)

The total energy equation in the radial direction is as follows,

$$\frac{1}{2}\frac{\partial\overline{u_r}^2}{\partial t}+\frac{1}{2}\frac{\partial\overline{u_r'^2}}{\partial t}+\overline{u_r}\cdot\overline{u_z}\frac{\partial\overline{u_r}}{\partial z}+\frac{\overline{u_r}^2}{2}\frac{\partial\overline{u_z}}{\partial z}+\frac{1}{2}\frac{\partial\overline{u_r'^2}\overline{u_z}}{\partial z}+\frac{\partial\overline{u_r}\overline{u_r'u_z'}}{\partial z}+\frac{1}{2}\frac{\partial\overline{u_r'^2u_z'}}{\partial z}$$
$$+\frac{3\overline{u_r}^2}{2}\frac{\partial\overline{u_r}}{\partial r}+\frac{3}{2}\frac{\partial\overline{u_r'^2}\overline{u_r}}{\partial r}+\frac{1}{2}\frac{\partial\overline{u_r'^3}}{\partial r}+\frac{\overline{u_r}\cdot\overline{u_\theta}}{r}\frac{\partial\overline{u_r}}{\partial\theta}+\frac{\overline{u_r}^2}{2r}\frac{\partial\overline{u_\theta}}{\partial\theta}+\frac{1}{2}\frac{\partial\overline{u_r'^2}\overline{u_\theta}}{r\partial\theta}$$
$$+\frac{\partial\overline{u_r}\overline{u_r'u_\theta'}}{r\partial\theta}+\frac{1}{2}\frac{\partial\overline{u_r'^2u_\theta'}}{r\partial\theta}+\frac{\overline{u_r}^3}{2r}+\frac{\overline{u_r}\overline{u_r'^2}}{2r}-\frac{\overline{u_r}\cdot\overline{u_\theta}^2}{r}-\frac{\overline{u_r}\cdot\overline{u_\theta'^2}}{r}+\frac{\overline{u_r'^3}}{2r}+\frac{\overline{u_r}\overline{u_r'^2}}{r}$$
$$-\frac{\overline{u_\theta'^2u_r'}}{r}-\frac{2\overline{u_\theta}\overline{u_\theta'u_r'}}{r}=-\frac{\overline{u_r}}{\rho}\frac{\partial\overline{p}}{\partial r}-\overline{\frac{u_r'}{\rho}\frac{\partial p'}{\partial r}}+2\upsilon[\frac{\partial\overline{u_r}\overline{S_{rz}}}{\partial z}+\frac{\partial r\overline{u_r}\overline{S_{rr}}}{r\partial r}+\frac{1}{r}\frac{\partial\overline{u_r}\overline{S_{r\theta}}}{\partial\theta}$$
$$-\overline{S_{rz}}\frac{\partial\overline{u_r}}{\partial z}-\overline{S_{rr}}\frac{\partial\overline{u_r}}{\partial r}-\frac{\overline{S_{r\theta}}}{r}\frac{\partial\overline{u_r}}{\partial\theta}-\frac{\overline{u_r}\overline{S_{\theta\theta}}}{r}+\frac{\partial\overline{u_r'S_{rz}'}}{\partial z}+\frac{\partial r\overline{u_r'S_{rr}'}}{r\partial r}+\frac{1}{r}\frac{\partial\overline{u_r'S_{r\theta}'}}{\partial\theta}$$
$$-\overline{S_{rz}'\frac{\partial u_r'}{\partial z}}-\overline{S_{rr}'\frac{\partial u_r'}{\partial r}}-\overline{\frac{S_{r\theta}'}{r}\frac{\partial u_r'}{\partial\theta}}-\overline{\frac{u_r'S_{\theta\theta}'}{r}}]$$

(A.26)

From equation (12) we have

$$\frac{1}{2}\frac{\partial\overline{u_r}^2}{\partial t}+\overline{u_r}\cdot\overline{u_z}\frac{\partial\overline{u_r}}{\partial z}+\overline{u_r}^2\frac{\partial\overline{u_r}}{\partial r}+\overline{u_r}\cdot\overline{u_\theta}\frac{\partial\overline{u_z}}{r\partial\theta}+\frac{\partial\overline{u_r}\cdot\overline{u_z'u_r'}}{\partial z}-\overline{u_z'u_r'}\frac{\partial\overline{u_r}}{\partial z}-\overline{u_r}\overline{u_r'\frac{\partial u_z'}{\partial z}}$$
$$+\frac{\partial\overline{u_r}\overline{u_r'u_r'}}{\partial r}-\overline{u_r'u_r'}\frac{\partial\overline{u_r}}{\partial r}-\overline{u_r}\overline{u_r'\frac{\partial u_r'}{\partial r}}+\frac{1}{r}\frac{\partial\overline{u_r}\overline{u_r'u_\theta'}}{\partial\theta}-\frac{1}{r}\overline{u_r'u_\theta'}\frac{\partial\overline{u_r}}{\partial\theta}-\frac{1}{r}\overline{u_r}\overline{u_r'\frac{\partial u_\theta'}{\partial\theta}}-\frac{\overline{u_r}\cdot\overline{u_\theta}^2}{r}-\frac{\overline{u_r}\overline{u_\theta'^2}}{r}$$
$$=-\frac{\overline{u_r}}{\rho}\frac{\partial\overline{p}}{\partial r}+2\upsilon(\frac{\partial\overline{u_r}\overline{S_{rz}}}{\partial z}+\frac{\partial r\overline{u_r}\overline{S_{rr}}}{r\partial r}+\frac{1}{r}\frac{\partial\overline{u_r}\overline{S_{r\theta}}}{\partial\theta}-\overline{S_{rz}}\frac{\partial\overline{u_r}}{\partial z}-\overline{S_{rr}}\frac{\partial\overline{u_r}}{\partial r}-\frac{\overline{S_{r\theta}}}{r}\frac{\partial\overline{u_r}}{\partial\theta}-\frac{\overline{u_r}\overline{S_{\theta\theta}}}{r})$$

On subtracting eqn (12) from eqn (26), we have

(The red, blue and green terms each add to 0)

$$\frac{1}{2}\frac{\partial\overline{\acute{u}_r^{\,2}}}{\partial t}+\frac{\overline{u_r}^2}{2}\frac{\partial\overline{u_z}}{\partial z}+\frac{\overline{\acute{u}_r^{\,2}}}{2}\frac{\partial\overline{u_z}}{\partial z}+\frac{\overline{u_z}}{2}\frac{\partial\overline{\acute{u}_r^{\,2}}}{\partial z}+\frac{1}{2}\frac{\partial\overline{\acute{u}_r^{\,2}\acute{u}_z}}{\partial z}+\overline{\acute{u}_z\acute{u}_r}\frac{\partial\overline{u_r}}{\partial z}+\overline{u_r}\overline{\acute{u}_r\frac{\partial\acute{u}_z}{\partial z}}$$
$$+\frac{\overline{u_r}^2}{2}\frac{\partial\overline{u_r}}{\partial r}+\frac{\overline{\acute{u}_r^{\,2}}}{2}\frac{\partial\overline{u_r}}{\partial r}+\frac{\overline{u_r}}{2}\frac{\partial\overline{\acute{u}_r^{\,2}}}{\partial r}+\frac{1}{2}\frac{\partial\overline{\acute{u}_r^{\,3}}}{\partial r}+\overline{\acute{u}_r\acute{u}_r}\frac{\partial\overline{u_r}}{\partial r}+\overline{u_r}\overline{\acute{u}_r\frac{\partial\acute{u}_r}{\partial r}}$$
$$+\frac{\overline{u_r}^2}{2r}\frac{\partial\overline{u_\theta}}{\partial\theta}+\frac{\overline{\acute{u}_r^{\,2}}}{2}\frac{\partial\overline{u_\theta}}{r\partial\theta}+\frac{\overline{u_\theta}}{2}\frac{\partial\overline{\acute{u}_r^{\,2}}}{r\partial\theta}+\frac{1}{2}\frac{\partial\overline{\acute{u}_r^{\,2}\acute{u}_\theta}}{r\partial\theta}+\frac{1}{r}\overline{\acute{u}_r\acute{u}_\theta}\frac{\partial\overline{u_r}}{\partial\theta}+\frac{1}{r}\overline{u_r}\overline{\acute{u}_r\frac{\partial\acute{u}_\theta}{\partial\theta}}$$
$$+\frac{\overline{u_r}^3}{2r}+\frac{\overline{u_r}\overline{\acute{u}_r^{\,2}}}{2r}+\frac{\overline{\acute{u}_r^{\,3}}}{2r}+\frac{\overline{u_r}\overline{\acute{u}_r^{\,2}}}{r}-\frac{\overline{u_\theta\acute{}^2\acute{u}_r}}{r}-\frac{2\overline{u_\theta}\overline{\acute{u}_\theta\acute{u}_r}}{r}=-\overline{\frac{\acute{u}_r}{\rho}\frac{\partial\acute{p}}{\partial r}}$$
$$+2\upsilon[\overline{\frac{\partial\acute{u}_r\acute{S_{rz}}}{\partial z}}+\overline{\frac{\partial r\acute{u}_r\acute{S_{rr}}}{r\partial r}}+\overline{\frac{1}{r}\frac{\partial\acute{u}_r\acute{S_{r\theta}}}{\partial\theta}}-\overline{\acute{S_{rz}}\frac{\partial\acute{u}_r}{\partial z}}-\overline{\acute{S_{rr}}\frac{\partial\acute{u}_r}{\partial r}}-\overline{\frac{\acute{S_{r\theta}}}{r}\frac{\partial\acute{u}_r}{\partial\theta}}-\overline{\frac{\acute{u}_r\acute{S_{\theta\theta}}}{r}}] \tag{A.27}$$

$$\frac{1}{2}\frac{\partial\overline{\acute{u}_r^{\,2}}}{\partial t}+\frac{\overline{u_z}}{2}\frac{\partial\overline{\acute{u}_r^{\,2}}}{\partial z}+\frac{1}{2}\frac{\partial\overline{\acute{u}_r^{\,2}\acute{u}_z}}{\partial z}+\overline{\acute{u}_z\acute{u}_r}\frac{\partial\overline{u_r}}{\partial z}+\frac{\overline{u_r}}{2}\frac{\partial\overline{\acute{u}_r^{\,2}}}{\partial r}+\frac{1}{2}\frac{\partial\overline{\acute{u}_r^{\,3}}}{\partial r}+\overline{\acute{u}_r\acute{u}_r}\frac{\partial\overline{u_r}}{\partial r}$$
$$+\frac{\overline{u_\theta}}{2}\frac{\partial\overline{\acute{u}_r^{\,2}}}{r\partial\theta}+\frac{1}{2}\frac{\partial\overline{\acute{u}_r^{\,2}\acute{u}_\theta}}{r\partial\theta}+\frac{1}{r}\overline{\acute{u}_r\acute{u}_\theta}\frac{\partial\overline{u_r}}{\partial\theta}+\frac{\overline{\acute{u}_r^{\,3}}}{2r}-\frac{\overline{u_\theta\acute{}^2\acute{u}_r}}{r}-\frac{2\overline{u_\theta}\overline{\acute{u}_\theta\acute{u}_r}}{r}=\overline{\frac{\acute{p}}{\rho}\frac{\partial\acute{u}_r}{\partial r}}$$
$$-\overline{\frac{1}{\rho}\frac{\partial\acute{u}_r\acute{p}}{\partial r}}+2\upsilon[\overline{\frac{\partial\acute{u}_r\acute{S_{rz}}}{\partial z}}+\overline{\frac{\partial r\acute{u}_r\acute{S_{rr}}}{r\partial r}}+\overline{\frac{1}{r}\frac{\partial\acute{u}_r\acute{S_{r\theta}}}{\partial\theta}}-\overline{\acute{S_{rz}}\frac{\partial\acute{u}_r}{\partial z}}-\overline{\acute{S_{rr}}\frac{\partial\acute{u}_r}{\partial r}}$$
$$-\overline{\frac{\acute{S_{r\theta}}}{r}\frac{\partial\acute{u}_r}{\partial\theta}}-\overline{\frac{\acute{u}_r\acute{S_{\theta\theta}}}{r}}] \tag{A.28}$$

The total energy equation in the tangential direction is as follows,

$$\frac{1}{2}\frac{\partial\overline{u_\theta}^2}{\partial t}+\frac{1}{2}\frac{\partial\overline{\acute{u}_\theta^{\,2}}}{\partial t}+\overline{u_\theta}\cdot\overline{u_z}\frac{\partial\overline{u_\theta}}{\partial z}+\frac{\overline{u_\theta}^2}{2}\frac{\partial\overline{u_z}}{\partial z}+\frac{1}{2}\frac{\partial\overline{\acute{u}_\theta^{\,2}}\overline{u_z}}{\partial z}+\frac{\partial\overline{u_\theta}\overline{\acute{u}_\theta\acute{u}_z}}{\partial z}+\frac{1}{2}\frac{\partial\overline{\acute{u}_\theta^{\,2}\acute{u}_z}}{\partial z}+\overline{u_r}\cdot\overline{u_\theta}\frac{\partial\overline{u_\theta}}{\partial r}$$
$$+\overline{u_\theta}^2\frac{\partial\overline{u_r}}{\partial r}+\frac{1}{2}\frac{\partial\overline{\acute{u}_\theta^{\,2}}\overline{u_r}}{\partial r}+\frac{\partial\overline{u_\theta}\overline{\acute{u}_\theta\acute{u}_r}}{\partial r}+\frac{1}{2}\frac{\partial\overline{\acute{u}_\theta^{\,2}\acute{u}_r}}{\partial r}+\frac{3\overline{u_\theta}^2}{2}\frac{\partial\overline{u_\theta}}{r\partial\theta}+\frac{3}{2}\frac{\partial\overline{\acute{u}_\theta^{\,2}}\overline{u_\theta}}{r\partial\theta}+\frac{1}{2}\frac{\partial\overline{\acute{u}_\theta^{\,3}}}{r\partial\theta}$$
$$+\frac{3\overline{u_r}\cdot\overline{u_\theta}^2}{2r}+\frac{3\overline{u_\theta}\overline{\acute{u}_\theta\acute{u}_r}}{r}+\frac{3\overline{u_r}\overline{\acute{u}_\theta}^2}{2r}+\frac{3\overline{u_\theta^2}\acute{u}_r}{2r}=-\overline{\frac{u_\theta}{r\rho}\frac{\partial p}{\partial\theta}}-\overline{\frac{\acute{u}_\theta}{r\rho}\frac{\partial\acute{p}}{\partial\theta}}+2\upsilon[\overline{\frac{\partial\overline{u_\theta}\overline{S_{\theta z}}}{\partial z}}+\overline{\frac{\partial r\overline{u_\theta}\overline{S_{r\theta}}}{r\partial r}}$$
$$+\overline{\frac{1}{r}\frac{\partial\overline{u_\theta}\overline{S_{\theta\theta}}}{\partial\theta}}-\overline{\overline{S_{\theta z}}\frac{\partial\overline{u_\theta}}{\partial z}}-\overline{\overline{S_{r\theta}}\frac{\partial\overline{u_\theta}}{\partial r}}-\overline{\frac{\overline{S_{\theta\theta}}}{r}\frac{\partial\overline{u_\theta}}{\partial\theta}}+\overline{\frac{\overline{u_\theta}\overline{S_{r\theta}}}{r}}+\overline{\frac{\partial\acute{u}_\theta\acute{S_{\theta z}}}{\partial z}}+\overline{\frac{\partial r\acute{u}_\theta\acute{S_{r\theta}}}{r\partial r}}$$
$$+\overline{\frac{1}{r}\frac{\partial\acute{u}_\theta\acute{S_{\theta\theta}}}{\partial\theta}}-\overline{\acute{S_{\theta z}}\frac{\partial\acute{u}_\theta}{\partial z}}-\overline{\acute{S_{r\theta}}\frac{\partial\acute{u}_\theta}{\partial r}}-\overline{\frac{\acute{S_{\theta\theta}}}{r}\frac{\partial\acute{u}_\theta}{\partial\theta}}+\overline{\frac{\acute{u}_\theta\acute{S_{r\theta}}}{r}}] \tag{A.29}$$

From equation (16) we have

$$\frac{1}{2}\frac{\partial\overline{u_\theta}^2}{\partial t}+\overline{u_\theta}\cdot\overline{u_z}\frac{\partial\overline{u_\theta}}{\partial z}+\overline{u_\theta}\cdot\overline{u_r}\frac{\partial\overline{u_\theta}}{\partial r}+\overline{u_\theta}^2\frac{\partial\overline{u_\theta}}{r\partial\theta}+\frac{\partial\overline{u_\theta}\cdot\overline{\acute{u}_z\acute{u}_\theta}}{\partial z}-\overline{\acute{u}_z\acute{u}_\theta}\frac{\partial\overline{u_\theta}}{\partial z}-\overline{u_\theta}\overline{\acute{u}_\theta\frac{\partial\acute{u}_z}{\partial z}}$$
$$+\frac{\partial\overline{u_\theta}\overline{\acute{u}_r\acute{u}_\theta}}{\partial r}-\overline{\acute{u}_r\acute{u}_\theta}\frac{\partial\overline{u_\theta}}{\partial r}-\overline{u_\theta}\overline{\acute{u}_\theta\frac{\partial\acute{u}_r}{\partial r}}+\frac{1}{r}\frac{\partial\overline{u_\theta}\overline{\acute{u}_\theta\acute{u}_\theta}}{\partial\theta}-\frac{1}{r}\overline{\acute{u}_\theta\acute{u}_\theta}\frac{\partial\overline{u_\theta}}{\partial\theta}-\frac{1}{r}\overline{u_\theta}\overline{\acute{u}_\theta\frac{\partial\acute{u}_\theta}{\partial\theta}}+\frac{\overline{u_r}\cdot\overline{u_\theta}^2}{r}+\frac{\overline{u_\theta}\overline{\acute{u}_\theta\acute{u}_r}}{r}$$
$$=-\overline{\frac{u_\theta}{r\rho}\frac{\partial p}{\partial\theta}}+2\upsilon[\overline{\frac{\partial\overline{u_\theta}\overline{S_{\theta z}}}{\partial z}}+\overline{\frac{\partial r\overline{u_\theta}\overline{S_{r\theta}}}{r\partial r}}+\overline{\frac{1}{r}\frac{\partial\overline{u_\theta}\overline{S_{\theta\theta}}}{\partial\theta}}-\overline{\overline{S_{\theta z}}\frac{\partial\overline{u_\theta}}{\partial z}}-\overline{\overline{S_{r\theta}}\frac{\partial\overline{u_\theta}}{\partial r}}-\overline{\frac{\overline{S_{\theta\theta}}}{r}\frac{\partial\overline{u_\theta}}{\partial\theta}}+$$
$$\overline{\frac{\overline{u_\theta}\overline{S_{r\theta}}}{r}}+\overline{\frac{\partial\acute{u}_\theta\acute{S_{\theta z}}}{\partial z}}+\overline{\frac{\partial r\acute{u}_\theta\acute{S_{r\theta}}}{r\partial r}}+\overline{\frac{1}{r}\frac{\partial\acute{u}_\theta\acute{S_{\theta\theta}}}{\partial\theta}}-\overline{\acute{S_{\theta z}}\frac{\partial\acute{u}_\theta}{\partial z}}-\overline{\acute{S_{r\theta}}\frac{\partial\acute{u}_\theta}{\partial r}}-\overline{\frac{\acute{S_{\theta\theta}}}{r}\frac{\partial\acute{u}_\theta}{\partial\theta}}+\overline{\frac{\acute{u}_\theta\acute{S_{r\theta}}}{r}}]$$

On subtracting (16) from (28) we have,

( The red, blue and green term add to 0)

$$\frac{1}{2}\frac{\partial\overline{\acute{u}_\theta^{\,2}}}{\partial t}+\frac{\overline{u_\theta}^{\,2}}{2}\frac{\partial\overline{u_z}}{\partial z}+\frac{\overline{\acute{u}_\theta^{\,2}}}{2}\frac{\partial\overline{u_z}}{\partial z}+\frac{\overline{u_z}}{2}\frac{\partial\overline{\acute{u}_\theta^{\,2}}}{\partial z}+\frac{1}{2}\frac{\partial\overline{\acute{u}_\theta^{\,2}\acute{u}_z}}{\partial z}+\overline{\acute{u}_z\acute{u}_\theta}\frac{\partial\overline{u_\theta}}{\partial z}+\overline{u_\theta}\overline{\acute{u}_\theta\frac{\partial\acute{u}_z}{\partial z}}$$
$$+\frac{\overline{u_\theta}^{\,2}}{2}\frac{\partial\overline{u_r}}{\partial r}+\frac{\overline{\acute{u}_\theta^{\,2}}}{2}\frac{\partial\overline{u_r}}{\partial r}+\frac{\overline{u_r}}{2}\frac{\partial\overline{\acute{u}_\theta^{\,2}}}{\partial r}+\frac{1}{2}\frac{\partial\overline{\acute{u}_\theta^{\,2}\acute{u}_r}}{\partial r}+\overline{\acute{u}_r\acute{u}_\theta}\frac{\partial\overline{u_\theta}}{\partial r}+\overline{u_\theta}\overline{\acute{u}_\theta\frac{\partial\acute{u}_r}{\partial r}}$$
$$+\frac{\overline{u_\theta}^{\,2}}{2}\frac{\partial\overline{u_\theta}}{r\partial\theta}+\frac{\overline{\acute{u}_\theta^{\,2}}}{2}\frac{\partial\overline{u_\theta}}{r\partial\theta}+\frac{\overline{u_\theta}}{2}\frac{\partial\overline{\acute{u}_\theta^{\,2}}}{r\partial\theta}+\frac{1}{2}\frac{\partial\overline{\acute{u}_\theta^{\,3}}}{r\partial\theta}+\frac{1}{r}\overline{\acute{u}_\theta\acute{u}_\theta}\frac{\partial\overline{u_\theta}}{\partial\theta}+\frac{1}{r}\overline{u_\theta}\overline{\acute{u}_\theta\frac{\partial\acute{u}_\theta}{\partial\theta}}$$
$$+\frac{\overline{u_r}\cdot\overline{u_\theta}^{\,2}}{2r}+\frac{\overline{u_\theta}\overline{\acute{u}_\theta\acute{u}_r}}{r}+\frac{\overline{u_\theta}\overline{\acute{u}_\theta\acute{u}_r}}{r}+\frac{\overline{u_r}\overline{\acute{u}_\theta^{\,2}}}{r}+\frac{\overline{u_r}\overline{\acute{u}_\theta^{\,2}}}{2r}+\frac{3\overline{u_\theta^{\acute{2}}\acute{u}_r}}{2r}=\overline{\frac{\acute{p}}{r\rho}\frac{\partial\acute{u}_\theta}{\partial\theta}}-\overline{\frac{1}{r\rho}\frac{\partial\acute{p}\acute{u}_\theta}{\partial\theta}}+2\upsilon[\overline{\frac{\partial\acute{u}_\theta S_{\theta z}^{\acute{}}}{\partial z}}$$
$$+\overline{\frac{\partial r\acute{u}_\theta S_{r\theta}^{\acute{}}}{r\partial r}}+\frac{1}{r}\overline{\frac{\partial\acute{u}_\theta S_{\theta\theta}^{\acute{}}}{\partial\theta}}-\overline{S_{\theta z}^{\acute{}}\frac{\partial\acute{u}_\theta}{\partial z}}-\overline{S_{r\theta}^{\acute{}}\frac{\partial\acute{u}_\theta}{\partial r}}-\overline{\frac{S_{\theta\theta}^{\acute{}}}{r}\frac{\partial\acute{u}_\theta}{\partial\theta}}+\overline{\frac{\acute{u}_\theta S_{r\theta}^{\acute{}}}{r}}] \tag{A.30}$$

$$\frac{1}{2}\frac{\partial\overline{\acute{u}_\theta^{\,2}}}{\partial t}+\frac{\overline{u_z}}{2}\frac{\partial\overline{\acute{u}_\theta^{\,2}}}{\partial z}+\frac{1}{2}\frac{\partial\overline{\acute{u}_\theta^{\,2}\acute{u}_z}}{\partial z}+\overline{\acute{u}_z\acute{u}_\theta}\frac{\partial\overline{u_\theta}}{\partial z}+\frac{\overline{u_r}}{2}\frac{\partial\overline{\acute{u}_\theta^{\,2}}}{\partial r}+\frac{1}{2}\frac{\partial\overline{\acute{u}_\theta^{\,2}\acute{u}_r}}{\partial r}+\overline{\acute{u}_r\acute{u}_\theta}\frac{\partial\overline{u_\theta}}{\partial r}$$
$$+\frac{\overline{u_\theta}}{2}\frac{\partial\overline{\acute{u}_\theta^{\,2}}}{r\partial\theta}+\frac{1}{2}\frac{\partial\overline{\acute{u}_\theta^{\,3}}}{r\partial\theta}+\frac{1}{r}\overline{\acute{u}_\theta\acute{u}_\theta}\frac{\partial\overline{u_\theta}}{\partial\theta}+\frac{\overline{u_\theta}\overline{\acute{u}_\theta\acute{u}_r}}{r}+\frac{\overline{u_r}\overline{\acute{u}_\theta^{\,2}}}{r}+\frac{3\overline{u_\theta^{\acute{2}}\acute{u}_r}}{2r}$$
$$=\overline{\frac{\acute{p}}{r\rho}\frac{\partial\acute{u}_\theta}{\partial\theta}}-\overline{\frac{1}{r\rho}\frac{\partial\acute{p}\acute{u}_\theta}{\partial\theta}}+2\upsilon[\overline{\frac{\partial\acute{u}_\theta S_{\theta z}^{\acute{}}}{\partial z}}+\overline{\frac{\partial r\acute{u}_\theta S_{r\theta}^{\acute{}}}{r\partial r}}+\frac{1}{r}\overline{\frac{\partial\acute{u}_\theta S_{\theta\theta}^{\acute{}}}{\partial\theta}}-\overline{S_{\theta z}^{\acute{}}\frac{\partial\acute{u}_\theta}{\partial z}}$$
$$-\overline{S_{r\theta}^{\acute{}}\frac{\partial\acute{u}_\theta}{\partial r}}-\overline{\frac{S_{\theta\theta}^{\acute{}}}{r}\frac{\partial\acute{u}_\theta}{\partial\theta}}+\overline{\frac{\acute{u}_\theta S_{r\theta}^{\acute{}}}{r}}] \tag{A.31}$$

On adding equations (25), (28) and (31), we have

(1st terms of LHS)

$$\frac{1}{2}\frac{\partial\overline{\acute{u}_z^{\,2}}}{\partial t}+\frac{1}{2}\frac{\partial\overline{\acute{u}_r^{\,2}}}{\partial t}+\frac{1}{2}\frac{\partial\overline{\acute{u}_\theta^{\,2}}}{\partial t}$$

(2nd terms of LHS)

$$+\frac{\overline{u_z}}{2}\frac{\partial\overline{\acute{u}_z^{\,2}}}{\partial z}+\frac{\overline{u_z}}{2}\frac{\partial\overline{\acute{u}_r^{\,2}}}{\partial z}+\frac{\overline{u_z}}{2}\frac{\partial\overline{\acute{u}_\theta^{\,2}}}{\partial z}$$

(3rd terms of LHS)

$$+\frac{1}{2}\frac{\partial\overline{\acute{u}_z^{\,3}}}{\partial z}+\frac{1}{2}\frac{\partial\overline{\acute{u}_r^{\,2}\acute{u}_z}}{\partial z}+\frac{1}{2}\frac{\partial\overline{\acute{u}_\theta^{\,2}\acute{u}_z}}{\partial z}$$

(4th terms of LHS)

$$+\overline{\acute{u_z}^2}\frac{\partial\overline{u_z}}{\partial z}+\overline{\acute{u_z}\acute{u_r}}\frac{\partial\overline{u_r}}{\partial z}+\overline{\acute{u_z}\acute{u_\theta}}\frac{\partial\overline{u_\theta}}{\partial z}$$

(5th terms of LHS)

$$+\frac{\overline{u_r}}{2}\frac{\partial\overline{\acute{u_z}^2}}{\partial r}+\frac{\overline{u_r}}{2}\frac{\partial\overline{\acute{u_r}^2}}{\partial r}+\frac{\overline{u_r}}{2}\frac{\partial\overline{\acute{u_\theta}^2}}{\partial r}$$

(6th terms of LHS)

$$+\frac{1}{2}\frac{\partial\overline{\acute{u_z}^2\acute{u_r}}}{\partial r}+\frac{1}{2}\frac{\partial\overline{\acute{u_r}^3}}{\partial r}+\frac{1}{2}\frac{\partial\overline{\acute{u_\theta}^2\acute{u_r}}}{\partial r}$$

(7th terms of LHS)

$$+\overline{\acute{u_z}\acute{u_r}}\frac{\partial\overline{u_z}}{\partial r}+\overline{\acute{u_r}\acute{u_r}}\frac{\partial\overline{u_r}}{\partial r}+\overline{\acute{u_r}\acute{u_\theta}}\frac{\partial\overline{u_\theta}}{\partial r}$$

(8th terms of LHS)

$$+\frac{\overline{u_\theta}}{2}\frac{\partial\overline{\acute{u_z}^2}}{r\partial\theta}+\frac{\overline{u_\theta}}{2}\frac{\partial\overline{\acute{u_r}^2}}{r\partial\theta}+\frac{\overline{u_\theta}}{2}\frac{\partial\overline{\acute{u_\theta}^2}}{r\partial\theta}$$

(9th terms of LHS)

$$+\frac{1}{2}\frac{\partial\overline{\acute{u_z}^2\acute{u_\theta}}}{r\partial\theta}+\frac{1}{2}\frac{\partial\overline{\acute{u_r}^2\acute{u_\theta}}}{r\partial\theta}+\frac{1}{2}\frac{\partial\overline{\acute{u_\theta}^3}}{r\partial\theta}$$

(10th terms of LHS)

$$+\frac{1}{r}\overline{\acute{u_z}\acute{u_\theta}}\frac{\partial\overline{u_z}}{\partial\theta}+\frac{1}{r}\overline{\acute{u_r}\acute{u_\theta}}\frac{\partial\overline{u_r}}{\partial\theta}+\frac{1}{r}\overline{\acute{u_\theta}\acute{u_\theta}}\frac{\partial\overline{u_\theta}}{\partial\theta}$$

(Remaining terms of LHS)

$$+\frac{\overline{\acute{u_z}^2\acute{u_r}}}{2r}+\frac{\overline{\acute{u_r}^3}}{2r}-\frac{\overline{u_\theta\acute{}^2\acute{u_r}}}{r}+\frac{3\overline{\acute{u_\theta^2}\acute{u_r}}}{2r}$$
$$-\frac{2\overline{u_\theta}\overline{\acute{u_\theta}\acute{u_r}}}{r}+\frac{\overline{u_\theta}\overline{\acute{u_\theta}\acute{u_r}}}{r}+\frac{\overline{u_r}\overline{\acute{u_\theta}^2}}{r}$$

(1st and 2nd terms of RHS)

$$=-\frac{1}{\rho}\left(\frac{\partial\overline{\acute{u_z}\acute{p}}}{\partial z}+\frac{1}{r}\frac{\partial r\overline{\acute{u_r}\acute{p}}}{\partial r}+\frac{1}{r}\frac{\partial\overline{\acute{u_\theta}\acute{p}}}{\partial\theta}\right)$$

(3rd terms of RHS)

$$+2\upsilon\left(\frac{\partial\overline{\acute{u_z}S_{zz}'}}{\partial z}+\frac{\partial\overline{\acute{u_r}S_{rz}'}}{\partial z}+\frac{\overline{\partial\acute{u_\theta}S_{\theta z}'}}{\partial z}\right.$$

(4th terms of RHS)

$$+\frac{\partial r\overline{\acute{u_z}S_{zr}'}}{r\partial r}+\frac{\partial r\overline{\acute{u_r}S_{rr}'}}{r\partial r}+\frac{\overline{\partial r\acute{u_\theta}S_{r\theta}'}}{r\partial r}$$

(5th terms of RHS)

$$+\frac{1}{r}\frac{\partial\overline{\acute{u}_z S'_{z\theta}}}{\partial\theta}+\frac{1}{r}\frac{\partial\overline{\acute{u}_r S'_{r\theta}}}{\partial\theta}+\frac{1}{r}\frac{\partial\overline{\acute{u}_\theta S'_{\theta\theta}}}{\partial\theta}$$

(6th terms of RHS)

$$-\overline{S'_{zz}\frac{\partial\acute{u}_z}{\partial z}}-\overline{S'_{zr}\frac{\partial\acute{u}_r}{\partial z}}-\overline{S'_{z\theta}\frac{\partial\acute{u}_\theta}{\partial z}}$$

(7th terms of RHS)

$$\overline{S'_{rz}\frac{\partial\acute{u}_z}{\partial r}}-\overline{S'_{rr}\frac{\partial\acute{u}_r}{\partial r}}-\overline{S'_{r\theta}\frac{\partial\acute{u}_\theta}{\partial r}} \qquad \text{(A.32)}$$

(8th terms of RHS)

$$\overline{S'_{\theta z}\frac{\partial\acute{u}_z}{\partial\theta}}-\overline{S'_{\theta r}\frac{\partial\acute{u}_r}{\partial\theta}}-\overline{S'_{\theta\theta}\frac{\partial\acute{u}_\theta}{\partial\theta}}$$

(Remaining terms of RHS)

$$-\overline{\frac{\acute{u}_r S'_{\theta\theta}}{r}}+\overline{\frac{\acute{u}_\theta S'_{r\theta}}{r}})$$

On rearranging the terms we have

$$
\begin{aligned}
&\frac{\partial q}{\partial t}+\overline{u_z}\frac{\partial q}{\partial z}+\overline{u_r}\frac{\partial q}{\partial r}+\overline{u_\theta}\frac{\partial q}{r\partial\theta}\\
&=-\frac{1}{\rho}(\frac{\partial\overline{\acute{u}_z\acute{p}}}{\partial z}+\frac{1}{r}\frac{\partial r\overline{\acute{u}_r\acute{p}}}{\partial r}+\frac{1}{r}\frac{\partial\overline{\acute{u}_\theta\acute{p}}}{\partial\theta})\\
&-\frac{\partial\overline{\acute{u}_z q}}{\partial z}-\frac{1}{r}\frac{\partial r\overline{\acute{u}_r q}}{\partial r}-\frac{1}{r}\frac{\partial\overline{\acute{u}_\theta q}}{\partial\theta}\\
&-\overline{\acute{u}_z{}^2}\frac{\partial\overline{u_z}}{\partial z}-\overline{\acute{u}_r\acute{u}_r}\frac{\partial\overline{u_r}}{\partial r}-\frac{1}{r}\overline{\acute{u}_\theta\acute{u}_\theta}\frac{\partial\overline{u_\theta}}{\partial\theta}\\
&-\overline{\acute{u}_z\acute{u}_r}(\frac{\partial\overline{u_z}}{\partial r}+\frac{\partial\overline{u_r}}{\partial z})-\overline{\acute{u}_z\acute{u}_\theta}(\frac{\partial\overline{u_z}}{r\partial\theta}+\frac{\partial\overline{u_\theta}}{\partial z})\\
&-\overline{\acute{u}_r\acute{u}_\theta}(\frac{\partial\overline{u_\theta}}{\partial r}+\frac{\partial\overline{u_r}}{r\partial\theta})+\frac{\overline{u_\theta}\overline{\acute{u}_\theta\acute{u}_r}}{r}-\frac{\overline{u_r}\overline{\acute{u}_\theta{}^2}}{r}\\
&+2\upsilon(\frac{\partial\overline{\acute{u}_z\acute{S}_{zz}}}{\partial z}+\frac{\partial\overline{\acute{u}_r\acute{S}_{rz}}}{\partial z}+\frac{\partial\overline{\acute{u}_\theta\acute{S}_{\theta z}}}{\partial z}\\
&+\frac{\partial r\overline{\acute{u}_z\acute{S}_{zr}}}{r\partial r}+\frac{\partial r\overline{\acute{u}_r\acute{S}_{rr}}}{r\partial r}+\frac{\partial r\overline{\acute{u}_\theta\acute{S}_{r\theta}}}{r\partial r}\\
&+\frac{1}{r}\frac{\partial\overline{\acute{u}_z\acute{S}_{z\theta}}}{\partial\theta}+\frac{1}{r}\frac{\partial\overline{\acute{u}_r\acute{S}_{r\theta}}}{\partial\theta}+\frac{1}{r}\frac{\partial\overline{\acute{u}_\theta\acute{S}_{\theta\theta}}}{\partial\theta}\\
&-\overline{\acute{S}_{zz}\frac{\partial\acute{u}_z}{\partial z}}-\overline{\acute{S}_{zr}\frac{\partial\acute{u}_r}{\partial z}}-\overline{\acute{S}_{z\theta}\frac{\partial\acute{u}_\theta}{\partial z}}\\
&\overline{\acute{S}_{rz}\frac{\partial\acute{u}_z}{\partial r}}-\overline{\acute{S}_{rr}\frac{\partial\acute{u}_r}{\partial r}}-\overline{\acute{S}_{r\theta}\frac{\partial\acute{u}_\theta}{\partial r}}\\
&\overline{\acute{S}_{\theta z}\frac{\partial\acute{u}_z}{\partial\theta}}-\overline{\acute{S}_{\theta r}\frac{\partial\acute{u}_r}{\partial\theta}}-\overline{\acute{S}_{\theta\theta}\frac{\partial\acute{u}_\theta}{\partial\theta}}\\
&-\overline{\frac{\acute{u}_r\acute{S}_{\theta\theta}}{r}}+\overline{\frac{\acute{u}_\theta\acute{S}_{r\theta}}{r}})
\end{aligned}
\tag{A.33}
$$

where, $q=\frac{1}{2}(\overline{u_r^2}+\overline{u_\theta^2}+\overline{u_z^2})$.

The terms can be classified as-

**Unsteady term**- $\frac{\partial q}{\partial t}$

**Convective Term**- $\overline{u_z}\frac{\partial q}{\partial z}+\overline{u_r}\frac{\partial q}{\partial r}+\overline{u_\theta}\frac{\partial q}{r\partial\theta}$

**Pressure Diffusion Term**- $-\frac{1}{\rho}(\frac{\partial\overline{\acute{u}_z\acute{p}}}{\partial z}+\frac{1}{r}\frac{\partial r\overline{\acute{u}_r\acute{p}}}{\partial r}+\frac{1}{r}\frac{\partial\overline{\acute{u}_\theta\acute{p}}}{\partial\theta})$

**Production Term**- $-\overline{\acute{u}_z{}^2}\frac{\partial\overline{u_z}}{\partial z}-\overline{\acute{u}_r\acute{u}_r}\frac{\partial\overline{u_r}}{\partial r}-\frac{1}{r}\overline{\acute{u}_\theta\acute{u}_\theta}\frac{\partial\overline{u_\theta}}{\partial\theta}-\overline{\acute{u}_z\acute{u}_r}(\frac{\partial\overline{u_z}}{\partial r}+\frac{\partial\overline{u_r}}{\partial z})-\overline{\acute{u}_z\acute{u}_\theta}(\frac{\partial\overline{u_z}}{r\partial\theta}+\frac{\partial\overline{u_\theta}}{\partial z})-\overline{\acute{u}_r\acute{u}_\theta}(\frac{\partial\overline{u_\theta}}{\partial r}+\frac{\partial\overline{u_r}}{r\partial\theta})+\frac{\overline{u_\theta}\overline{\acute{u}_\theta\acute{u}_r}}{r}-\frac{\overline{u_r}\overline{\acute{u}_\theta{}^2}}{r}$

**Turbulent Diffusion Term**- $-\frac{\partial\overline{\acute{u}_z q}}{\partial z}-\frac{1}{r}\frac{\partial r\overline{\acute{u}_r q}}{\partial r}-\frac{1}{r}\frac{\partial\overline{\acute{u}_\theta q}}{\partial\theta}$

**Viscous Diffusion Term**-

$$
\begin{aligned}
&2\upsilon(\frac{\partial\overline{\acute{u}_z\acute{S}_{zz}}}{\partial z}+\frac{\partial\overline{\acute{u}_r\acute{S}_{rz}}}{\partial z}+\frac{\partial\overline{\acute{u}_\theta\acute{S}_{\theta z}}}{\partial z}\\
&+\frac{\partial r\overline{\acute{u}_z\acute{S}_{zr}}}{r\partial r}+\frac{\partial r\overline{\acute{u}_r\acute{S}_{rr}}}{r\partial r}+\frac{\partial r\overline{\acute{u}_\theta\acute{S}_{r\theta}}}{r\partial r}\\
&+\frac{1}{r}\frac{\partial\overline{\acute{u}_z\acute{S}_{z\theta}}}{\partial\theta}+\frac{1}{r}\frac{\partial\overline{\acute{u}_r\acute{S}_{r\theta}}}{\partial\theta}+\frac{1}{r}\frac{\partial\overline{\acute{u}_\theta\acute{S}_{\theta\theta}}}{\partial\theta})
\end{aligned}
$$

**Viscous Dissipation Term**-

$$2\upsilon(-\overline{S_{zz}^{'}\frac{\partial u_z^{'}}{\partial z}}-\overline{S_{zr}^{'}\frac{\partial u_r^{'}}{\partial z}}-\overline{S_{z\theta}^{'}\frac{\partial u_\theta^{'}}{\partial z}}$$
$$\overline{S_{rz}^{'}\frac{\partial u_z^{'}}{\partial r}}-\overline{S_{rr}^{'}\frac{\partial u_r^{'}}{\partial r}}-\overline{S_{r\theta}^{'}\frac{\partial u_\theta^{'}}{\partial r}}$$
$$\overline{S_{\theta z}^{'}\frac{\partial u_z^{'}}{\partial \theta}}-\overline{S_{\theta r}^{'}\frac{\partial u_r^{'}}{\partial \theta}}-\overline{S_{\theta\theta}^{'}\frac{\partial u_\theta^{'}}{\partial \theta}}$$
$$-\overline{\frac{u_r^{'}S_{\theta\theta}^{'}}{r}}+\overline{\frac{u_\theta^{'}S_{r\theta}^{'}}{r}})$$

Assuming homogeneity along the z-diection and smmetry along the azimuthal direction, we have $\overline{u_r}=\overline{u_\theta}=0$ and derivatives of statistical quantities along z-direction are $0$.

Hence, we have

$$\begin{aligned}\frac{\partial q}{\partial t}=&-\frac{1}{\rho}(\frac{1}{r}\frac{\partial r\overline{u_r^{'}p^{'}}}{\partial r})-\frac{1}{r}\frac{\partial r\overline{u_r^{'}q}}{\partial r}-\overline{u_z^{'}u_r^{'}}(\frac{\partial\overline{u_z}}{\partial r})+2\upsilon(\overline{\frac{\partial u_z^{'}S_{zz}^{'}}{\partial z}}+\overline{\frac{\partial u_r^{'}S_{rz}^{'}}{\partial z}}+\overline{\frac{\partial u_\theta^{'}S_{\theta z}^{'}}{\partial z}}+\overline{\frac{\partial r u_z^{'}S_{zr}^{'}}{r\partial r}}\\&+\overline{\frac{\partial r u_r^{'}S_{rr}^{'}}{r\partial r}}+\overline{\frac{\partial r u_\theta^{'}S_{r\theta}^{'}}{r\partial r}}+\frac{1}{r}\overline{\frac{\partial u_z^{'}S_{z\theta}^{'}}{\partial\theta}}+\frac{1}{r}\overline{\frac{\partial u_r^{'}S_{r\theta}^{'}}{\partial\theta}}+\frac{1}{r}\overline{\frac{\partial u_\theta^{'}S_{\theta\theta}^{'}}{\partial\theta}}-\overline{S_{zz}^{'}\frac{\partial u_z^{'}}{\partial z}}-\overline{S_{zr}^{'}\frac{\partial u_r^{'}}{\partial z}}-\overline{S_{z\theta}^{'}\frac{\partial u_\theta^{'}}{\partial z}}\\&-\overline{S_{rz}^{'}\frac{\partial u_z^{'}}{\partial r}}-\overline{S_{rr}^{'}\frac{\partial u_r^{'}}{\partial r}}-\overline{S_{r\theta}^{'}\frac{\partial u_\theta^{'}}{\partial r}}-\overline{S_{\theta z}^{'}\frac{\partial u_z^{'}}{\partial\theta}}-\overline{S_{\theta r}^{'}\frac{\partial u_r^{'}}{\partial\theta}}-\overline{S_{\theta\theta}^{'}\frac{\partial u_\theta^{'}}{\partial\theta}}-\overline{\frac{u_r^{'}S_{\theta\theta}^{'}}{r}}+\overline{\frac{u_\theta^{'}S_{r\theta}^{'}}{r}})\end{aligned}\tag{A.34}$$

The terms can be classified as-

**Unsteady term**- $\frac{\partial q}{\partial t}$

**Pressure Diffusion Term**- $-\frac{1}{\rho}(\frac{1}{r}\frac{\partial r\overline{u_r^{'}p^{'}}}{\partial r})$

**Production Term**- $-\overline{u_z^{'}u_r^{'}}(\frac{\partial\overline{u_z}}{\partial r})$

**Turbulent Diffusion Term**- $-\frac{1}{r}\frac{\partial r\overline{u_r^{'}q}}{\partial r}$

**Viscous Diffusion Term**-

$$2\upsilon(\overline{\frac{\partial u_z^{'}S_{zz}^{'}}{\partial z}}+\overline{\frac{\partial u_r^{'}S_{rz}^{'}}{\partial z}}+\overline{\frac{\partial u_\theta^{'}S_{\theta z}^{'}}{\partial z}}$$
$$+\overline{\frac{\partial r u_z^{'}S_{zr}^{'}}{r\partial r}}+\overline{\frac{\partial r u_r^{'}S_{rr}^{'}}{r\partial r}}+\overline{\frac{\partial r u_\theta^{'}S_{r\theta}^{'}}{r\partial r}}$$
$$+\frac{1}{r}\overline{\frac{\partial u_z^{'}S_{z\theta}^{'}}{\partial\theta}}+\frac{1}{r}\overline{\frac{\partial u_r^{'}S_{r\theta}^{'}}{\partial\theta}}+\frac{1}{r}\overline{\frac{\partial u_\theta^{'}S_{\theta\theta}^{'}}{\partial\theta}})$$

**Viscous Dissipation Term**-

$$2\upsilon(-\overline{S_{zz}^{'}\frac{\partial u_z^{'}}{\partial z}}-\overline{S_{zr}^{'}\frac{\partial u_r^{'}}{\partial z}}-\overline{S_{z\theta}^{'}\frac{\partial u_\theta^{'}}{\partial z}}$$
$$\overline{S_{rz}^{'}\frac{\partial u_z^{'}}{\partial r}}-\overline{S_{rr}^{'}\frac{\partial u_r^{'}}{\partial r}}-\overline{S_{r\theta}^{'}\frac{\partial u_\theta^{'}}{\partial r}}$$
$$\overline{S_{\theta z}^{'}\frac{\partial u_z^{'}}{\partial \theta}}-\overline{S_{\theta r}^{'}\frac{\partial u_r^{'}}{\partial \theta}}-\overline{S_{\theta\theta}^{'}\frac{\partial u_\theta^{'}}{\partial \theta}}$$
$$-\overline{\frac{u_r^{'}S_{\theta\theta}^{'}}{r}}+\overline{\frac{u_\theta^{'}S_{r\theta}^{'}}{r}})$$

On scaling these terms,

**Unsteady term**- $\mathcal{O}(\mathcal{U}/\mathcal{T})$

**Pressure Diffusion Term**- $\mathcal{O}(\mathcal{U}^3/\mathcal{L})$

**Production Term**-$\mathcal{O}(\mathcal{U}^3/\mathcal{L})$

**Turbulent Diffusion Term**- $\mathcal{O}(\mathcal{U}^3/\mathcal{L})$

**Viscous Diffusion Term**- $\mathcal{O}(\upsilon\mathcal{U}^2/\mathcal{L}^2)$

**Viscous Dissipation Term**- $\mathcal{O}(\upsilon \quad u^2/\eta^2)$

Here, $\mathcal{U}$ and $\mathcal{L}$ refer to the velocity and length scale respectively of large scale eddies; $u$ and $\eta$ refer to the velocity and length scale respectively of small scale eddies

# B

# Appendix 2

PIV is a non-intrusive optical flow measurement technique in which tracer particles are added to the fluid and quick consecutive images of the laser illuminated flow field are taken. The displacement of the particles over a time interval Δt between the images provides the velocity of the flow field. Unlike other 'point' measurement techniques, it is a 'whole field' flow measurement technique in which the entire image is divided into 'interrogation windows'. The image intensity of an interrogation window is cross-correlated with that of the interrogation window of successive images to obtain a correlation function. The peak of this cross-correlation function is approximated to sub-pixel accuracy to obtain the displacement of particles in the interrogation window.The displacement divided by the time interval Δt is the velocity of the particle. This time interval Δt needs to be small for the obtained velocity to be the 'true' velocity. In this manner information about the velocity of the particles over the entire flow field is obtained. In an ideal case the particles would have the same velocity as the flow, would not interact with each other and would not distort the flow field. However in the constraints of the 'real' world some errors do persist, but they are often negligible.The velocity of the fluid is then deduced to be equal to the velocity of the particles. Techniques like Interrogation window overlap, Multi-grid interrogation is used to further improve the accuracy of the estimation of the velocity field.

In standard 2D PIV the light sheet is perpendicular to the optical axis of the camera, hence the 2D velocity field of the plane illuminated by the laser sheet can be obtained. In S-PIV more than one camera with different viewing angles are used to obtain 3 components of the spatial velocity field. Standard 2D-PIV algorithms are used to construct velocity fields from images at different angles using multiple cameras (quite often it is two cameras). Davis 8.3.1 uses a 3D calibration method to reconstruct a 3-component velocity field using these velocity fields. A non-linear mapping function is used to project the coordinates from the image plane of the cameras $\mathbf{x} = (x_1^{(1)}, x_2^{(1)}, x_1^{(2)}, x_2^{(2)})$ (superscript 1 and 2

denotes cameras 1 and 2 respectively) into the the measurement plane $\mathbf{X} = (X_1, X_2, X_3)$ (subscript 3 denotes the out -of-plane coordinate). This non-linear function **F** takes into account the effects of perspective and distortions due to the various optical media between the image plane and the object plane. The mapping is as follows.

$$\mathbf{x} = \mathbf{F}(\mathbf{X}) \tag{B.1}$$

**F** is generally approximated by a polynomial function which is cubic in $X_1$ and $X_2$ and quadratic in $X_3$. It is given as,

$$\begin{aligned}\mathbf{F} =& \mathbf{a_0} + \mathbf{a_1}X_1 + \mathbf{a_2}X_2 + \mathbf{a_3}X_3 + \mathbf{a_4}X_1^2 + \mathbf{a_5}X_1X_2 + \mathbf{a_6}X_2^2 + \mathbf{a_7}X_1X_3 + \mathbf{a_8}X_2X_3 \\ &+ \mathbf{a_9}X_3^2 + \mathbf{a_{10}}X_1^3 + \mathbf{a_{11}}X_1^2X_2 + \mathbf{a_{12}}X_1X_2^2 + \mathbf{a_{13}}X_2^3 + \mathbf{a_{14}}X_1^2X_3 + \mathbf{a_{15}}X_1X_2X_3 \\ &+ \mathbf{a_{16}}X_2^2X_3 + \mathbf{a_{17}}X_1^2X_3 + \mathbf{a_{18}}X_2X_3^2\end{aligned} \tag{B.2}$$

The coefficients $\mathbf{a_i}$ have 4 values for 4 equations ( 2 displacement coordinates from 2 cameras) and are obtained via a calibration process in which a calibration plate is placed in the measurement plane $(X_3 = 0)$ within a pipe. The calibration plate consists of markers printed on a surface at precisely known locations. (See Fig 1.3). Hence, the coordinates of the markers in the measurement plane are known. Images of the calibration plate are then recorded using both the cameras to obtain the coordinates of the markers in the image plane. The coefficients of equation 1.2 are then obtained using a least squares approach. The calibration plate needs to be traversed with a known displacement along the out of plane coordinate twice, to use three $X_3$ planes to satisfy the quadratic dependence on $X_3$. Hence, three sets of images from both the cameras are used to obtain the aforementioned coefficients.

Displacements in the coordinates in the image plane are given by,

$$x + \Delta x = F(X + \Delta X) - F(X) \tag{B.3}$$

Using taylor expansion and neglecting higher order terms we get a mapping of the displacements of the measurement plane into the image plane

$$\Delta x = \nabla F \Delta X \tag{B.4}$$

where, $(\nabla F)_{ij} = \frac{\partial F_i}{\partial X_j}$

The displacements of the measurement plane are obtained from the displacements of cameras 1 and 2 as,

$$\Delta X = (\nabla F)^{-1} \Delta x \tag{B.5}$$

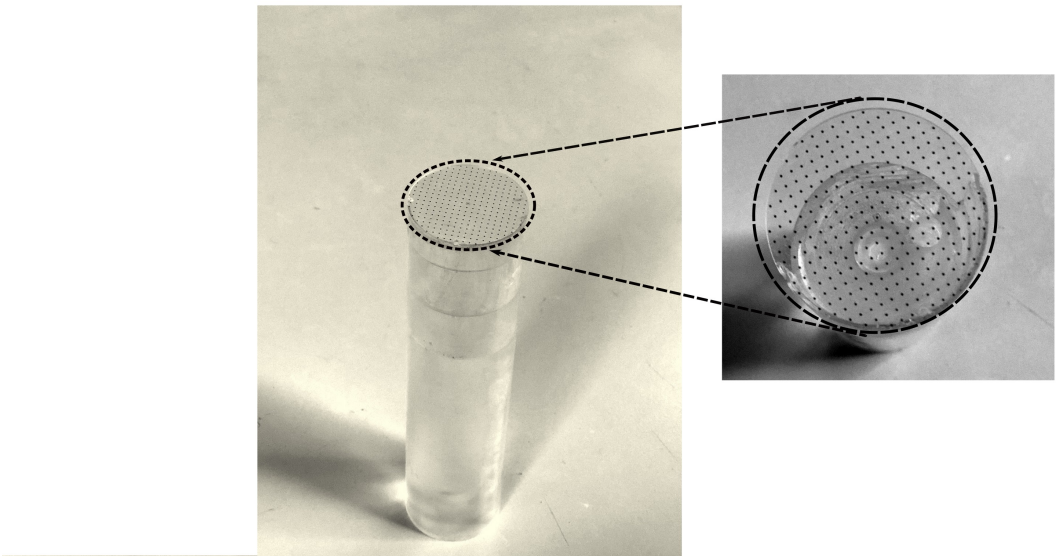

Figure B.1: Calibration plate used in the experiments

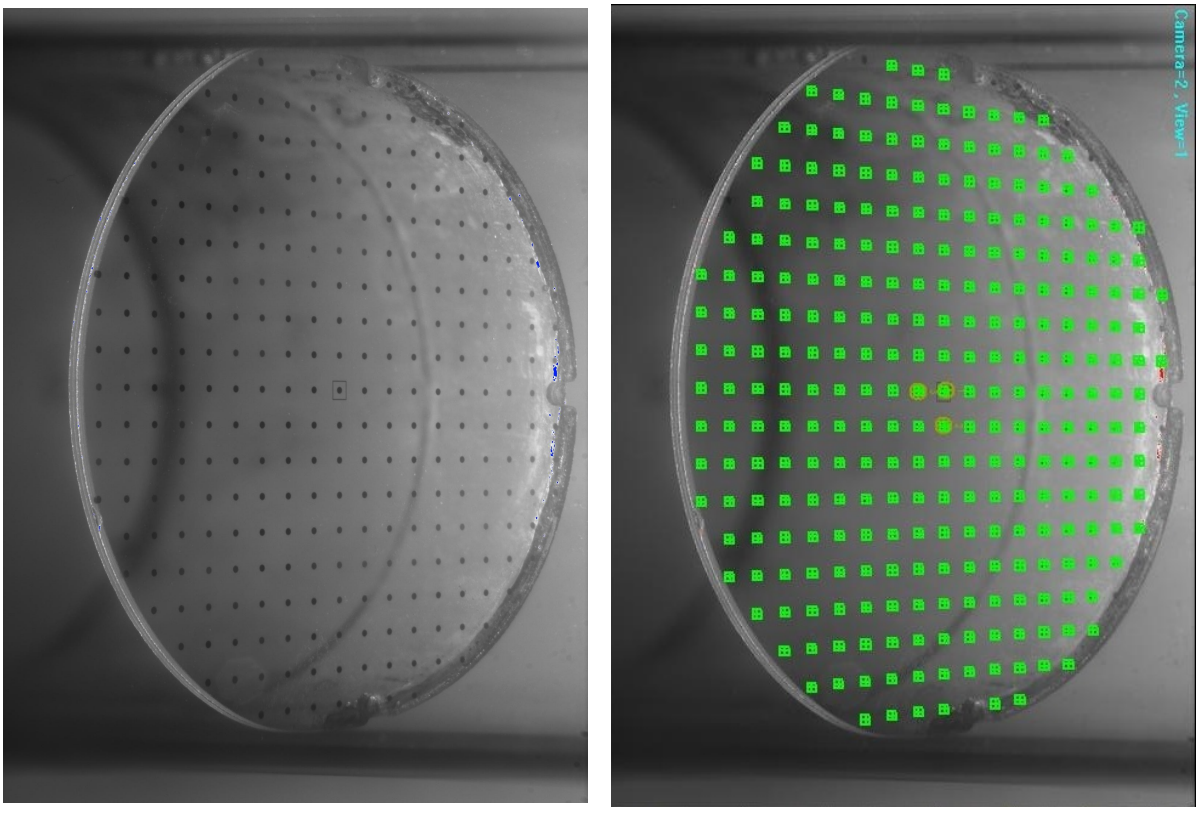


(a) (b)

Figure B.2: In **Figure (a)** Image of the calibration plate inside the pipe captured by a camera In **Figure (b)** the markers detected by Davis software are indicated with green boxes

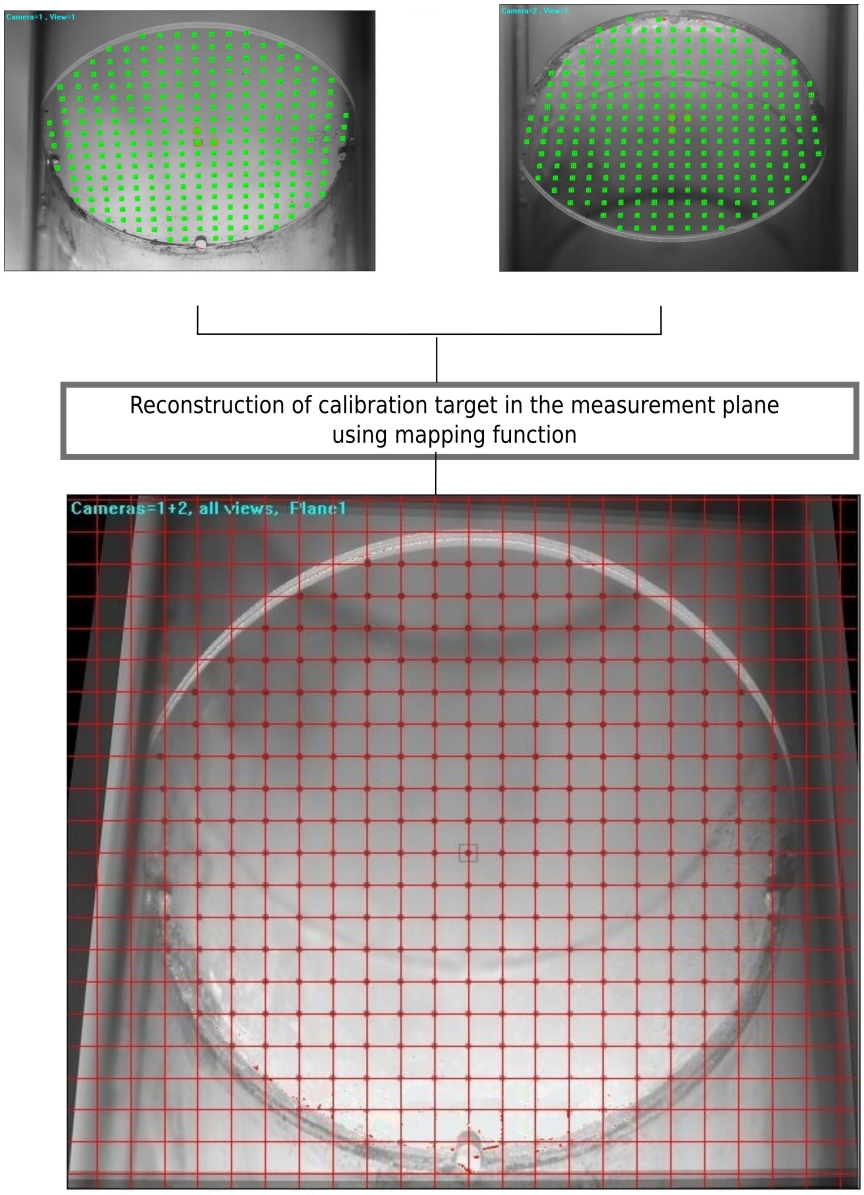


Figure B.3: Schematic showing the image of the measurement plane reconstructed using the images of the calibration plate in the pipe obtained from both the cameras

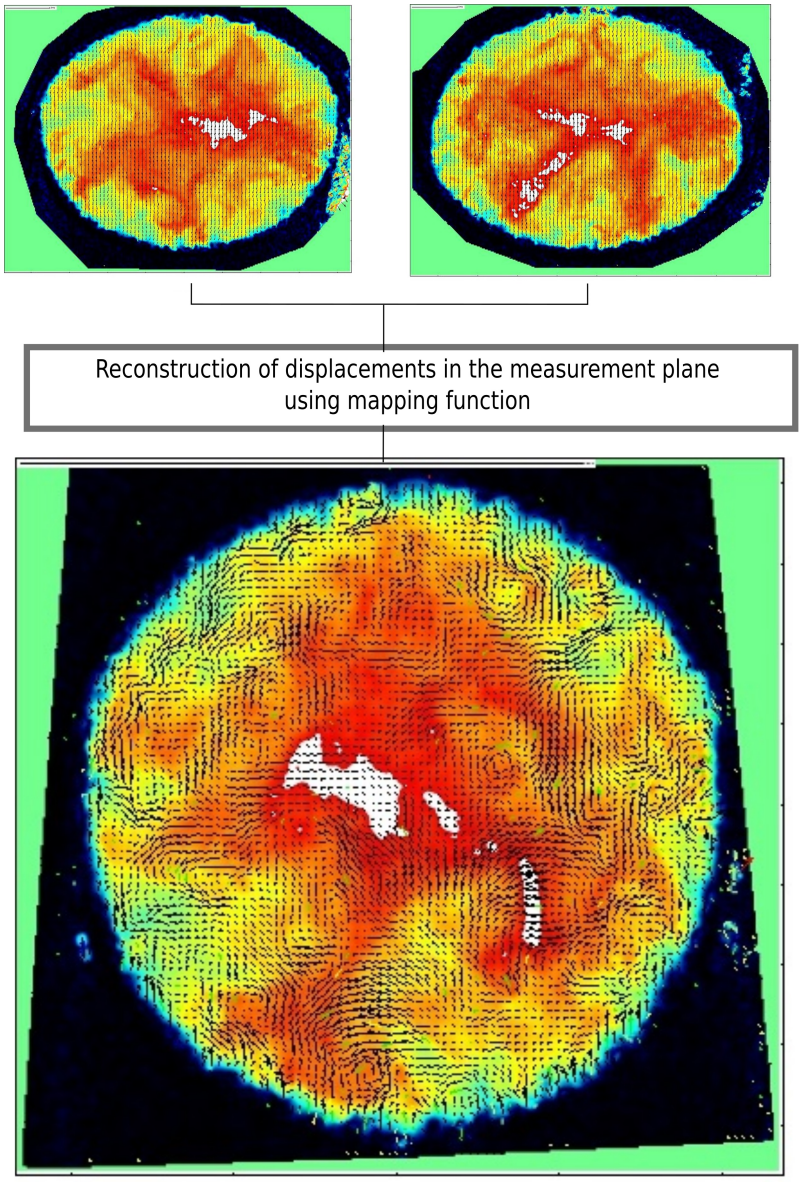


Figure B.4: Schematic showing the reconstruction of the velocity field of the measurement plane using vector field obtained from both the cameras

# C

# Appendix 3

Fig C.1 shows the dissipation rate in comparison with the Production term for different Gaussian Filter strengths ($\sigma = 0.65$, $\sigma = 1.1$ and $\sigma = 1.65$. The value of $\sigma = 1.1$ was chosen in this present work as it qualitatively matches the dissipation rates shown in Lawn (1971) and Laufer (1953).

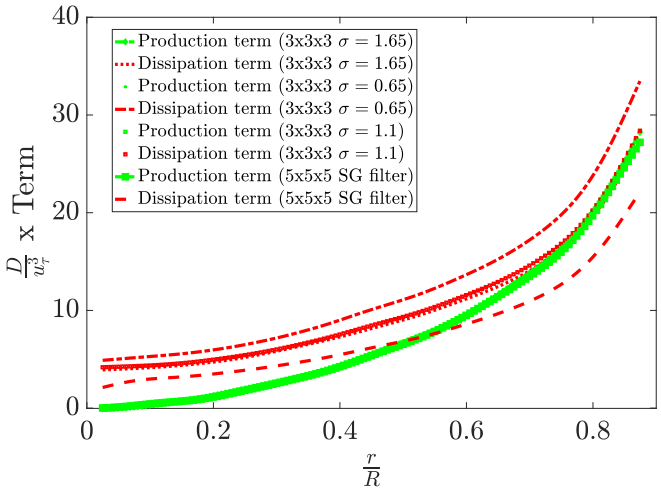


Figure C.1: Comparison of results from different filter strengths.

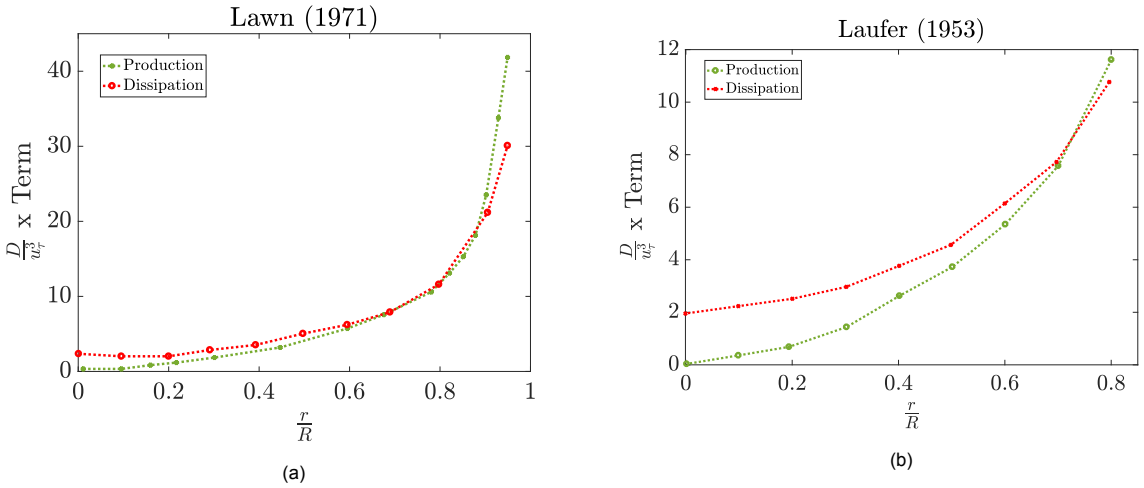


Figure C.2: **Figure (a)** Results from Lawn (1971) **Figure (b)** Results from Laufer (1953)

Fig C.2a shows the dissipation rate are shown in Lawn (1971). The values are measured using the Energy spectrum and using the Kolmogorov's hypothesis. C.2b shows the dissipation rate presented by Laufer (1953), the data is calculated using isotropic relations.